

Reversed-Phase Liquid Chromatography of Peptides for Bottom-Up Proteomics: A Tutorial

Juraj Lenčo,* Siddharth Jadeja, Denis K. Naplekov, Oleg V. Krokhin, Maria A. Khalikova, Petr Chocholouš, Jiří Urban, Ken Broeckhoven, Lucie Nováková, and František Švec



Cite This: <https://doi.org/10.1021/acs.jproteome.2c00407>



Read Online

ACCESS |

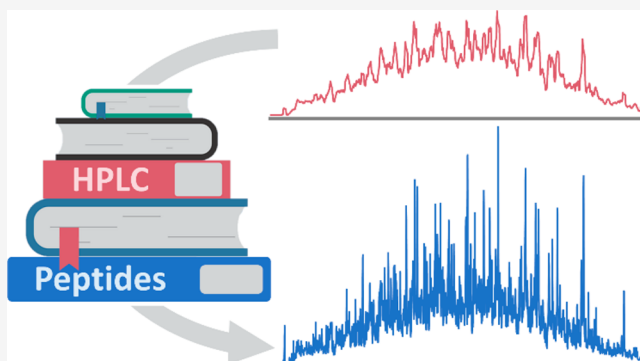
Metrics & More

Article Recommendations

Supporting Information

ABSTRACT: The performance of the current bottom-up liquid chromatography hyphenated with mass spectrometry (LC-MS) analyses has undoubtedly been fueled by spectacular progress in mass spectrometry. It is thus not surprising that the MS instrument attracts the most attention during LC-MS method development, whereas optimizing conditions for peptide separation using reversed-phase liquid chromatography (RPLC) remains somewhat in its shadow. Consequently, the wisdom of the fundaments of chromatography is slowly vanishing from some laboratories. However, the full potential of advanced MS instruments cannot be achieved without highly efficient RPLC. This is impossible to attain without understanding fundamental processes in the chromatographic system and the properties of peptides important for their chromatographic behavior. We wrote this tutorial intending to give practitioners an overview of critical aspects of peptide separation using RPLC to facilitate setting the LC parameters so that they can leverage the full capabilities of their MS instruments. After briefly introducing the gradient separation of peptides, we discuss their properties that affect the quality of LC-MS chromatograms the most. Next, we address the in-column and extra-column broadening. The last section is devoted to key parameters of LC-MS methods. We also extracted trends in practice from recent bottom-up proteomics studies and correlated them with the current knowledge on peptide RPLC separation.

KEYWORDS: *bottom-up proteomics, peptide separation, reversed-phase liquid chromatography, peptide properties, method development, protein separation, tutorial*



INTRODUCTION

Bottom-up proteomics based on protein cleavage using a sequence-specific protease followed by analysis utilizing liquid chromatography hyphenated with mass spectrometry (LC-MS) has become the core approach in the realm. Mass spectrometry combined with advanced MS data evaluation strategies is undoubtedly the leading analytical technology, thanks to which bottom-up proteomics can identify thousands of proteins from complex proteomic samples during a single LC-MS analysis. Indeed, the progress in mass spectrometry in the recent decade is stunning, and it is difficult not to be fascinated by the capabilities of state-of-the-art MS instruments.^{1–8} Relative to this, the progress in liquid chromatography for the analysis of peptide mixtures since the introduction of sub-2 µm particles,⁹ the resurrection of superficially porous particles in 2006,¹⁰ and the recent introduction of micropillar array columns¹¹ is not that dramatic. These facts, however, must not reduce the importance of liquid chromatographic separation in LC-MS-based proteomics. Quite the contrary, the quality of peptide chromatography can dramatically affect the results of bottom-

up LC-MS proteomic analyses. Without outstanding chromatographic separation, the full potential of the most advanced mass spectrometers can never be fully exploited.¹²

It may sound surprising that we feel a tutorial on peptide separation using reversed-phase liquid chromatography (RPLC) is needed more than 25 years after the fully automated bottom-up proteomic analyses employing chromatographic separation were brought to life.¹³ Nevertheless, if the key to efficiently utilizing the full potential of current mass spectrometers for bottom-up proteomics is liquid chromatography, we rationalize that this is impossible without understanding chromatography fundamentals. For our recent publication,¹⁴ we inspected 60 LC-MS data files deposited in the ProteomeXchange repository.¹⁵ The quality of chromato-

Received: July 7, 2022

graphic separation observed in a substantial portion of those data files did not correspond to the current state-of-the-art liquid chromatography of peptides. To get an independent and even broader insight into the quality of chromatographic separation in recent bottom-up LC-MS proteomic analyses, we inspected data files deposited in the ProteomeXchange repository from July 27, 2020, onward. We imported one LC-MS file with an average size to Skyline software compatible with data formats from all major mass spectrometer vendors from each data set.¹⁶ In total, one hundred chromatograms were exported and uniformly visualized (*Supporting Information*, Figure S1). This deeper inspection confirmed our previous observation. The separation quality differs much between laboratories, and what is more important, a significant number of chromatograms obtained in various proteomic laboratories do not represent results corresponding to highly efficient peptide separation. We further collected specifications of how RPLC prior to the MS analysis was carried out. What first caught our attention most was the incomplete specification of the liquid chromatography methods. We had to inspect a several-fold higher number of deposited data sets to obtain at least 50 records for essential chromatography parameters. The parsimony in reporting the details of LC parameters further underlined that the role of chromatography in bottom-up proteomics is somewhat underestimated.

In this tutorial, we want to communicate the critical aspects of liquid chromatography of peptides that can show practitioners how better peptide separation can be achieved so that they can utilize the full performance of their state-of-the-art mass spectrometers. Besides, we would like to contribute to dispelling some chromatographic myths circulating in the community. Despite the recent progress in top-down proteomics (for reviews, see refs 17–20), the workhorse of proteomics nowadays is still bottom-up proteomics relying on converting proteins to more manageable peptides in the earliest stages. Hence, we have mainly focused on the chromatographic aspects of peptides. Nevertheless, where we consider it necessary or worthy, we address important aspects of separating the proteins using reversed-phase liquid chromatography.

BENEFITS OF EFFICIENT AND REPRODUCIBLE CHROMATOGRAPHY IN BOTTOM-UP PROTEOMICS

The primary purpose of RPLC in bottom-up proteomics is to timely distribute the sample components to reduce the number of peptides simultaneously entering the mass spectrometer. This gives the MS instrument time to acquire and interpret MS1 scans and isolate and fragment individual precursors. Nevertheless, liquid chromatography must not only be considered an indispensable step for delivering peptides into a mass spectrometer. It is vital to recognize that this stage of a bottom-up LC-MS analysis can dramatically impact the quality of data recorded by the mass spectrometer and, eventually, the number of identified and quantified peptides in both data-dependent and data-independent analyses.

The most readily observable benefit of more efficient peptide chromatography is the boost in MS signal intensity. To a first approximation, the peak area is constant and independent of the peak shape. Consequently, the narrower the peaks, the higher their signals must be, and thereby the higher the likelihood that the intensity crosses a threshold value for triggering a data-dependent scan (Figure 1). Sharper

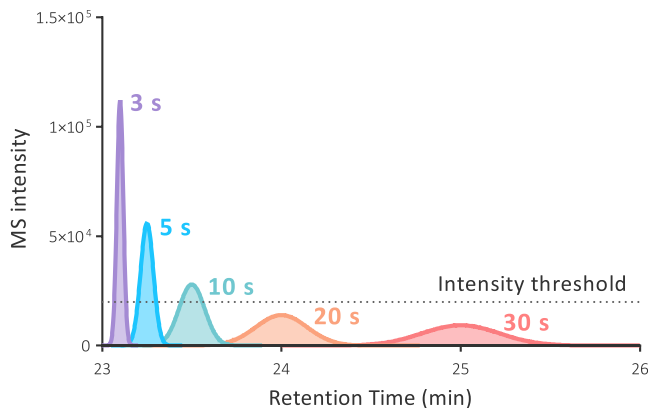


Figure 1. Simulated LC-MS peaks of a representative low abundant peptide chromatographed under five conditions with diverse separation performance resulting in peak widths at half-height w_h of 3, 5, 10, 20, and 30 s. Because the quantity of the peptide is the same and the peak area must be constant among peaks, broader peaks have a significantly reduced intensity. Only the three sharpest peaks cross the virtual intensity threshold of 2×10^4 for triggering a data-dependent scan in this simulation.

and more intense chromatographic peaks deliver more precursor ions for fragmentation per unit of time, resulting in a better quality of MS2 spectra and/or less time needed to accumulate the desired signal in the MS2 spectra. Our recent experiments have also demonstrated that thinner, thus, more intense chromatographic peaks lead to triggering data-dependent scans closer to their apex (Figure 2). This can further increase the quality of recorded MS2 spectra and/or decrease the time to obtain high-quality MS2 spectra. Besides, increased MS intensity due to better chromatography should rationally improve the accuracy of m/z of low abundant peptides as they are concentrated in sharper, more intense MS peaks. These facts collectively result in a higher number of fragmented unique precursors, improved quality of data, and, in turn, more identified peptides and proteins. Better peptide chromatography also contributes to accurate quantification. The better the peak shape, the more reliable peak integration is, and the more reliable quantification based on the precursor peak area.

A lower number of data points across the peak profile is often a proclaimed drawback associated with sharp chromatographic peaks in bottom-up LC-MS analyses that may affect the accuracy and reproducibility of quantification. Recent studies suggest that fewer than at least 15 data points recommended in the past for the analysis of small molecules²¹ are satisfactory for achieving accurate and repeatable quantification using LC-MS.^{7,22,23} A very recent LC-MS study focused on small molecules demonstrated that even six data points per peak could yield comparable quantitation results matched to those obtained using 10 and 20 data points.²⁴ Strikingly, Doellinger et al.²⁵ demonstrated that even mere 1.8 data points above the half-maximum of the peak sufficed to achieve a mean coefficient variation for protein quantification of 4%. One factor contributing to the differences between the recent studies and earlier recommendations may be that the intensity level from which data points are counted has not been established. In any case, experimental studies convincingly invalidate the concerns of some practitioners that sharper peaks due to improved performance of chromatography impair quantification. Nevertheless, if more data points per peak are genuinely needed for any reason, simple

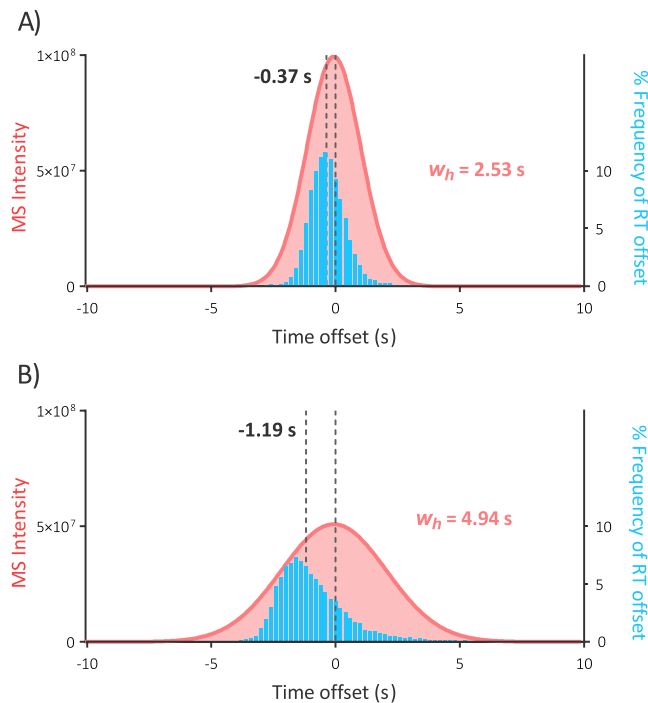


Figure 2. Effect of peptide separation quality on time offset between peak apex and triggering MS2 scans in data-dependent analyses. (A) MS2 scans are recorded closer to the peak apex when peptides elute as sharp peaks (the average w_h was 2.53 s, and the median offset time between peak apex and time of triggering MS2 spectra -0.37 s, 14980 PSMs were evaluated). (B) For broader peaks, the offset between the peak apex and the time when MS2 scans are recorded is significantly larger (the average w_h was 4.94 s, and the median offset time -1.19 s, 12888 PSMs were evaluated). Data from LC-MS analyses of a tryptic digest of a bacterium *F. tularensis* is demonstrated. Peptides were separated using a 12 min linear gradient from 2 to 38% acetonitrile with 0.1% formic acid in a 1.0×150 mm Acuity UPLC CSH C₁₈ 1.7 μm , 130 Å column (Waters). The column temperature was 60 °C, and the flow rate was 50 $\mu\text{L}/\text{min}$. The postcolumn band broadening in the bottom graph was enhanced by installing an additional 0.1 × 300 mm PEEK capillary (see the section [Band Dispersion in the Tubing](#)). The induced band broadening reduced the number of identified peptides by 15.7% and the median Byonic score⁴² of identified spectra by 13.4%. Combined data from duplicates are presented for each condition.

adjustments to the method, such as decreasing the flow rate or extending the gradient time, can be leveraged. Provided that the other chromatography parameters are optimized to obtain highly efficient peptide separation, such adjustments have a

secondary positive effect on the number of identifications without any significant drawback.

Sharper peaks are better timely resolved from each other, and the chance of coisolation and fragmentation of interfering precursors with similar m/z values is minor.²⁶ Coisolation is no longer a real issue in purely qualitative experiments and quantitative analyses relying on reconstructed peaks based on m/z values of precursors because dedicated bioinformatics tools that can identify multiple peptides from chimeric spectra have been developed.^{27–30} Yet, precursor coisolation represents a substantial issue in quantification methods based on isobaric tags.^{31–33} Sharper chromatographic peaks due to more efficient separation can thus improve the accuracy of quantification from reporter ions. Moreover, the time overlap between sharper peaks is vastly reduced, meaning that fewer interfering peptides are present in the ion source at one moment. The decreased competition between peptides for charging in the electrospray ion source can enhance their total MS intensity (Figure 3).

Efficiently optimized peptide chromatography also improves additional aspects important for proteomic studies based on bottom-up LC-MS analyses. The optimized chromatographic method does not only improve peak shapes as such but also their uniformity. The peak profiles are alike and independent of the peptide length, amino acid composition, and retention time. This effect brings a secondary benefit of better chromatography of peptides. The more uniform the peak widths of eluting peptides, the easier it is to set the dynamic exclusion time in data-dependent experiments to avoid repeated fragmentation of precursors and the maximum cycle time for collecting the preferred number of data points across chromatographic peaks for label-free quantification. The optimized method should also bring stability to retention times across injections. Arguably, the more stable the retention times, the more reliable the alignment of unidentified to identified precursors between runs, reducing the number of missing values in studies involving a large number of samples. In addition, repeatable retention times make scheduling in targeted LC-MS analyses reliable and safe.

RPLC itself provides an additional level of useful information. LC-MS data contain the retention time of peptides, i.e., specific and informative features of their sequences that can be compared with predicted values to improve the confidence of MS2 spectra identification.^{30,34–38} In addition, robust chromatography with retention time prediction algorithms improves confidence in assigning peptides to chromatographic peaks in targeted analyses, facilitates targeted methods scheduling,^{16,36,39} and even

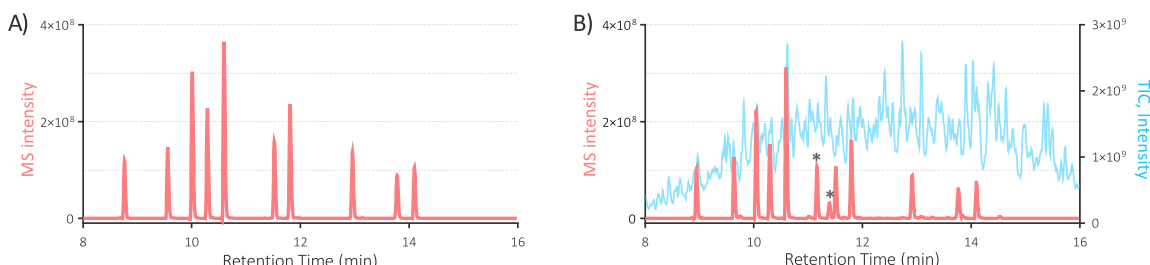


Figure 3. Comparison of LC-MS chromatograms of peptide standards when analyzed alone (A) and when injected from the same vial quickly followed by injecting a complex peptide mixture (B). Only ten peptides eluting along with the major portion of tryptic peptides from the complex sample (total ion chromatogram (TIC) in blue aligned to the right y-axis) are shown. Peaks extracted nonspecifically with an accuracy of 5 ppm are labeled with an asterisk. The experimental conditions were similar to those described in Figure 2.

enables on-the-fly generation of inclusion and exclusion lists.⁴⁰ Various approaches for predicting the retention time of peptides are currently available (for a review, see ref 41).

The text above focused on the benefits of efficient separation in data-dependent analyses. However, the same or similar benefits of better RPLC separation of peptides can also be seen in ever more popular data-independent analyses (DIAs). More uniform peak shapes facilitate calculating cycle time to obtain the desired number of points across peaks for reliable quantification. Sharper and more intense chromatographic peaks provide more intense fragments in DIA scans. In addition and perhaps most importantly, highly efficient separation facilitates aligning extracted chromatograms of peptide fragments from DIA scans and assigning them to particular precursors from MS1 scans.

RPLC IN PROTEOMICS

Peptides can be separated using various liquid chromatographic modes. These can be combined to achieve orthogonal 2D LC separations in comprehensive proteomic analyses.^{43,44} Yet, RPLC introduced already in the 1970s⁴⁵ remains the dominant chromatography mode for the final stage peptide separation when hyphenated to mass spectrometry. Undoubtedly, this is due to its intrinsic compatibility with soft ionization techniques for mass spectrometry. All commonly used mobile phase components for proteomic applications are perfectly compatible with online electrospray ionization-mass spectrometry via a robust and straightforward interface. The components are also compatible with the crystallization of matrices used in matrix-assisted laser desorption/ionization-mass spectrometry that is utilized for offline LC-matrix-assisted laser desorption/ionization mass spectrometry analysis. In addition, RPLC provides an unprecedented separation performance and very decent versatility. In contrast to some other modes, samples to be loaded into RPLC columns are dissolved in an aqueous environment that is well suited for peptides and proteins. A significant additional advantage of reversed-phase liquid chromatography is its exceptional robustness. The exclusive position of RPLC in proteomics is further strengthened by the fact that it efficiently separates also intact proteins for top-down analyses.

Retention Mechanism in RPLC

Despite numerous studies, considerable uncertainty still exists concerning the nature of the retention mechanism in RPLC.⁴⁶ The most widely discussed retention models involve (i) Horváth's model based on solvophobic theory⁴⁵ (analyte is rejected from the unfriendly polar environment and attached to a nonpolar bonded ligands), (ii) partitioning⁴⁷ (analyte is embedded within the bonded ligands), and (iii) adsorption⁴⁸ (analyte is positioned at the ends of bonded ligands). The only certain conclusion that has been drawn is that the retention mechanism at the molecular level is very complex and most likely varies with the stationary and mobile phases, analyte, and other conditions of the RPLC method. The retention mechanism of proteins is more complex because it involves changes in their conformation.^{49,50} We assume that further discussion of the retention mechanism is beyond the interest of the results-oriented practitioners in proteomics as it has only very little practical significance for their RPLC methods.

Independently of the mechanism, the retention of analytes in RPLC is controlled by the polarity of the analyte and both mobile and stationary phases. The polarity of the mobile phase

is modulated by adding a strong solvent to water, which is considered a weak solvent. Various solvents are used in RPLC that are ordered into an eluotropic series based on their elution strength which negatively correlates with their polarity. For instance, the elution strength of acetonitrile in RPLC of peptides is 2× stronger than methanol but 1.5× weaker than propanol.⁵¹

The mobile phase for RPLC of peptides and proteins typically contains a small portion of an acid such as formic acid, trifluoroacetic acid (TFA), and acetic acid (see the section [Additives for pH Adjustments](#)). The respective counteranions create neutral ion pairs with peptides and proteins protonated at the acidic pH and thus reduce the complexity of their ionic equilibria, modulate their hydrophobicity, and facilitate their interaction with the neutral hydrophobic stationary phase.⁵² Therefore, the separation of peptides and proteins under these conditions is often referred to as ion-pair RPLC. Two equivalent models that provide similar predictions describe the separation in ion-pair liquid RPLC.⁵³ The first assumes that an ion-pair is formed in the mobile phase, while the second suggests that the ion-pairing reagent is retained by the stationary phase and retention follows the ion-exchange process.

Gradient RPLC of Peptides

In proteomic applications, peptides and proteins are efficiently separated by RPLC only using gradient elution. It would be difficult, if not impossible, to explain how gradient elution works without describing the fundamental aspect of isocratic elution. Therefore, the first part of this section is devoted to the basics of isocratic elution.

Isocratic Elution. Regardless of the exact retention mechanisms, the main events leading to the separation of peptides in an RPLC column are similar to those during the extraction in a separatory funnel filled with two immiscible polar and nonpolar liquids, i.e., establishing dynamic equilibria between the concentration of the analytes in the polar mobile phase and the nonpolar phase represented by ligands bonded to stationary phase support. Hence, in principle, a separation column can be imagined as a lineup of a very high number of separatory funnels.

In RPLC, the hydrophobicity of analytes dictates their relative affinity to given polar mobile phase and nonpolar bonded ligands. A very polar analyte has no affinity to the bonded ligands. Hence, 100% of its molecules are situated in the mobile phase. Consequently, this analyte passes along the column with an overall speed that matches the mobile phase velocity (u). Suppose another analyte has precisely the same affinity to both phases. In that case, 50% of its molecules remain in a position being attached to nonpolar ligands while the other 50% moves to the column end with the speed of mobile phase velocity at each moment. The exchange of analyte molecules between both compartments is continuous. Therefore, the overall speed of this analyte through the column equals 50% of the mobile phase velocity. Analogously, the analyte with an 87.5% relative affinity to the nonpolar ligands passes the column with 12.5% mobile phase velocity.

The fraction of moles of the analyte in the stationary phase (n_S) relative to the number of moles in the mobile phase (n_M) determines the retention factor (k). The amount of the analyte in each phase is related to the concentration of the analyte in the stationary (c_S) and mobile (c_M) phase, together with the

total volume of stationary (V_S) and the mobile phase (V_M) (eq 1).

$$k = \frac{n_S}{n_M} = \frac{c_S \cdot V_S}{c_M \cdot V_M} \quad (1)$$

The retention factors for the three abovementioned examples are 0, 1, and 7. Distinct retention factors of analytes affect their retention times and, therefore, separation in the isocratic elution. By knowing the retention factor, one can predict the retention time t_R in isocratic elution from a particular column if the elution time of a nonretained compound (t_0) is also known (eqs 2 and 3).

$$k = \frac{t_R - t_0}{t_0} \quad (2)$$

$$t_R = t_0(k + 1) \quad (3)$$

In isocratic RPLC, the retention factor decreases with increasing volume fraction of strong solvent in the mobile phase (ϕ). A simple semilogarithmic linear-solvent-strength model introduced by Snyder⁵⁴ is widely used to describe the effect of the volume fraction of strong solvent in the mobile phase on the analyte retention factor (eq 4).

$$\log k = \log k_0 - S \cdot \phi \quad (4)$$

The parameter $\log k_0$ is extrapolated logarithm of the analyte retention factor in the purely aqueous mobile phase, while the parameter S determines how responsive its retention is to changes in the volume fraction of strong solvent (see the section S Parameter).⁵⁵

The volume fraction of the strong solvent is constant during isocratic elution. Therefore, isocratic elution is useful for separating a few or several analytes with relatively close hydrophobicity. In such cases, finding a percentage of strong solvent that separates all analytes in the mixture with reasonable retention factors is feasible. The retention factors should ideally be between 2 and 10. However, if all analytes significantly differ in their hydrophobicity, they cannot be isocratically eluted with retention factors in a reasonable range. Moreover, peptides have a significantly higher value of the S parameter than small molecules. Subsequently, the elution window of certain mobile phase compositions is very narrow for peptides and extremely narrow for proteins.⁵⁶ Hence, even a small change in the volume fraction of the strong solvent in the mobile phase can provide either strong retention or no retention at all. As a result, it is impossible to find a mobile phase composition that allows reasonable isocratic elution of peptides in a complex proteomic sample; therefore, gradient elution must be utilized.

Gradient Elution. In gradient RPLC, the concentration of the strong solvent such as acetonitrile increases, most often linearly, over the gradient span ($\Delta\phi$), i.e., from an initial concentration (ϕ_0) to a final concentration (ϕ_F) within the framework of preselected gradient time (t_G), defining the slope of the gradient run (B) (eq 5).

$$B = \frac{\Delta\phi}{t_G} = \frac{\phi_F - \phi_0}{t_G} \quad (5)$$

The retention factor at the initial conditions of the gradient of most peptides, except for the least hydrophobic ones, is very high because the mobile phase mostly constitutes water. In such an environment, typical peptides strongly interact with

the nonpolar ligands bonded to the stationary phase support. This limits their concentration in the mobile phase and increases their retention factor. Thereby, their passing speed through the column is close to zero or zero. The volume fraction of the strong solvent in the mobile phase increases during the gradient program, gradually weakening the affinity of the peptides to the stationary phase in the order of their raising hydrophobicity while increasing their affinity to the mobile phase. As a result, retention factors of individual peptides, and therefore their retention, with the ever-increasing acetonitrile fraction in the mobile phase, start progressively decreasing, and the migration of peptides through the column accelerates until they eventually leave the column.

To compare isocratic and gradient elution, Snyder introduced the “median” gradient retention factor at the midpoint of the column (k^*) that is equivalent to the isocratic retention factor and enables to treat the gradient data similarly to data from isocratic elution (eq 6).

$$k^* = \frac{1}{1.15 \cdot b} \quad (6)$$

For some calculations, the gradient retention factor at the beginning of the gradient (k_0) and at the time when the analyte elutes from the column (k_e) must be characterized (eqs 7 and 8).⁵⁷

$$k_0 = \frac{1}{b} (e^{b \cdot k_0} - 1) \quad (7)$$

$$k_e = \frac{k_0}{b \cdot k_0 + 1} \quad (8)$$

The gradient retention factor k_0 is calculated from the “apparent” gradient retention factor (k_g) based on the observed in-column residence time of the analyte (eq 9).

$$k_g = \frac{t_R - t_0}{t_0} \quad (9)$$

Equation 9 is accurate when gradient delay time (t_D) equals zero (see the section Gradient Program and Gradient Time). Otherwise, the gradient delay time t_D must be subtracted from t_R . The coefficient b in the equations for calculating gradient retention factors at those three different positions in the column represents the steepness of the gradient in the linear-solvent-strength model of gradient elution (eq 10).

$$b = \frac{t_0 \cdot S \cdot \Delta\phi}{t_G} = \frac{V_0 \cdot S \cdot \Delta\phi}{F \cdot t_G} \quad (10)$$

The elution time of a nonretained compound t_0 can also be predicted from the column void volume (V_0) and flow rate (F). The void volume can be estimated from the volume of an empty cylinder and the total column porosity (ε_T) (eq 11).

$$V_0 = V_e \cdot \varepsilon_T \quad (11)$$

The total porosity of a column ideally packed with fully porous particles is between 0.55 and 0.66. Columns packed with superficially porous particles have a 10–20% lower total porosity depending on the thickness of the porous layer.⁵⁸

In isocratic elution, the peak widths increase with later retention times of the analytes due to longitudinal broadening (see the section The B Term: Longitudinal Broadening Due to Molecular Diffusion). In contrast, peak widths in gradient elution are almost constant for early and late eluting

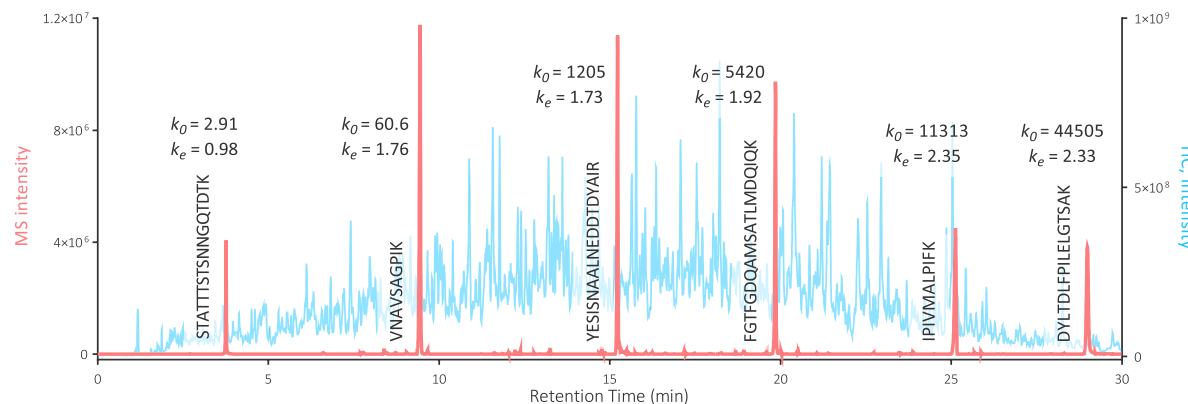


Figure 4. Gradient retention factors at the beginning of the gradient (k_0) and at the elution from the column (k_e) estimated for six selected tryptic peptides using eqs 7–10. Peptides with similar MS intensities eluting at different retention times were extracted with an accuracy of 5 ppm from a chromatogram of a tryptic digest of a bacterium *F. tularensis* (total ion chromatogram (TIC) in blue aligned to the right y-axis). The peptides were separated in a 2.1×150 mm bioZen Peptide column packed with $1.7 \mu\text{m}$ XB-C₁₈, 100 Å superficially porous particles (Phenomenex) held at 50 °C using a 30 min gradient. The other parameters of the separation method were: $F = 225 \mu\text{L}/\text{min}$, $t_0 = 1.18 \text{ min}$, and $\Delta\Phi = 0.384$. The values of the parameter S were predicted using an online calculator (<https://proteome.ad.umanitoba.ca/ssrcalc>). A gradient delay volume (V_D) of 152 μL was considered.

compounds, which is caused by the increase in migration velocity of the band along the column and the corresponding decrease in retention factor as the elution power of the mobile phase increases during the analysis. Hence, their passage along the column takes a very similar time, and despite the differences in their retention factor at the beginning of the gradient k_0 , analytes leave the column with a very similar instantaneous elution factor k_e (Figure 4). Peptides leave the column with low k_e , and similarly to isocratic elution, a small retention factor is associated with narrow peaks. Gradient retention factor k_e linearly increase with gradient time t_G and decrease inversely with gradient span $\Delta\phi$ and the column length (Figure 5). This explains why sharper peaks are observed in short steep gradients, whereas long shallow gradients yield significantly broader peaks, and also why better gradient separation of peptides is usually, not in 100% cases though, achieved using longer columns.

The column void volume is typically higher than the volume of the mobile phase delivered per minute. Therefore, the difference in the volume fraction of the strong solvent at the column inlet and the column outlet is higher than the programmed change of the strong solvent per minute, creating a gradient inside the column. As a result, the tail of a chromatographic band is always present in a slightly stronger mobile phase, thereby having a lower retention factor and higher velocity than the front of the band. Consequently, bands in the column are constantly compressed due to the higher velocity of the tails and the slower velocity of the fronts. This effect is known as gradient compression and further contributes to narrowing peaks in the gradient elution. The gradient peak-compression factor (G) can be estimated from the simplified relation proposed by Poppe (eq 12) using a parameter p (eq 13).⁵⁹

$$G = \frac{\sqrt{1 + p + \left(\frac{p^2}{3}\right)}}{1 + p} \quad (12)$$

$$p = \frac{2.3 \cdot k_0 \cdot b}{k_0 + 1} \quad (13)$$

In extremely steep gradients, the minimum theoretical value of the peak-compression factor is 0.58, compressing the peak width to only 58% of the peak width observable upon isocratic elution, with the isocratic retention factor k being equal to k_e . In long shallow gradients, it approaches the limit of 1, meaning there is no compression effect at all.⁶⁰ Because larger analytes have higher S parameter values, peak widths of peptides and particularly proteins can significantly profit from the compression factor in the gradient elution. Dependencies of the gradient peak-compression factor on selected parameters of gradient RPLC methods are listed in Table 1. By taking into account the gradient peak-compression factor, the peak bandwidth (w_b) of the analyte in a gradient elution can then be determined by eq 14.⁶⁰

$$w_b = \frac{4 \cdot t_0}{\sqrt{N}} \cdot G(1 + k_e) \quad (14)$$

The important parameter in the peak width prediction is the column efficiency specified as the number of theoretical plates. The determination of the theoretical plate number in isocratic elution (N) is a simple procedure. In contrast, it cannot be directly calculated from retention times and peak widths in gradient elution. Therefore, the theoretical plate number determined under isocratic conditions in the mobile phases good for analyte elution, a “median” plate number,⁶¹ or subtraction of extra-column contributions on peak width⁶² are usually utilized in the first approximation.

CHROMATOGRAPHIC PEAKS

The result of chromatographic separation processes within a column is a chromatographic band. As the band enters the detector, its concentration profile is recorded as a chromatographic peak. Under ideal conditions, the peak shape should fit the Gaussian function. The quality of peaks can be defined in multiple ways.^{63,64} Peak widths at half-height (w_h , symbols $w_{0.5}$ and $w_{50\%}$) are also frequently used in the literature, but they are not in alignment with the “Nomenclature for Chromatography” issued by IUPAC⁶⁵) are most easy to determine. w_h equals the peak width at 2.355 standard deviations (σ) of the Gaussian function. The base width of the peak, where the tangents through the inflection points intersect the baseline

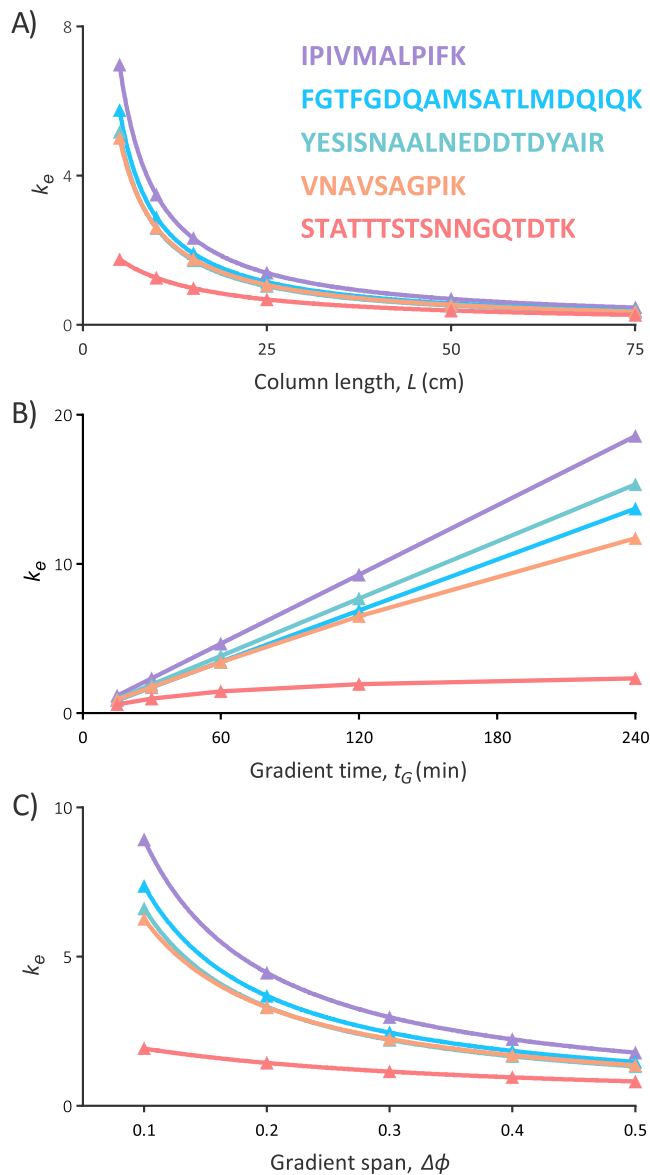


Figure 5. Relationship of gradient retention factor at the elution (k_e) with column length (A), gradient time (B), and gradient span (C) for the first five peptides from the chromatogram presented in Figure 4 (the values for the last peptide DYLTDLFFPILELGTSAK from the chromatogram essentially copied values calculated for the peptide IPIVMALPIFK). If not indicated otherwise, parameters present in Figure 4 or derived from it ($\varepsilon_T = 0.51$) were used.

Table 1. Relationship of Gradient Compression Factor G with Column Length (L), Gradient Time (t_G), and Gradient Span ($\Delta\Phi$)^a

L (mm)	G	t_G (min)	G	$\Delta\Phi$	G
50	0.851	15	0.671	0.1	0.875
100	0.777	30	0.734	0.2	0.804
150	0.734	60	0.809	0.3	0.760
250	0.685	120	0.879	0.4	0.730
500	0.637	240	0.930	0.5	0.707
750	0.619	480	0.962	0.6	0.691

^aValues calculated for the peptide YESISNAALNEDDTDYAIR that eluted at 15.2 min in the chromatogram shown in Figure 4 are present. If not stated otherwise, other parameters were the same as specified in the caption of Figure 4.

(w_b), is defined at 4σ . The width at 4σ can be converted to the peak width at 13.4% height. Similarly, the peak width at 5σ equals the peak width at 4.4% height ($w_{5\sigma}$). Unlike the w_h values of w_b and $w_{5\sigma}$ are not commonly calculated by software for proteomic LC-MS data evaluation. Where it is necessary, such as for calculating peak capacity, w_b can be extrapolated by multiplying w_h by a factor of 1.7 ($4\sigma/2.355\sigma$).

In practice, the Gaussian profile of peaks in proteomic analyses is barely achieved. Thus, w_h cannot define the quality of the peak in its entire profile. Peaks of separated peptides are not perfectly symmetrical, and peaks recorded from peptide RPLC separation often exhibit tailing. Assessment of peak quality can be improved using asymmetry factor (A_s) or U.S. Pharmacopeia tailing factor (T_f) that are defined at $w_{10\%}$ and $w_{5\%}$, respectively.⁶⁴

To assess the quality of a peak more realistically, at least two values are thus needed: w_h and asymmetry factor or tailing factor. This is not very practical. In addition, even the combination of these two criteria fails to reveal problems in separation resulting in symmetrical peaks suffering from both fronting and tailing. These issues can be tackled by calculating the peak variance (σ^2). It measures how far each data point in the peak profile is from the apex time of the peak. As a result, only one number is sufficient to measure the quality of chromatographic peaks. The most accurate method for calculating the peak variance is based on the second statistical moment.⁶⁵ At the time of writing this tutorial, the authors were not aware of any software for evaluating bottom-up proteomic data that determines the variance of chromatographic peaks. However, if it is vital, a semiautomated calculation in MS Excel based on numerical integration of peak profiles can be successfully used.⁶⁷ Although less accurate, the peak variance can be obtained from w_h values because $w_h = 2.355\sigma$ (eq 15).⁶⁶

$$\sigma^2 = \frac{w_h^2}{5.545} \quad (15)$$

Definition of Separation Performance in Isocratic Elution

Based on the plate theory developed by Martin and Synge,⁶⁸ the column performance in the isocratic elution mode is measured as the column efficiency expressed as the theoretical plate number N that relativizes retention time of a peak to its time variance (σ_t^2) (eq 16).

$$N = \frac{t_R^2}{\sigma_t^2} = \left(\frac{t_R}{w_h/2.355} \right)^2 = 5.545 \left(\frac{t_R}{w_h} \right)^2 \quad (16)$$

Beginners in chromatography are sometimes told that the theoretical plate number can be imagined as the number of imaginary separatory funnels in a column in which the dynamic equilibria between the concentration of the analytes in the mobile phase and the stationary phase can establish. When column length (L) is divided by the theoretical plate number N , a height equivalent to a theoretical plate (HETP or shortly theoretical plate height, H), that is commonly given in μm , is determined (eq 17).

$$H = \frac{L}{N} \quad (17)$$

Analogously to the theoretical plate number, theoretical plate height H can be imagined as the distance between the two adjacent imaginary separatory funnels in the column. The general effort in chromatography is to minimize H to achieve

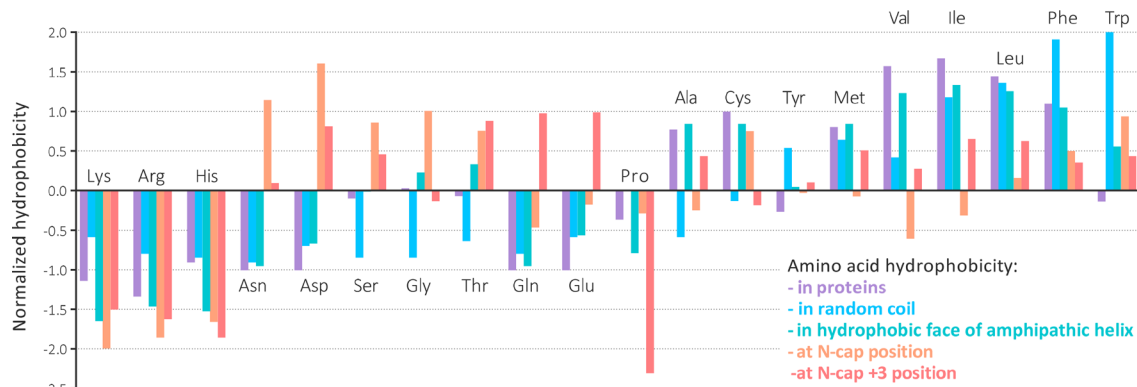


Figure 6. Hydrophobicity scales of amino acids in proteins and peptides. Kyte–Doolittle scale⁹⁵ for amino acids in proteins (purple); scale by Kovacs et al.⁸¹ for amino acids in peptides with a random coil conformation (blue); scale by Sereda et al.⁸⁴ for amino acid substitutions within the hydrophobic face of an amphipathic helix (green); scale for amino acids at the N-cap (orange) and N-cap+3 positions (red) in an amphipathic helical peptide.⁸⁵ Normalized hydrophobicity values are presented. The plot earlier published by Spicer et al.⁸⁵ in *Analytical Chemistry* was adapted for the figure.

superior chromatographic efficiency. Van Deemter et al.⁶⁹ postulated an equation that determines how H is associated with three main types of in-column band dispersion (see the section **In-Column Band Dispersion**).

The theoretical plate height H can be divided by the particle diameter (d_p) to obtain a reduced theoretical plate height (h) (eq 18). This simple relativization subsequently allows comparing the efficiency of columns independently of the particle size, i.e., other aspects impacting the differences in column efficiency, such as the quality of packing, can be evaluated. Modern, well-packed columns with the particulate stationary phase are expected to deliver reduced theoretical plate height h as low as twice the particle diameter or less when operated close to their optimal mobile phase velocity.⁷⁰

$$h = \frac{H}{d_p} \quad (18)$$

Definition of Separation Performance in Gradient Elution

Evaluating the separation performance in gradient separation using the theoretical plate number the same way as it is calculated for isocratic elution (eq 16) is inherently not possible. If the knowledge of column efficiency expressed in theoretical plate number for gradient methods is necessary, the retention time in eq 16 must be replaced by the expression $t_0(1 + k_e)$ based on eq 3 and then plate number for gradient elution (N^*) can be calculated (eq 19).

$$N^* = \left(\frac{t_0(1 + k_e)}{\sigma_t} \right)^2 = 5.545 \left(\frac{t_0(1 + k_e)}{w_h} \right)^2 \quad (19)$$

Because the determination of theoretical plate number for gradient elution is less straightforward than in the isocratic elution, peak capacity (n_p , symbol P_c is also frequently used) is commonly used for assessing the separation performance in gradient mode. The peak capacity was initially defined as the maximum number of peaks that can be separated in a given elution window of isocratic chromatography with a resolution of 1.⁷¹ Horváth subsequently applied this concept to gradient separations.⁷² The widths of peaks are relatively constant within a gradient run. Hence, experimental peak capacity can be calculated by dividing the gradient time t_G by the average peak width at 4σ (eq 20).^{57,73}

$$n_p = 1 + \frac{t_G}{w_b} = 1 + \frac{t_G}{1.7 \cdot w_h} \quad (20)$$

If the analytes occupy only a fraction of the effective elution window of the gradient program, the separation quality should be characterized by the sample peak capacity introduced by Snyder⁷⁴ that calculates the peak capacity from the elution time of the last and the first analyte (eq 21).

$$n_p = 1 + \frac{t_R^{last} - t_R^{first}}{w_b} \quad (21)$$

Inappropriate calculation of peak capacity based on w_h instead of w_b overestimates its true value 1.7-fold. Unfortunately, except for a few exceptional LC-MS proteomic studies,^{75–78} reporting peak capacity close to and above 1000 is most likely a result of incorrect calculation rather than a significant advance in the peptide separation. Improper use of the formula for calculating the peak capacity, whether conscious or unconscious, unnecessarily complicates the comparison of the separation performance among studies, particularly if the calculation is not specified.

Peak capacity in the gradient separation of larger molecules, including peptides, can be predicted using an approximate model proposed by Neue (eq 22).⁵⁷

$$n_p = 1 + \frac{\sqrt{N^*} \cdot S \cdot \Delta \phi}{4 \cdot b + 1} \quad (22)$$

The practitioners can use this equation to readily predict a possible gain when basic parameters of a gradient method for the separation of peptides with a characterized performance need to be optimized to increase the peak capacity.

■ PROPERTIES OF PEPTIDES AFFECTING THEIR RPLC SEPARATION

Peptides possess several quite specific properties affecting their separation using RPLC. Some of them make their separation more troublesome compared to small-size analytes. These features are worthy of consideration during RPLC method development for superior results in bottom-up proteomics.

Hydrophobicity

The hydrophobicity of peptides is the property that uppermost affects their chromatographic behavior in an RPLC column.

The hydrophobicity of any compound, and therefore its retention in an RPLC column, can be assessed from a decadic logarithm of its partition coefficient between water and octanol ($\log P$). In the case of RPLC separation, this translates into the partition between water and usually acetonitrile and hydrophobic C₁₈ chains bound to stationary phase support. The ultimate goal of predicting peptide hydrophobicity/retention in this system has driven Hodges's group and subsequently others to seek features that contribute most to peptide retention in RPLC.

The hydrophobicity of a peptide is not only a sum of contributions of individual amino acids, i.e., retention coefficients (R_c), to the total hydrophobicity as assumed in the additive models,^{79–81} but the position of individual amino acids also plays an important role.⁸² For instance, based on the single amino acid substitution experiments, Trp and Phe are often exemplified as amino acids with the greatest contribution to peptide hydrophobicity.^{80,81} However, this is not true for all peptide sequences, and assembling a simple list that would rank all amino acids based on their retention coefficients is impossible (Figure 6).

Eventually, several composition- and sequence-specific features affecting peptide retention under particular chromatographic conditions have been established: (i) peptide length (longer peptides exhibit decreased retention due to spatial hindrance preventing interactions),⁸³ (ii) peptide secondary structure (amphipathic helical peptides are characterized by very high retention due to specific orientation upon contact with C₁₈ ligands favoring hydrophobic and disfavoring hydrophilic interactions),⁸⁴ (iii) N-capping (specific amino acid motifs stabilize secondary structures before amphipathic helices, which allows hydrogen bond formation to cap unpaired NH/C=O groups at the edge of the helix, and thus, a favorable N-capping arrangement prior to amphipathic helix may result in the highest hydrophobicity of Asp/Asn or Glu/Gln peptide analogues among all naturally occurring amino acids when placed in the N-cap or N₃ position, respectively),⁸⁵ (iv) ion-pairing properties (counteranions hinder hydrophobic interaction of close proximity side chains leading to significant reduction of retention coefficients for hydrophobic residues near charged groups such as near N-terminal amino group at acidic pH),⁸⁶ and (v) overall peptide hydrophobicity (concentration of the strong solvent required for peptide elution alters ion-pairing interactions and as consequence, hydrophobicity values for all charged residues).⁸⁷

Understanding the complexity of peptide behavior in RPLC enabled the development of algorithms that can predict hydrophobicity and, therefore, the retention time of any possible peptide sequence. The retention time prediction in bottom-up proteomics is simplified because most conditions of peptide separation are generally constant among studies. Perhaps the most complex algorithm for predicting the retention times of peptides in an absolute manner is the Sequence-Specific Retention Calculator (SSRCalc, <https://proteome.ad.umanitoba.ca/ssrcalc>).^{88,89} SSRCalc estimates the retention of peptides using a hydrophobicity index (HI), i.e., the concentration of acetonitrile that yields a retention factor $k = 10$ under isocratic elution conditions.⁹⁰ The hydrophobicity index correlates well with retention time, and thus, it allows to accurately estimate the retention time of specific peptides if the retention time of a subset of calibrating peptides separated using the same method is known (Figure 7).

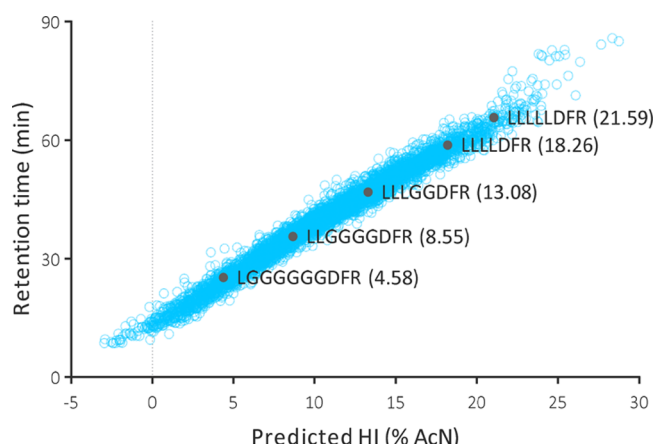


Figure 7. Peptide retention time prediction using SSRCalc.⁸⁹ The retention time of 5000 peptides was plotted against predicted SSRCalc hydrophobicity index (HI) values. Five calibrating peptides and their tabulated HI values are shown in gray. The plot earlier published by Krokkin et al.⁹⁰ in *Analytical Chemistry* was adapted for the figure.

The hydrophobicity of peptides is also responsible for unwanted losses in sample vials. This issue is significant when dilute peptide samples are processed and analyzed. Therefore, specific countermeasures must be undertaken to avoid such losses.^{91–93} Currently, adding a trace amount of polyethylene glycol with an average molecular mass of 20 000 is perhaps the most efficient means to reduce losses of hydrophobic peptides.^{91,94}

S Parameter

The larger the analyte molecular weight, the more interaction sites it possesses, and the more responsive its retention is to changes in the composition of the mobile phase. For instance, if the mobile phase strength in the isocratic elution of salicylic acid is increased or decreased by 1% acetonitrile, it would only slightly affect its retention time. However, if we make the same changes in the isocratic elution of a peptide, the retention time will differ significantly (Figure 8, A and B). This “retention sensitivity” is quantified using the parameter S. It was derived from the linear-solvent-strength model of gradient elution (eq 4) and represents the absolute steepness of a slope in the plot of the logarithm of the analyte retention factor against the volume fraction of the strong solvent in the mobile phase (Figure 8, C).^{96,97} To a first approximation, the parameter S is determined by the molecular weight of the peptide or protein. Due to their very high S values, retention of large polypeptides and proteins is sometimes simplified as a “catch and release” or “on-off” process.⁹⁸

S parameter can be estimated based on the peptide sequence and chromatographic conditions (<https://proteome.ad.umanitoba.ca/ssrcalc>).^{99,100} For predictions in bottom-up LC-MS analyses, a value between 29 to 38 can be a reasonable approximation (Figure 9).^{99,101–103} For intact proteins, S parameter is much higher.^{56,97} The association of the S parameter with molecular weight implies that the larger the polypeptide, the more likely the contribution of adsorption in the retention mechanism, whereas partitioning becomes less important.¹⁰⁴ A detailed investigation using extended sets of peptides demonstrated the influence of peptide charge and hydrophobicity^{99,100} in addition to their size, showing the

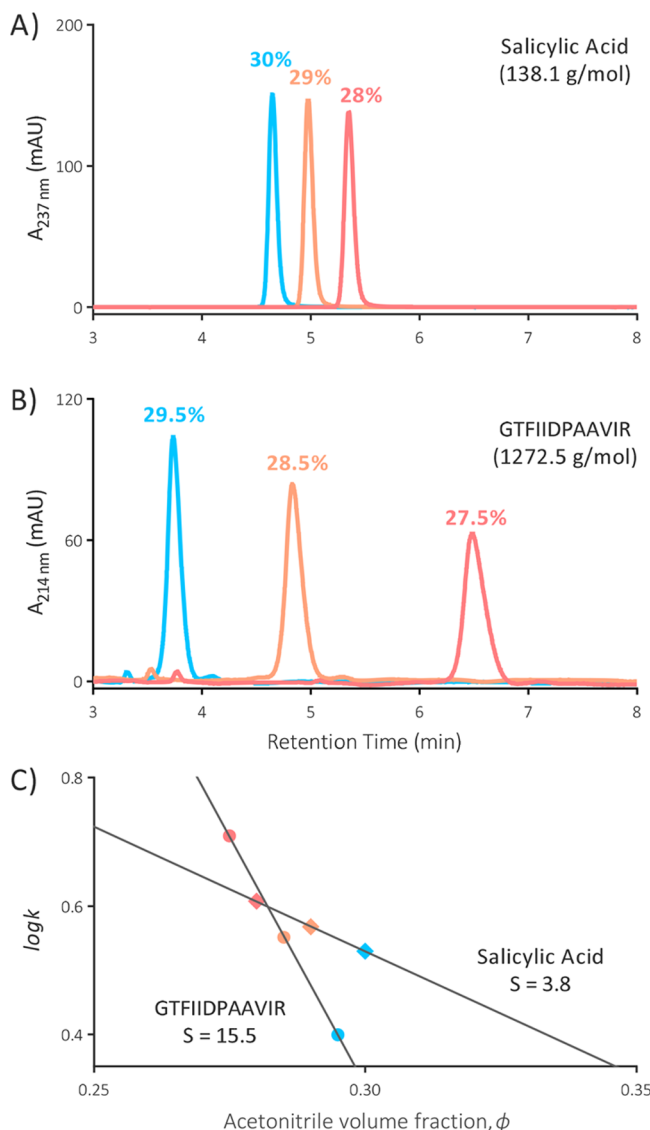


Figure 8. LC-UV chromatograms of isocratic elution of salicylic acid (A) and a peptide GTFIIDPAAVIR (B) obtained using a 2.1×100 mm column Zorbax SB-C₁₈ Rapid Resolution HD, $1.8 \mu\text{m}$, 80 \AA (Agilent). The column was maintained at 30°C . The mobile phase was acidified using 0.1% TFA, and the flow rate was $200 \mu\text{L}/\text{min}$. The initial acetonitrile volume fraction was optimized so that the analytes eluted around 5 min (orange peaks). Subsequently, the acetonitrile volume fraction was increased (blue peaks) and decreased (red peaks) by 1%. The percentual values above each peak represent the acetonitrile volume fraction in the mobile phase used for the isocratic elution. The bottom graph (C) illustrates the determination of the parameter S as a slope in the plot of the logarithm of the isocratic retention factor k drawn against the volume fraction of acetonitrile in the mobile phase ϕ .

complexity of the still disputed retention mechanism of RPLC.⁴⁶

The greater S parameter of peptides helps them virtually refocus at the head of a column after sample injection. This is important for the hydrophilic peptides in a direct injection setup. In a trap-elute configuration, this concerns all peptides. The effective refocusing of peptides at the head of a separation column virtually eliminates the contribution of the extra-column dispersion upstream of the column to total peak broadening (see the section **Extra-Column Dispersion and**

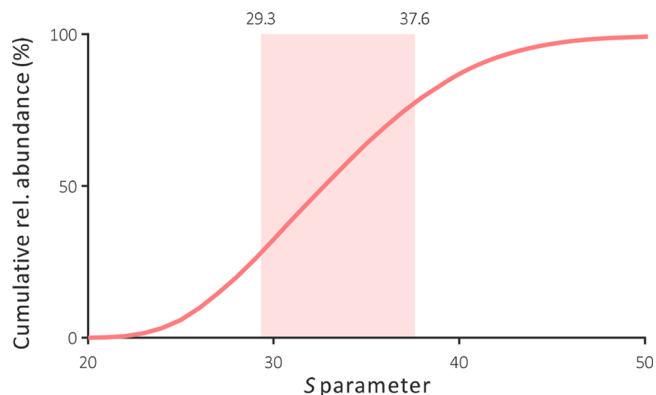


Figure 9. Prediction of S parameter for approximately 46,500 tryptic peptides with a length between 7 and 50 amino acids identified from Jurkat cells in a recent study.¹⁰⁷ No peptide modification was considered. Prediction is valid for a C₁₈ stationary phase with a pore size of 100 \AA and mobile phase acidified using 0.1% formic acid.¹⁰⁰ Red area represents the interquartile range.

Remaining Column Efficiency). Moreover, refocusing at the head of a column due to the greater S parameter enables the injection of large sample volumes relative to the column's inner diameter without disturbing the peak shape of the vast majority of peptides. This is particularly important in nanoLC, where injected sample volumes significantly exceed the volume of nanoflow separation columns or trap columns.¹⁰⁵ Furthermore, the gradient compression effect (see the section **Gradient Elution**) will be more important in the gradient separation of peptides (Table 1). Finally, small molecule contaminants with similar hydrophobicity as the hydrophilic peptides in the sample can be eluted by an initial isocratic step before the gradient elution of peptides commences.

On the other hand, the relative sensitivity of peptides to the elution strength of the solvent requires the chromatographic systems to generate reproducible gradients to maintain stable retention times across analyses. Moreover, as temperature impacts the elution strength of the mobile phase,¹⁰⁶ the column should be placed in a thermostat to eliminate ambient temperature fluctuation that would result in unpredictable shifts of retention times. The S parameter can also affect the separation selectivity of peptides. Providing that two peptides with close hydrophobicity have markedly different numbers of amino acids, they also have significantly different S parameters. As a result, they can elute in a different order if the slope of the gradient run changes significantly between methods.¹⁰⁰

Acid–Base Properties

Peptides are polyprotic amphoteric molecules. C-terminal carboxyls and carboxyl groups on Asp and Glu side chains represent functional groups with low pK_a values, while the N-terminal amino groups and side chains of His, Arg, Lys, and Tyr represent major sites with high pK_a values. The exact pK_a values of individual amino acids are well-known.¹⁰⁸ However, within a polypeptide chain, the acidity and basicity of the groups are under the influence of surrounding amino acids. Therefore, pK_a values of the amino acids joined via peptide bonds and their N-termini and C-termini are distinct from the pK_a values of isolated amino acids and vary depending on the position in the sequence.^{109–111} For instance, the pK_a of Asp was measured to be 3.7 in an alanine pentapeptide¹¹⁰ but can be as low as 0.5 in other sequences.¹¹² The pK_a values, together with the pH of the mobile phase, determine the

dissociation state of peptides. Depending on their composition and sequence, distinct dissociation states of peptides have distinct hydrophobicity, thereby retention. This behavior can be exploited to achieve an orthogonal selectivity in peptide prefractionation and 2D separation by RPLC using mobile phases with opposite pH.^{43,44,113}

The dissociation at equilibrium is a dynamic state, and the kinetics of dissociation and dedissociation is much faster than the interactions of peptides with the stationary phase. Thus, peptides in different dissociation states cannot be separated from each other. Instead, the retention of a peptide at certain pH is a sum of retentions of its possible dissociation states multiplied by their relative abundances. For a robust separation with stable retention times across analyses, the pH of the mobile phase should be far below the lowest or above the highest pK_a values of peptides. Here, minor inaccuracies in the pH adjustments do not significantly change the abundances of various possible dissociation states. To illustrate, the Henderson–Hasselbalch equation predicts that if the lowest pK_a is 3.5, and the pH of the mobile phase is adjusted incorrectly to 1.9 instead of 2.0, such an error in the pH results in only a 0.6% change in the abundance of corresponding dissociation states and does not have a significant effect on the retention time.

Typical tryptic peptides have at least two positive charges under the preferentially used acidic pH of the mobile phase. Such peptides and ionic compounds in general, tend to exhibit signs of overloading when analyzed using a low-ionic-strength mobile phase.^{114–116} This behavior explains why 0.1% TFA provides better peak shapes than 0.1% formic acid for the overwhelming majority of stationary phases. For superior peak shapes, peptides must be analyzed considering column loading capacities for them significantly lower than is typical for neutral analytes, or the ionic strength of the mobile phase must be increased.^{115,117,118} Dedicated stationary phases have also been developed to facilitate the separation of positively charged analytes, including peptides, using a low-ionic-strength acid mobile phase (see the section [Chemistry of Bonded Ligands](#)).

Molecular Diffusion

The mobile phase passages through the paths of the least flow resistance, which means it percolates through the interstitial spaces formed between the adjacent stationary phase particles in a packed bed column or through macropores in a monolithic media. Because of their nanoscale dimensions and, therefore, extreme flow resistance, the mobile phase does not flow through the tortuous and highly interconnected nanometer-sized pores, also known as mesopores, that furnish the large surface area necessary for efficient chromatography. The pores are filled with the stagnant mobile phase. Although it does not move, its composition changes during a gradient program because of the fast diffusion of solvents.

The only possibility for analytes to exploit the chromatographic ligands covering the surface of pores is diffusion through the stagnant mobile phase governed by the analyte concentration gradient. The faster the molecular diffusion of the analyte, the more rapidly it can diffuse inside the pores for chromatographic interaction and back to the mobile phase stream, and the more efficient the chromatographic separation can be. Molecular diffusion is proportional to the molecular weight of analytes. Peptides thus have roughly an order of magnitude lower diffusion coefficient (D_m) than small molecules have. For instance, the diffusion coefficient of

bradykinin and insulin in 50% acetonitrile is $2.85 \times 10^{-6} \text{ cm}^2/\text{s}$ and $1.50 \times 10^{-6} \text{ cm}^2/\text{s}$, respectively,¹¹⁹ whereas the diffusion coefficient of acetophenone is $1.77 \times 10^{-5} \text{ cm}^2/\text{s}$ (measured in 75% acetonitrile).¹²⁰ The issue related to the slow diffusion of peptides is further aggravated by the fact that the diffusion inside porous chromatographic media is significantly slower than is in the bulk solvent depending on the ratio of the analyte hydrodynamic diameter (see the section [Hydrodynamic Diameter](#)) to the size of pores.^{121–123} This is a consequence of the tortuosity and steric hindrance inside the pores.

The diffusion coefficient can be estimated using semi-empirical models. Wilke–Chang equation is the most popular for predicting the diffusion coefficient.¹²⁴ Nevertheless, the Young equation (eq 23) is more appropriate for larger molecules, such as peptides and proteins.^{125,126}

$$D_m = \frac{8.34 \cdot 10^{-8} \cdot T}{\eta \cdot \sqrt[3]{M_w}} \quad (23)$$

As seen from the Young equation, molecular diffusion is faster at a higher temperature (T). Temperature also reduces the viscosity of solvents (η) that subsequently hinders less the Brownian motion of molecules, the phenomenon behind diffusion. Collectively, raising the temperature from 20 to 60 °C directly and via the impact of lower viscosity accelerates the molecular diffusion of peptides approximately 2.5 times (Figure 10). Temperature thus represents an exceptionally

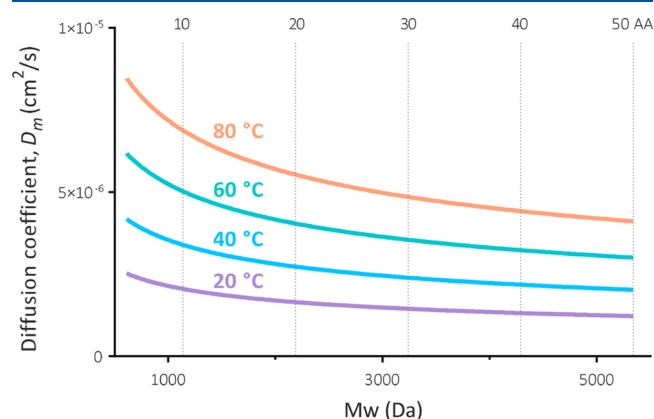


Figure 10. Diffusion coefficient (D_m) of peptides with various lengths estimated using the Young equation (eq 23) at four different temperatures.¹²⁵ Temperature-relevant viscosities of 20% acetonitrile at 200 bar reported by Billen et al.¹²⁷ were used.

effective means for coping up with the slow diffusion of peptides and proteins (see the section [Column Temperature](#)). Besides, particles with a reduced length of the diffusion paths, such as sub-2 μm particles and superficially porous particles, should be preferred media for separating analytes with slow diffusion.

Hydrodynamic Diameter

From the surface area of the particulate stationary phase, it can be estimated that more than 99% of the chromatographic surface is located in pores inside the particles. Hence, peptides must enter the pores to exploit the full separation potential of the columns packed with porous particles. However, if their hydrodynamic diameter is too large, a lower portion of the internal volume of particles with the chromatographic surface area is accessible to them, leading to reduced retention, peak

broadening, and/or tailing. The fraction of the pore volume that is accessible to peptides and proteins can be roughly estimated based on their hydrodynamic diameter (D_h) as $\left(1 - \left(\frac{D_h}{d}\right)\right)^3$ with d being the mean pore diameter.¹²⁸ Thus, if peptides shall use at least 50% of the pore volume, the nominal pore size must be five times larger than their hydrodynamic diameter. Gritti et al.^{128,129} proposed that the average pore size should be three times the hydrodynamic diameter of proteins to avoid a secondary size-exclusion retention mechanism that would result in peak broadening. In addition, the effective diffusion rate inside pores considerably decreases when the hydrodynamic diameter of peptides is significant relative to the size of the pores, aggravating the problem with their resistance to mass transfer (see the section **The C Term: Resistance to Mass Transfer**).¹²³

Hydrodynamic diameter is the diameter of a sphere formed by rotating a molecule in all possible directions with the center of rotation in its midpoint. Thus, it equals the longest distance between the two ends of a peptide shape in a typical RPLC separation carried out under denaturing conditions. For globular proteins in their native conformation, the hydrodynamic diameter equals the diameter of the molecule. If the molecular diffusivity of a peptide is known or was previously estimated using the Young correlation (eq 23),¹²⁵ its hydrodynamic diameter D_h can be determined according to the Stokes–Einstein law. Alternatively, hydrodynamic diameter in Å (10 Å = 1 nm) can be estimated to a rough approximation from the number of amino acids in a linearized polypeptide (N_p) using an empirical equation derived by Wilkins et al. (eq 24).¹³⁰

$$D_h = 4.42 \cdot N_p^{0.57} \quad (24)$$

For example, the hydrodynamic diameter of bradykinin can be estimated to be 15.5 Å, which is for purposes of separation optimization in proteomic LC-MS analysis in reasonable agreement with 17.0 Å determined using a direct application of the Stokes–Einstein law.¹¹⁹ The hydrodynamic diameter of proteins in native conformation is smaller.¹³⁰ Therefore, the optimum pore size for denaturing RPLC and native chromatography using nondenaturing conditions can differ.

Without any doubt, trypsin is the protease of choice for bottom-up proteomics analyses. It cleaves the carboxyterminal of Arg and Lys residues with high specificity and kinetics, resulting in peptides with desirable length and charge characteristics for identification using collision-induced dissociation and related techniques.^{131–134} The molecular weight of 90% of theoretic human tryptic peptides does not exceed 3 kDa, and the molecular weight of only 10% of tryptic peptides with two missed cleavages exceeds 5.6 kDa. Therefore, most of the peptides for the bottom-up analyses have a quintuple hydrodynamic diameter lower than 100 Å (Figure 11), which is the pore size of a typical particulate stationary phase for RPLC. For less restricted diffusion inside the pores and thereby more efficient separation, practitioners can take advantage of the stationary phases with a pore size larger than 100 Å. Also, in particular cases, such as peptidomics analyses, analyses of peptides generated with enzymatic digestion using Lys-C protease, or perhaps analyses of cross-linked peptides, the larger hydrodynamic diameter of some peptides would very likely benefit from using a stationary phase with wider pores (Figure 12). Nevertheless, one should be

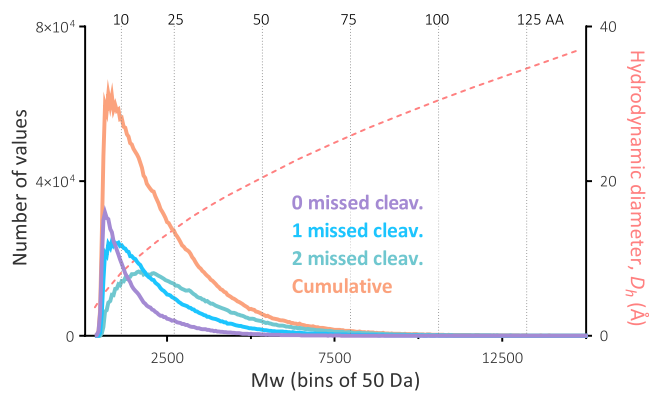


Figure 11. Distribution of molecular weight of predicted tryptic peptides generated *in silico* from the UniProt human protein database. Peptide molecular weight is correlated with the number of amino acids and the hydrodynamic diameter (D_h) predicted based on the equation derived by Wilkins et al.¹³⁰

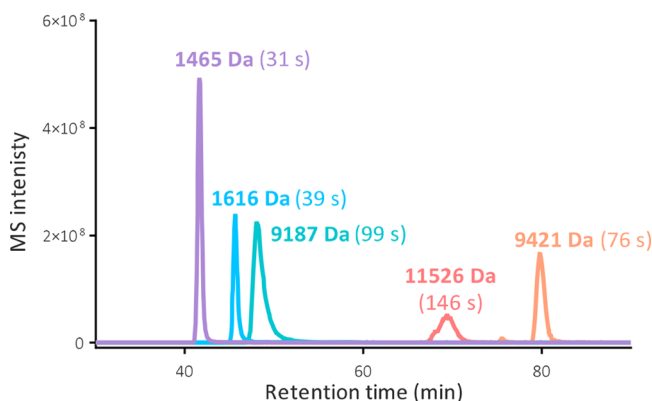


Figure 12. Extracted ion chromatograms of two short (1465 and 1616 Da) and three large peptides (9187, 11526, and 9421 Da) separated using a column packed with particles with a pore size of 100 Å. Although other effects cannot be excluded, the peak widths w_h in seconds noticeably correlate with the molecular weight of the peptides, suggesting restricted accessibility of particle pores. Reported molecular weights were calculated from the precursor m/z values and the charge states. LC-MS data were recorded within a human plasma peptidomics study by Kay et al.¹³⁵

aware that the surface area decreases with a larger pore size, which can result in slightly less efficient chromatography of shorter peptides. As a result, a rational balance between pore size and the surface area should be found for superior peptide RPLC.

Specific Amino Acid Composition of Peptides

Amino Acids with Chelating Properties. The hexahistidine tag is a well-known amino acid motif used for protein purification via interaction with immobilized metal ions.¹³⁶ Hence, it should not be surprising that the separation of peptides containing amino acids with chelating properties, such as just His but also Asp and Glu, can result in poor peak shapes, recovery, and in the worst scenario, can remain irreversibly bound to trace of metals accumulated on active sites in the column and flow paths. This issue is detectable mainly in LC-MS analyses with mobile phases acidified with weak acidifiers. Caution must be paid, particularly in analyses of phosphopeptides with an intrinsic affinity to metal ions, which is the property effectively exploited for their enrichment

using immobilized metal ion affinity chromatography, also known as IMAC.¹³⁷

NanoLC systems typically used for bottom-up LC-MS analyses are fabricated as biocompatible by design, meaning only materials such as PEEK, titanium, and MP35N, which is a nickel–cobalt-based alloy with a minimized risk of generating active metal sites, are used for the components that come in contact with the mobile phase. Nevertheless, practitioners should be aware that trace metals are virtually ubiquitous, and metal ions can accumulate in the stationary phase even in a biocompatible chromatograph.¹³⁸ Special care should be taken for systems used to analyze global proteomic samples and simultaneously phosphopeptides previously enriched using IMAC. In such situations, a significant risk of introducing metals released from the phosphopeptide enrichment columns exists.¹³⁹

If the chelating capacity is significant, the chromatograph and column should be flushed using a chelating agent such as salts of ethylenediaminetetraacetic acid. Alternatively, the chelating tendencies can be mitigated by adding MS-friendly deactivation agents to the mobile phase in low concentrations (see the section *Other Additives*).^{136,140} Dissolving peptides in the presence of deactivation agents can provide a similar service without changing the mobile phase composition.

Peptides with Vicinal Prolines. Peptide bonds in polypeptides have a partial double bond character. Hence, they are planar and rigid, and two α -carbons can be located in *trans* and *cis* positions. In Pro residue, the peptide bond-forming nitrogen and α -carbon are entrapped in a five-membered rigid ring. Unlike other amino acids, Pro may exist in *cis* and *trans* conformations under denaturing conditions with slow isomerization kinetics.¹⁴¹ The conformers often have distinct retentivity under typical RPLC conditions, leading to peak broadening. In an extreme case, when peptides contain a Pro–Pro bond endowed by extremely slow isomerization kinetics, the conformers can be separated from each other.¹⁴² Accelerating the isomerization kinetics via raising temperature tackles this issue. Bottom-up LC-MS analyses of samples expected to contain a considerable amount of Pro-rich proteins, such as saliva,¹⁴³ should be carried out using a column kept at a temperature of 60 °C and higher to achieve a superior separation of resulting tryptic peptides.¹⁰⁷

Chemical Inertness of Peptides. The chemical reactivity of amino acid residues and stability of peptide bonds during LC-MS analyses is vastly disregarded. The predicted pH of the typical mobile phase acidified using 0.1% formic acid is 2.68, and in combination with elevated column temperature exploited for a more efficient peptide separation, it may damage peptides. This is particularly important for single-shot analyses that rely on long gradients, sometimes even several hours long. Upon such conditions, the column is easily transformed into a chemical reactor, resulting in artifacts such as Glu and Gln converted to pyroglutamic acid, dehydration of Asp, and peptide bond cleavage at Asp.¹⁰⁷ An additional source of unwanted in-column reaction is associated with metal traces that induce oxidation, with the most common target being Met residue.¹⁴⁴ Such in-column oxidation can be sorted out by remedies that remove metal traces already discussed in the section above. Even though the artificial modifications can be identified using unbiased search strategies,^{145,146} their presence indirectly decreases the number of identified peptides and proteins with biologically and clinically relevant information. This is because a significant amount of the instrument time is

wasted on MS2 scans of artificially modified peptides with the same amino acid sequences covered by MS2 scans of their unmodified parent peptides.

BAND AND PEAK BROADENING

If the column and the chromatographic system performed ideally, the rear and front boundaries of the eluted peaks would overlap, and practitioners would observe signals with an infinite intensity instead of peaks with Gaussian-like profiles.^{147,148} In practice, the chromatographic bands inevitably broaden on their way through the column, giving the column a finite efficiency. Moreover, the detected peaks do not reflect the intrinsic separation performance of the column because the chromatographic bands also broaden on their way toward the column and downstream from the column to a mass spectrometer (or other types of detector), where they are transformed into peak profiles. Hence, the observed separation quality expressed as peak variance (σ_{obs}^2) is a result of the intrinsic performance of the column; in other words, in-column band dispersion (σ_{col}^2), and the inevitable dispersion due to the extra-column contributors (σ_{ec}^2). These two contributors have the same importance for obtaining narrow peaks and, thus, highly efficient chromatographic separation (eqs 25 and 26).

$$\sigma_{obs}^2 = \sigma_{col}^2 + \sigma_{ec}^2 \quad (25)$$

$$w_h = 2.355 \cdot \sigma_{obs} = \frac{\sqrt{\sigma_{col}^2 + \sigma_{ec}^2}}{2.355} \quad (26)$$

In-Column Band Dispersion

The chromatographic column itself significantly contributes to the peak width. The in-column band broadening is primarily attributed to three independent contributors: (i) broadening due to unequal flow paths, (ii) longitudinal broadening due to molecular diffusion, and (iii) broadening due to resistance to mass transfer between mobile and stationary phases. Their total effect on the column efficiency expressed in the theoretical plate height H was mathematically derived by van Deemter,⁶⁹ who, for the first time, assigned a physicochemical background to the plate theory developed earlier by Martin and Synge (eq 27).⁶⁸

$$N = \frac{L}{H} = \frac{L}{A + \frac{B}{u} + C_u} \quad (27)$$

The van Deemter equation describes the theoretical plate height as the sum of three independent contributors to the band dispersion with different dependencies on the flow velocity of the mobile phase u ($u = L/t_0$). If the plot is constructed to find an optimum for a particular column, the linear flow velocity can be replaced by the flow rate. The van Deemter model is not flawless,¹⁴⁹ and later more complex models were derived by Giddings,¹⁵⁰ Horváth,¹⁵¹ and Knox.¹⁵² Nevertheless, the original van Deemter equation fits the experimental data very accurately¹⁵³ and will serve competently for this tutorial.

The dependence of the theoretical plate height on those three terms has a typical curvilinear relationship. Its notoriously known graphical expression is called the van Deemter curve. It should be noted that the van Deemter curve is easily constructed for analytes reasonably eluting under isocratic conditions. This is not very practical for the analysis

of peptides and, in particular, proteins. A viable alternative for finding an optimal flow rate with the minimal in-column band broadening during a gradient elution of peptides is the use of the pseudo van Deemter plot introduced by Gilar and Neue.¹⁵⁴ The plot is constructed from the squared peak volume V_p^2 ($V_p = F \cdot w_b$) versus mobile phase flow rate. The total gradient volume V_G ($V_G = F \cdot t_G$) must be kept constant across different flow rates used for the pseudo van Deemter plot to preserve the same gradient steepness b (see the section Gradient Elution).¹⁵⁵ Then, the curve in the pseudo van Deemter plot is similar to the curve in the van Deemter plot obtained for the same analyte using isocratic elution (Figure 13).

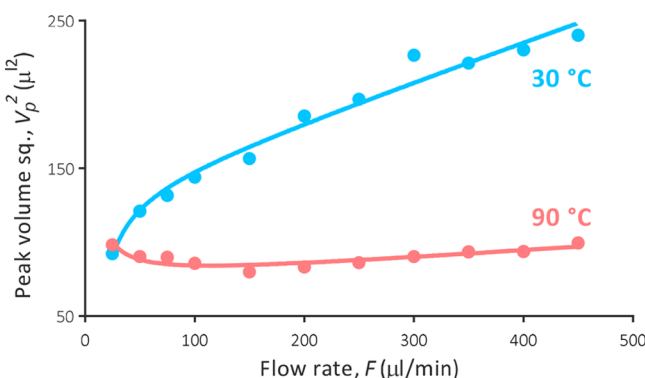


Figure 13. Pseudo van Deemter plot constructed using five standard peptides at 30 and 90 °C separated in a 2.1 × 150 mm Acuity UPLC column packed with 1.7 μm CSH C₁₈, 130 Å fully porous particles (Waters). The plot was constructed using squared peak volumes (V_p^2) against varying flow rates (F) as proposed by Gilar and Neue.¹⁵⁴ The contribution of the longitudinal dispersion becomes apparent at 90 °C at very low flow rates. The plot earlier published by Lenčo et al.¹⁰⁷ in *Journal of Proteome Research* was adapted for the figure.

The B Term: Longitudinal Broadening due to Molecular Diffusion. The longitudinal broadening due to molecular diffusion is the least important type of broadening in bottom-up proteomic analyses. It is dictated by the analyte diffusion inside and outside the particles and their time on the way along the column. The shorter the time it takes to pass the column, the shorter the time the analyte has to diffuse axially.¹⁵⁶ Peptides diffuse much more slowly than small molecules do. Besides, all peptides need roughly the same time to pass the column length in the gradient elution because they are refocused at the head of the column upon injection, where they wait for a critical concentration of stronger solvent that initiates their elution. Lastly, the gradient peak-compression factor G contributes to efficiently mitigating longitudinal broadening. Thus, peptides eluting at later retention times do not suffer from longitudinal broadening typical for later eluting analytes in isocratic elution. As a result, the longitudinal broadening in proteomic analyses may become noticeable only under very impractical conditions, i.e., when a shallow gradient at extremely low flow rates is applied, and simultaneously, the peptide diffusion rate is dramatically enhanced by elevating the column temperature (see the left part of the pseudo van Deemter curve obtained at 90 °C in Figure 13).

The A Term: Eddy Dispersion due to Flow Path Inequalities. The A term combines broadening due to various types of flow inhomogeneities in the interstitial volume of the column. This broadening is more complex than van Deemter presumed initially, and experimentally, some of the effects

contributing to the A term are absorbed by the C term in the van Deemter curve that is flow rate-dependent.¹⁵⁷ Giddings, who linked the A-term to mass transport in the mobile phase, defined two main categories of dispersion due to flow inhomogeneities, namely short-range and long-range dispersion.¹⁵⁸ The short-range eddy dispersion results from inequalities in the mobile phase velocity due to the random nature of the local bed packing and faster local flow in the center of the channels formed by the adjacent particles than is the flow at the surface of particles.

The long-range dispersion is caused by differences in the mobile phase velocity between more distant sites in the column, again due to the random nature of the packed bed. Moreover, the particles are not packed uniformly across the column cross-section, and the existence of three coaxial zones with distinct mobile phase velocities can be distinguished.^{70,158–160} The central bulk zone is packed randomly. This zone is surrounded by an intermediate region of densely packed particles with an average velocity of 5% slower than the bulk velocity. A very thin zone of around $1.5d_p$ at the very wall of the column is loose, and the mobile phase velocity here is about 50% faster than in the bulk zone. These three zones can occupy various relative portions of the column volume, depending on the column diameter (d_c) and particle diameter that determine the aspect ratio (d_c/d_p). In case the zones with different mobile phase velocities occupy comparable portions, such as in columns with an inner diameter between 0.5 and 1.0 mm packed with modern small-size particles, the column efficiency is significantly reduced by so-called trans-column eddy dispersion because of the radial flow heterogeneity.¹⁶⁰

Typical nanoflow columns with an inner diameter of 75 μm were predicted to exhibit a very low trans-column eddy dispersion.¹⁶⁰ The bed should be formed dominantly with the intermediate zone of densely packed particles, and the negative effect of faster velocity at the wall should be reduced by the fast radial dispersion of analytes. Theoretical models also presumed columns with an inner diameter of 20 and 30 μm to suffer more from trans-column eddy dispersion than nanoflow columns with an inner diameter of 75 μm. Astonishingly, experiments demonstrated that these columns could provide even better separation than those of 75 μm inner diameter because of the presence of fewer voids at the column wall-particulate bed interface.¹⁶¹ On the other hand, extremely efficient packing of nanoflow columns with a diameter of 75 μm can yield a reduced theoretical plate height h of 1.05.¹⁶²

The columns are equipped with porous frits to allow packing them and hold the particle bed in its position. Frits inherently operate as mixers. The inlet frit does not represent an obstacle in achieving high efficiency in gradient peptide separation, but the outlet frit contributes to the extra-bed in-column broadening, particularly in short columns.^{163,164} The contribution of frits to band broadening should be, by nature, absorbed by the A term; however, it was proven to be flow rate dependent.^{163,165} The performance of frits that can be assembled to nanoflow columns remains to be thoroughly evaluated for peptide separation.^{166,167} In this regard, a not fully recognized merit of nonparticulate columns is that they do not need frits.

The A term is likely the main reason why narrow-diameter regular columns used in bottom-up proteomic analyses usually do not reach the separation performance of conventional-flow columns packed with identical particles. The A term can be reduced by more effective packing procedures^{162,168–171} or,

analogously, by casting monoliths with a more homogeneous size of both polymer globules and flow-through macropores.^{172,173} Narrower particle size distribution has also been linked to smaller A term in columns packed by superficially porous particles.¹⁷⁴ Nevertheless, it is questionable whether this effect can be attributed to a narrow particle size distribution per se.^{175–177} The outlet frit structure and length should be optimized to minimize its mixing effect. A pulled capillary end can take over the role of the outlet frit in particulate nanoflow columns packed in fused silica tubing.¹⁷⁸ However, such a conical column ending can increase the mobile phase velocity-dependent resistance to mass transfer. For instance, if the velocity in a 75 μm segment of the pulled-capillary column is 1 mm/s, it increases to a value of 56.25 mm/s in its 10 μm opening.

The A-term is the major contributor to the in-column band broadening near the optimum flow rate.¹⁵⁷ This fact inspired chromatographers to develop columns with strictly oriented chromatographic beds embodied by superficially porous micropillars (see the section **Micropillar Array Columns**).^{179–183} Such micropillar array columns are equipped with ordered flow distributors instead of frits, also eliminating their mixing effect from the total in-column band dispersion.^{184,185}

The C Term: Resistance to Mass Transfer. To reach the chromatographic surface to interact with, peptides must first diffuse from the interstitial mobile phase stream close to the stationary phase support. Then, they diffuse through a thin film of the stagnant layer of the mobile phase surrounding the stationary phase support. In the case of porous chromatographic media, peptides further diffuse through the pores filled with the stagnant mobile phase and along the pore surface.¹⁸⁶ The concentration gradient enables peptides to leave the pores by diffusion-driven transfer and return to the interstitial mobile phase stream.

The slower the molecular diffusion, the greater the delay in migration through the column between the subset of peptides entering the stationary phase and the subset of the same peptides carried by the mobile phase stream forward along the column, inevitably resulting in band dispersion. As already mentioned, the diffusion of peptides is much slower than the diffusion of small molecules. The issue is further aggravated by the fact that the diffusion in pores is dramatically slower than in the bulk solvent due to steric hindrance and tortuous pathways.^{187,188} As a result, despite the positive impact of the surface diffusion,¹⁸⁶ the overall diffusion inside porous chromatographic media is significantly slower than diffusion in the bulk solvent.^{121–123}

The processes described in the previous paragraph only transfer the peptides to the active chromatographic surface. The chromatographic interaction itself is realized by numerous adsorption–desorption steps to and from the chromatographic surface, i.e., ligands bonded to the stationary phase support (the term adsorption does not suggest the possible retention mechanism but is used here in its physical sense). Their number is governed by the rate constant of adsorption (k_{ads}). If the adsorption–desorption processes are virtually instantaneous or k_{ads} is larger than 10^4 s^{-1} at least, there is no noticeable impact of adsorption–desorption kinetics on the band broadening.¹⁸⁹ While this is the case for RPLC of small molecules,¹⁹⁰ the adsorption–desorption kinetics of peptides and proteins is slower because k_{ads} is inversely proportional to molecular weight,^{149,191} contributing to the band broadening

and peak shape skewing. To illustrate, Gritti et al.¹²² calculated the rate constant of adsorption of human insulin in the C_{18} phase in the presence of 0.1% TFA to be 80 s^{-1} at 50 °C.

At flow rates and column temperatures commonly employed in bottom-up proteomics, the resistance to mass transfer represents the major obstacle to achieving maximum column separation performance in bottom-up LC-MS analyses. The band broadening due to diffusion from the mobile phase stream to the stationary phase support (C_m) and due to diffusion in the stagnant mobile phase entrapped in the pores of stationary phase support (C_s) depends on the diffusion distance.¹⁹² Therefore, C_m can be minimized by reducing the dimensions of the flow-through channels formed by globules of monolithic stationary phase¹⁷⁸ or adjacent particles in a packed bed column. In an ideally packed column, the latter can be accomplished by reducing the particle size.¹⁹² Obviously, smaller particles concurrently reduce C_s by shortening the average length of the diffusion path. The superficially porous particles have the same impact because peptides diffuse only in a thin surface layer. Alternatively, polymer monolithic columns formed by globules virtually with no pores accessible for diffusion can be used for rapid, efficient separation of slowly diffusing analytes.

Both the molecular diffusion and the rate constant of adsorption are temperature-dependent.^{122,125,191} Hence, elevating the column temperature reduces the band broadening due to the resistance to mass transfer in bottom-up LC-MS analyses. Indeed, peptide separations cannot provide optimum results when carried out close to ambient temperature (Figure 13).¹⁰⁷ For the efficient separation of proteins, the use of high column temperature is absolutely essential (see the section **Column Temperature**).^{193,194}

Other Sources of In-Column Band Broadening. Additional factors contributing to in-column band broadening include broadening due to frictional heating^{195,196} and broadening due to mobile phase temperature mismatch.^{197,198} However, under the conditions typically applied for the separation of peptides, i.e., slow mobile phase velocities and small column inner diameters allowing a fast exchange of heat between the column and environment, these contributions to band broadening are usually irrelevant in bottom-up proteomic analyses.

Extra-Column Dispersion and Remaining Column Efficiency

Even the best-performing separation column cannot provide superior peaks without minimizing volumetric and time-related dispersion in the chromatographic system and MS detector.^{199–201} The loss in the separation efficiency caused by the extra-column contributors determines the remaining column efficiency (E_r), which depends on the in-column dispersion σ_{col}^2 and the extra-column dispersion σ_{ec}^2 (eq 28).

$$E_r = 100 \cdot \frac{\sigma_{col}^2}{\sigma_{col}^2 + \sigma_{ec}^2} \quad (28)$$

The column band dispersion σ_{col}^2 (eq 29) can be calculated from the gradient retention factor at the elution k_e (eq 8), the column void volume V_0 (eq 11), and the gradient theoretical plate number N^* (eq 19).

$$\sigma_{col}^2 = \frac{V_0^2}{N^*} \cdot (1 + k_e)^2 \quad (29)$$

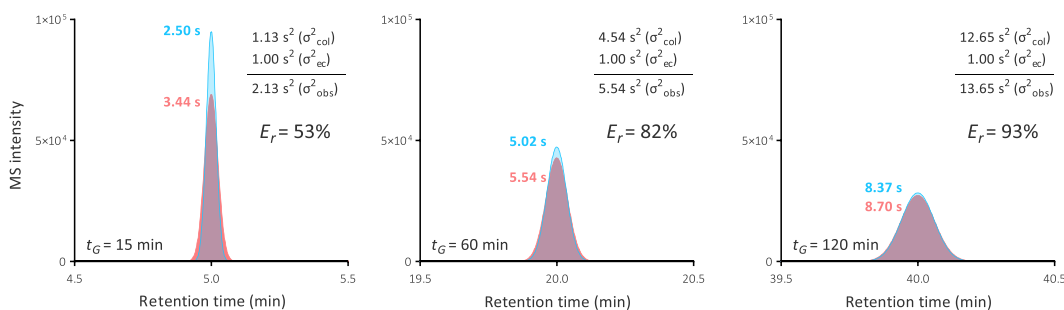


Figure 14. Effect of extra-column band dispersion σ_{ec}^2 on observed peak variance σ_{obs}^2 and remaining column efficiency E_r in peptide LC-MS analyses carried out using various gradient times. Peak width w_h without the impact of extra-column dispersion were calculated from the peak capacity n_c that was predicted using eq 22. The following parameters were used: $L = 250$ mm, $d_c = 75$ μm , $N = 42\,500$, $e_T = 0.55$, $F = 250$ nL/min, $\Delta\Phi = 0.35$, and $S = 35$. Gradient time t_G was 15 min (chromatogram on the left), 60 min (middle chromatogram), and 120 min (chromatogram on the right). The time extra-column dispersion σ_{ec}^2 was selected to be 1 s^2 . Blue peaks indicate the intrinsic gradient separation performance of the column. Red peaks are broadened due to an extra-column dispersion of 1 s^2 downstream of the column. The values of w_h in seconds are shown above each peak. The peak area was kept constant across all peaks so that the peak heights reflect w_h .

Because the extra-column dispersion σ_{ec}^2 is given by the instrument configuration and can be readily minimized, we describe this phenomenon in more detail in the following section. The parts of the chromatographic system that generally contribute to the extra-column dispersion include the injector (σ_{inj}^2), precolumn tubing ($\sigma_{\text{tubing,pre-col}}^2$), postcolumn tubing ($\sigma_{\text{tubing,post-col}}^2$), volumetric and time-related peak dispersion in a detector (σ_{det}^2), and nonquantifiable influences that are *a priori* unknown (σ_{other}^2), such as the quality of connections and flow paths in valve channels. To a first approximation, the contribution of all sources to the total extra-column dispersion is independent of each other and, therefore, additive (eq 30).

$$\sigma_{\text{ec}}^2 = \sigma_{\text{inj}}^2 + \sigma_{\text{tubing,pre-col}}^2 + \sigma_{\text{tubing,post-col}}^2 + \sigma_{\text{det}}^2 + \sigma_{\text{other}}^2 \quad (30)$$

Providing that peptides arrive into a column at a weaker mobile phase than is required to initiate their elution and their retention factor is high, they are virtually trapped at the head of the column because of their large S parameter. As a result, the parts upstream of the analytical column have only a negligible impact on the total extra-column dispersion σ_{ec}^2 in proteomic analyses relying on direct injection of peptides in the column.^{67,202} The total extra-column dispersion in the gradient elution of peptides is then reduced to parts downstream of the column (eq 31).

$$\sigma_{\text{ec}}^2 = \sigma_{\text{tubing,post-col}}^2 + \sigma_{\text{det}}^2 + \sigma_{\text{other}}^2 \quad (31)$$

Volumes of chromatographic bands eluting from a typical nanoflow column with an inner diameter of 75 μm occupy only a few tens of nanoliters, making them extremely sensitive to dispersion even due to minor extra-column volumes. This is one of several reasons why it is a real challenge to obtain nanoLC chromatograms truly reflecting the progress in column technology. The issue will be exacerbated by further reducing the inner diameter of columns for ultrasensitive bottom-up LC-MS analyses.

At a constant flow rate, the extra-column band dispersion downstream of the column is, to a first approximation, independent of the gradient time and thereby constant. Therefore, its effect on the observed peaks and remaining column efficiency E_r is more pronounced in steep gradients where sharp chromatographic peaks are expected to be observed. The remaining column efficiency E_r is higher in longer gradients because the bands eluting from the column

are inherently broader (see the section [Gradient Elution](#)), and the additive effect of the extra-column dispersion is thus less pronounced (Figure 14).

Band Dispersion in the Tubing. The major source of extra-column band broadening in proteomic analyses is likely the dispersion in the outlet tubing. The band dispersion due to the laminar flow in capillaries (σ_{tubing}^2) can be estimated by a transition equation derived from the Taylor–Aris and Attwood–Golay eqs (eq 32).²⁰³

$$\sigma_{\text{tubing}}^2 = \frac{\pi^2 \cdot r^4 \cdot L^2}{3 + \left(24 \cdot \pi \cdot L \cdot \frac{D_m}{F} \right)} \quad (32)$$

As can be seen from the equation, larger molecules are more susceptible to dispersion in tubing because of their low diffusion coefficient D_m . The equation also implies that the major influence on the dispersion in tubing possesses the inner radius (r , fourth power dependency, Figure 15), whereas the impact of its length is dramatically weaker (second power dependency). Therefore, a capillary with a smaller diameter should be preferred, even if it is longer than a capillary with a wider inner diameter. The negative effect of using thinner tubing is the higher backpressure that is governed by the Poiseuille law (eq 33).

$$P = \frac{L \cdot 8\eta \cdot F}{\pi \cdot r^4} \quad (33)$$

As a result, to preserve the maximum separation performance for proteomic LC-MS analyses with moderate backpressure, the column shall be placed as close to the MS instrument as possible, and the capillary connecting the column to the ion source shall be as short as possible.

The dispersion in the tubing is because of the laminar flow of the mobile phase. It is almost a forgotten wisdom that when the perfect laminar flow is disrupted by secondary flow effects or replaced by a turbulent flow, the longitudinal band dispersion in the tubing decreases. It may sound like a joke, but knotting and twisting an outlet capillary made from a flexible material can improve the total separation performance of a chromatographic system without increasing the backpressure and additional financial costs (Figure 16).^{204–207}

The data in Figure 15 show that the maximum separation efficiency is preserved when the ratio between the squared inner diameter of the 2.1 mm column and the squared inner

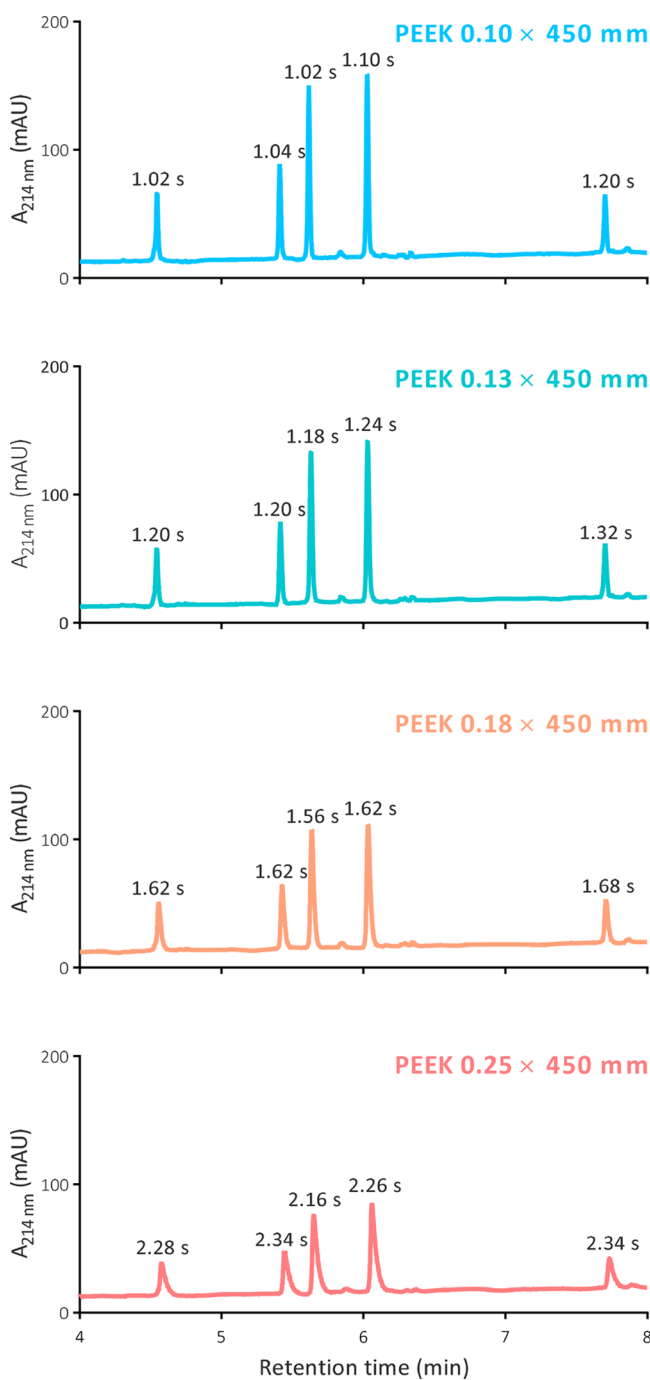


Figure 15. Effect of the inner diameter of an outlet capillary on the apparent separation performance of an LC-UV system. Five standard peptides were separated using a gradient from 2 to 40% acetonitrile with 0.1% TFA in a 2.1 × 150 mm bioZen Peptide column packed with 1.7 μm XB-C₁₈, 100 Å superficially porous particles (Phenomenex). The column temperature was 60 °C, and the flow rate was 400 μL/min. The column was connected using hand-cut PEEK capillaries with a length of 450 mm to a UV detector. The absorbance was monitored at 214 nm. The values of w_h in seconds are shown above each peak. Averaged values from three consecutive injections are presented.

diameter of the 0.10 mm capillary was 441. If we extrapolate this ratio to a nanoflow column with an inner diameter of 75 μm, the outlet capillary should have an inner diameter of 3.6 μm for maximum remaining column efficiency. This dimension

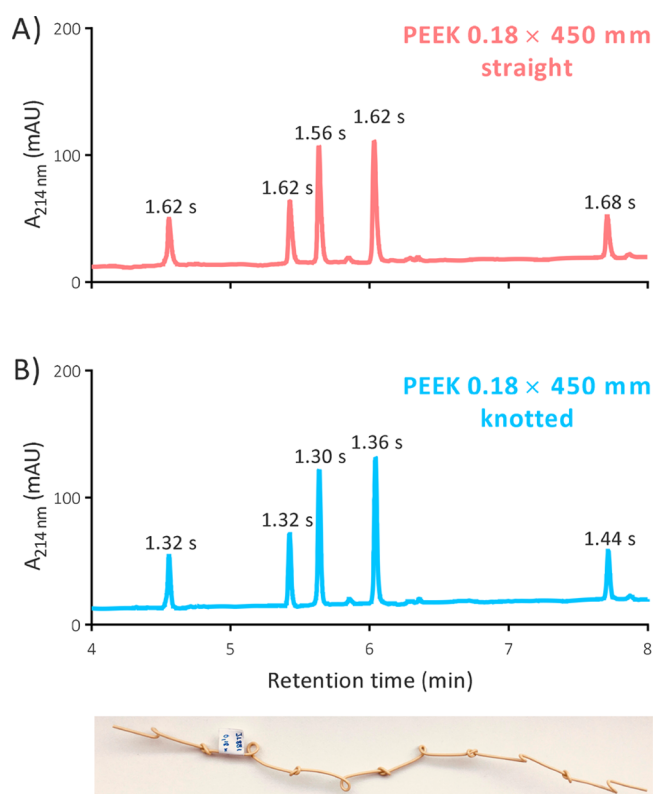


Figure 16. Band broadening in a PEEK capillary (A) before and (B) after twisting and knotting (see the figure below the chromatograms) on the apparent separation performance of an LC-UV system. For further details, see the legend in Figure 15. The values of w_h in seconds are shown above each peak. Averaged values from three consecutive injections are presented.

is too far from the capillary inner diameter of 20 μm typically used in nanoLC connections. The spray needles and emitters essentially behave as capillaries with all the consequences for band dispersion due to the laminar flow. Therefore, their diameter must be selected proportionally to the inner diameter of the column too.^{67,208}

The major contributors to the nonquantifiable influences are capillary connections because of void volumes and changes in the inner diameter of flow channels. This requires that the number of connections downstream of the analytical column is kept at a minimum. If a connection is necessary, capillaries with integrated fittings should be preferred as these produce the lowest band dispersion (Figure 17).²⁰⁹ Numerous high-quality products are currently available, such as Viper and nanoViper capillaries (Thermo Fisher Scientific), Security-LINK capillaries (Phenomenex), ZenFit capillaries (Waters), and MarvelXACT capillaries (IDEX). Optionally, PEEKTite Ti-Lok EXP UHPLC fittings (SGE/Trajan Scientific) for precisely cut and polished PEEKsil capillaries can be used. These products provide fingertight, reusable tubing connections that can withstand maximum pressures even above 1000 bar. Capillaries of different materials and in various dimensions are available. Of course, the ease of their use is balanced by their price. A more economical solution represents self-made connections with reusable fittings and fused silica capillaries that can be cut according to the current needs. However, even the best-performing capillary cutter cannot provide a clean and smooth cut surface. To prepare true zero-dead volume connections for nanoLC, the cuts must be

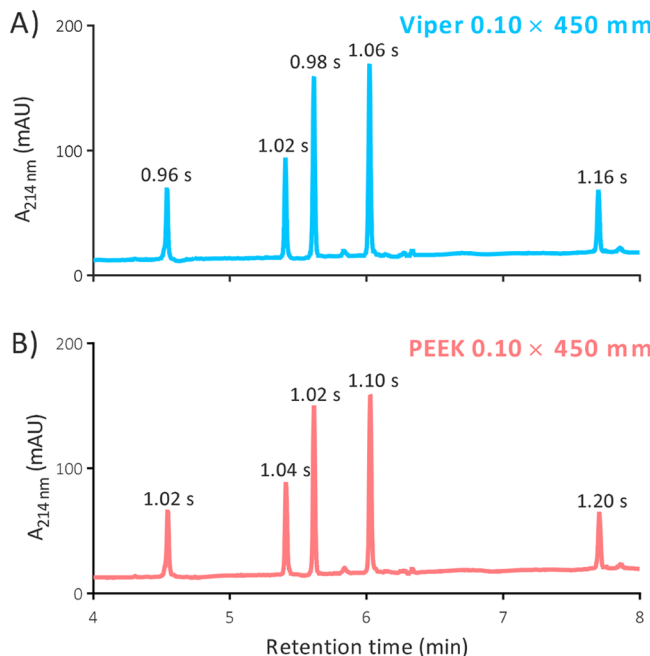


Figure 17. Comparison of band broadening in a commercial capillary with integrated fittings (A) and in a cut PEEK capillary with reusable fittings (B). For further details, see the legend in Figure 15. The values of w_h in seconds are shown above each peak. Averaged values from three consecutive injections are presented.

smoothed and polished using a dedicated device, such as Capillary Polishing Station (ESI Source Solutions) or Fused Silica Tube End Prep Kit (VICI Jour).

The knowledge summarized above suggests that the most straightforward approach for preserving maximum separation efficiency in proteomic nanoLC-MS analyses is the use of packed spray emitters or nanoflow columns seamlessly integrated with short and thin emitters. Such accessories include, but are not limited to, Aurora Series emitter columns (Ion Opticks), PicoFrit nanospray columns (New Objective), Pulled tip columns (ESI Source Solutions), EASY-Spray LC columns (Thermo Fisher Scientific), and MonoSpray (GL Sciences). The extra-column broadening theory predicts that similar products will be vital for achieving reasonable separation efficiency using columns with an inner diameter <75 μm dedicated to ultrasensitive applications such as single-cell proteomic analyses.

Band Dispersion in Trap-Elute Setups. NanoLC systems usually operate in a trap-elute setup to shorten the time needed for delivering the sample from the autosampler to the column. The sample is injected at a higher flow rate onto a trap column installed between two ports of a switching valve.²¹⁰ To decrease the pressure resistance, the trap columns are short, usually have a larger inner diameter, or are packed with larger particles. After delivering the sample, the switching valve creates a flow path interconnecting the pump delivering the gradient, the trap column, and the separation column (Figure 18). In an economical version that does not require an additional pump, the trap-elute configuration is often realized as a vented column (Figure 19).²¹¹

The mobile phase is diverted to waste during sample injection in a trap-elute setup. Hence an additional advantage of this configuration is that it enables an online solid-phase extraction for sample cleanup.²¹² If the trap-elute setup is not

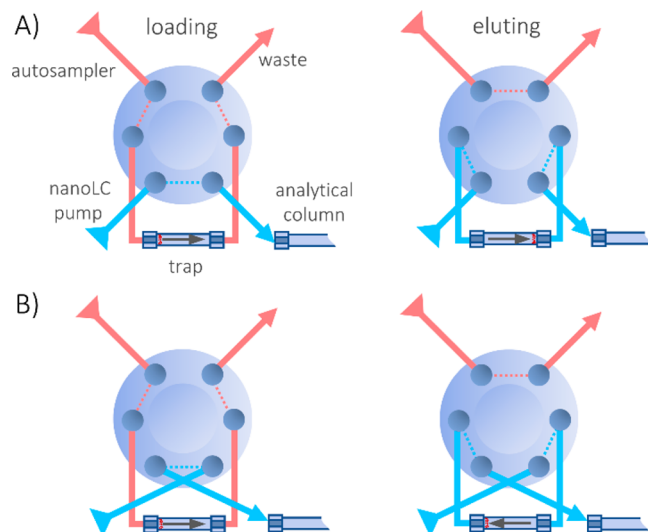


Figure 18. Two configurations of the trap-elute setup with the column switching. In the front-flush configuration (A), peptides pass the whole trap column length during elution. In the back-flush configuration (B), peptides pass only the distance of the trap column that they occupy upon injection.

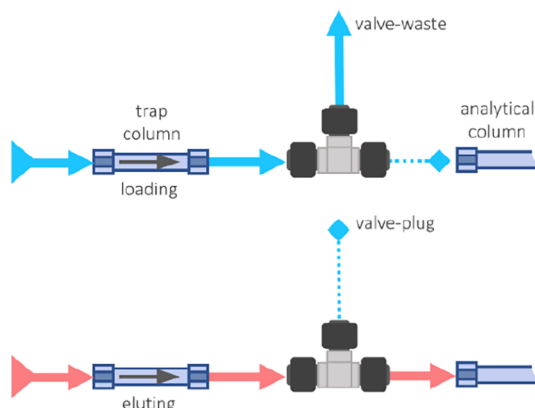


Figure 19. Trap-elute setup realized via a vented column. Peptides can be eluted from the trap column only in the same direction as they were loaded.

ideally optimized, peptides may arrive in the separation column at a mobile phase strength that does not allow them to refocus at the head of the column well. Under such conditions, all components between the peptide band focused on the trap column and the MS inlet, including the dispersion in the rest of the trap column (σ_{trap}^2) and downstream capillary ($\sigma_{tubing,post-trap}^2$), contribute to the total extra-column band broadening (eq 34).

$$\sigma_{ec}^2 = \sigma_{trap}^2 + \sigma_{tubing,post-trap}^2 + \sigma_{tubing,pre-col}^2 + \sigma_{tubing,post-col}^2 + \sigma_{det}^2 + \sigma_{other}^2 \quad (34)$$

This dispersion ultimately results in peak shapes that do not reflect the intrinsic efficiency of the separation column (Figure 20).^{212–215} The trap column must have lower retentivity than the analytical column to minimize broadening upstream of the separation column in the trap-elute setup. This allows the peptides to leave the trap column at mobile phase strength that still permits their refocusing on the head of the more retentive separation column. A less retentive stationary phase for the

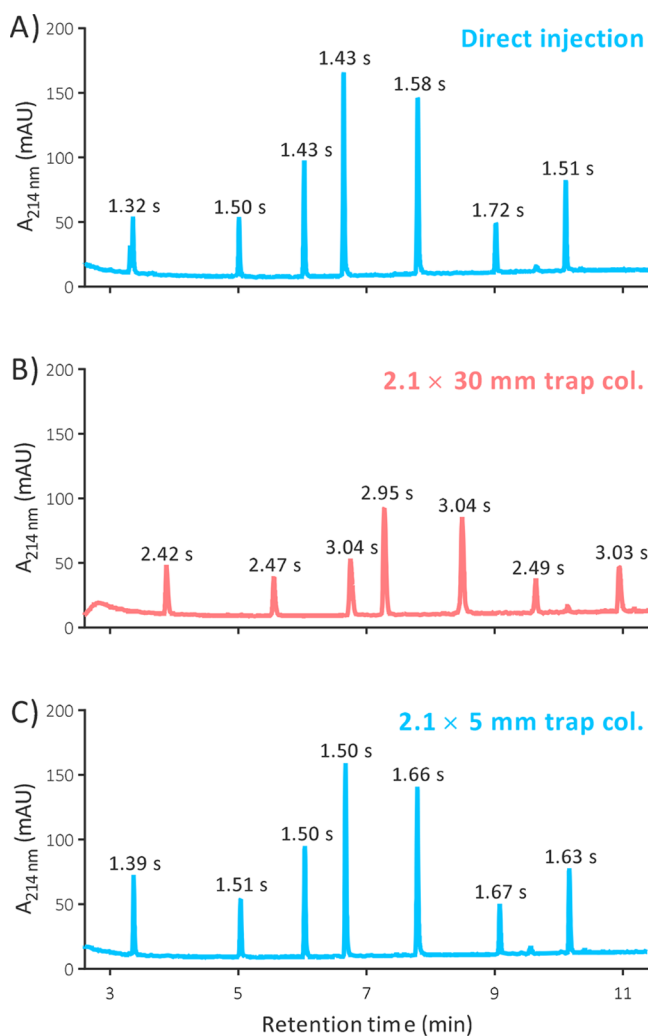


Figure 20. Importance of adjusting retentivity and dimensions of a trap column for minimizing band broadening in a trap-elute setup. Seven standard peptides were separated using a 10 min linear gradient from 1 to 31% acetonitrile with 0.05% formic acid in a 2.1 × 150 mm Acuity UPLC CSH C₁₈ 1.7 μm, 130 Å column (Waters). The peptide mixture was injected directly in the separation column (A), or in a 2.1 × 30 mm trap column with a 2-fold lower retentivity than the separation column (B), or in a 2.1 × 5 mm trap column with 8-fold lower retentivity than the separation column (C). The setup simulated a vented column configuration. The separation column temperature was 70 °C, and the trap columns were maintained at temperatures that afforded them the desired retentivity. The flow rate was 300 μL/min. The absorbance was monitored at 214 nm. The retentivity of columns was estimated based on isocratic retention factors of three small neutral compounds. The values of w_h in seconds are shown above each peak. Averaged values from three consecutive injections are presented.

trap column can lead to losing most hydrophilic peptides upon injection. Replacing formic acid in the loading mobile phase with an acid providing more hydrophobic anion, such as TFA, can mitigate the issue.²¹³

The theory of gradient elution predicts that the longer the column distance the peptides pass, the lower their retention factor at elution (Figure 5). This means that a larger portion of peptides tends to be in the mobile phase relative to the stationary phase. Such distribution of the peptides prevents them from efficiently refocusing at the head of the separation column after eluting from a lengthy trap column, and

subsequently, band broadening downstream worsens the peak shape of peptides. To shorten the distance the peptides travel in the trap column and thereby increase their retention factor at elution, the loading in and elution from the trap column shall be carried out in a reversed direction whenever possible. This can be readily realized by interchanging two connections on the switching valve accommodating the trap column (Figure 18). Such a minor modification dramatically reduces the distance in a trap column that the peptides travel along during their elution and hence, increases the retention factor at elution. This remedy cannot be realized in the vented column setup. Here, a partial increase in the retention factor at elution can be accomplished by decreasing the physical length of the trap column and/or decreasing its inner diameter.

Even an optimized trap-elute system cannot provide 100% separation performance compared to direct injection. Nevertheless, in the direct injection setup, the most hydrophilic peptides also migrate along a significant fraction of the column length under isocratic conditions due to the gradient delay volume. They then do not profit from the gradient compression. Depending on the extra-column band dispersion upstream of the column, those not retained hydrophilic peptides can elute as broader peaks than the peaks at later retention times. The gradient delay volume should be minimized, or the mobile phase delivering peptides should be weak enough to allow even the least hydrophobic peptides to refocus at the head of the separation column to let these peptides benefit from the separation power of highly efficient columns.²¹⁶ The gain in the chromatographic separation of the most hydrophilic peptides will then be outbalanced by a longer analysis time. Alternatively, a delayed injection can be applied if the instrument has this capability.

Peak Dispersion in UV Detector and Mass Spectrometer. A UV detector is much more robust than MS detection and provides reproducible monitoring of gradient elution. Hence, some practitioners have recommended UV detection for quality control in proteomics.^{214,217} However, connecting the UV detector between a nanoflow column and a mass spectrometer in real-life proteomic analyses is questionable. The volumetric contribution of the detector cell to the total band broadening depends on the volume of the detector cell (V_{cell}) and a constant characteristic of the UV cell geometry (k_{cell}) (eq 35).

$$\sigma_{det}^2 = \frac{V_{cell}^2}{k_{cell}} \quad (35)$$

The value k_{cell} was previously reported to lie between 1 and 12,²⁰⁰ but for modern analytical ultrahigh performance liquid chromatography (UHPLC) systems with small volume cells, values around 1 are more realistic.²¹⁸ The capillaries connecting the UV detector increase significantly the total length that a band eluting from a column has to pass to reach the mass spectrometer. This extra volume and the potential void volume in the associated extra connections further contribute to the total band broadening registered in the resulting LC-MS chromatogram (eq 31).

The mass spectrometers alone can contribute to the volumetric band broadening, but their impact is not as important as the broadening upstream.²¹⁹ If the acquisition rate is at least 10 data points across a peak, the time-dependent contribution to the peak width in the resulting chromatograms can also be neglected.^{203,220} However, this means that the

Table 2. Typical Setting of Chromatographic Parameters in Recent Bottom-Up LC-MS Proteomic Analyses^a

Injection configuration	Trap-elute setup	Direct injection						
2020 (n=261)	52.9%	47.1%						
2022 (n=203)	54.2%	45.8%						
Loading solvent strength	0% AcN	1% AcN	2% AcN	3% AcN	4% and 5% AcN	5% MeOH	2% DMSO	
2020 (n=57)	49.1%	7.0%	35.1%	3.5%	3.5%	1.8%	0.0%	
2022 (n=50)	48.0%	10.0%	20.0%	6.0%	13.7%	0.0%	2.0%	
Loading solvent acidifier	Formic ac.	TFA	HFBA					
2020 (n=57)	64.9%	31.6%	3.5%					
2022 (n=50)	90.0%	10.0%	0.0%					
Separation column origin	Commercial	Prepared in-house						
2020 (n=240)	68.8%	31.2%						
2022 (n=195)	68.7%	31.3%						
Separation column type	Particulate	Monolithic	μPAC					
2020 (n=242)	98.4%	0.8%	0.8%					
2022 (n=202)	98.0%	0.0%	2.0%					
Particle type	Totally porous	Superficially porous						
2020 (n=238)	96.3%	3.7%						
2022 (n=188)	96.3%	3.7%						
Stationary phase brand	Acclaim PepMap	ReproSil	BEH	Magic	ChromXP	HSS T3	Others	
2020 (n=207)	45.9%	24.2%	8.7%	2.4%	1.0%	1.4%	< 2.0%	
2022 (n=175)	46.9%	21.1%	8.6%	2.3%	4.6%	4.0%	< 1.8%	
Particle diameter	1.7 and 1.8 μm	1.9 and 2.0 μm	2.7 μm	3.0 μm	5.0 μm	Others		
2020 (n=179)	15.6%	46.4%	2.8%	24.6%	6.1%	< 1.1%		
2022 (n=166)	13.9%	39.2%	3.0%	31.9%	5.4%	< 1.8%		
Pore size	80 Å	100 Å	120 and 130 Å	200 Å	300 Å	Others		
2020 (n=170)	2.4%	61.8%	27.1%	1.2%	5.3%	< 0.6%		
2022 (n=171)	0.0%	55.6%	37.4%	2.9%	0.6%	< 1.2%		
Bonded ligand/chemistry	C ₁₈	C ₈						
2020 (n=224)	99.1%	0.9%						
2022 (n=200)	100.0%	0.0%						
Column format	Nanoflow	Capillary	Microbore	Narrow-bore				
2020 (n=224)	90.2%	4.5%	3.1%	2.2%				
2022 (n=198)	92.9%	4.0%	1.0%	2.0%				
Nanoflow- and capillary column inner diameter	50 μm	75 μm	100 μm	150 μm	300 μm	Others		
2020 (n=212)	0.9%	86.3%	7.1%	4.2%	0.5%	< 0.5%		
2022 (n=192)	4.2%	84.4%	6.8%	1.0%	2.6%	< 0.6%		

Table 2. continued

Commercial columns length	5 cm	10 cm	15 cm	20 cm	25 cm	50 cm	Others
2020 (n=149)	0.0%	10.1%	25.5%	2.0%	20.8%	37.6%	< 1.4%
2022 (n=129)	2.3%	7.0%	18.6%	3.1%	26.4%	38.8%	< 1.6%
Self-packed columns length	≥ 5 to ≤ 10 cm	> 10 to ≤ 15 cm	> 15 to ≤ 25 cm	> 25 to ≤ 35 cm	> 35 to ≤ 45 cm	> 45 to ≤ 70 cm	> 75 to ≤ 100 cm
2020 (n=71)	4.2%	32.4%	31.0%	12.7%	7.0%	12.7%	2.8%
2022 (n=62)	9.7%	30.6%	25.8%	12.9%	12.9%	8.1%	0.0%
Column temperature (bins of 10 °C)	> 0 to ≤ 10 °C	> 10 to ≤ 20 °C	> 20 to ≤ 30 °C	> 30 to ≤ 40 °C	> 40 to ≤ 50 °C	> 50 to ≤ 60 °C	> 60 °C
2020 (n=50)	2.0%	0.0%	4.0%	22.0%	38.0%	34.0%	0.0%
2022 (n=50)	4.0%	0.0%	6.0%	28.0%	26.0%	34.0%	2.0%
Mobile phase strong solvent	AcN	MeOH	AcN/PrOH	Others			
2020 (n=244)	96.7%	1.6%	0.0%	< 0.5%			
2022 (n=192)	98.4%	0.0%	1.6%				
Mobile phase pH	Acidic	Alkaline/neutral					
2020 (n=236)	98.3%	1.7%					
2022 (n=189)	100.0%	0.0%					
Mobile phase acidifier	Formic ac.	Acetic ac.	Others				
2020 (n=229)	96.1%	2.2%	< 0.5%				
2022 (n=192)	99.0%	0.5%	< 0.5%				
Mobile phase acidifier concentration	0.08% Formic ac.	0.1% Formic ac.	0.2% Formic ac.	Others			
2020 (n=220)	0.5%	90.9%	3.6%	< 0.5%			
2022 (n=190)	2.1%	91.1%	1.6%	< 0.5%			
Flow rate for 75 μm ID column	200 nL/min	250 nL/min	300 nL/min	350 nL/min	400 nL/min	500 nL/min	Others
2020 (n=138)	8.0%	22.5%	54.3%	5.1%	5.8%	0.7%	< 0.8%
2022 (n=151)	6.6%	18.5%	55.6%	4.0%	6.0%	4.0%	< 1.4%
Gradient program	Segmented	Linear	Non-linear				
2020 (n=204)	51.0%	49.0%	0.0%				
2022 (n=190)	36.3%	63.7%	0.0%				
Gradient time (bins of 30 min)	≥30 to < 60 min	≥60 to < 90 min	≥90 to < 120 min	≥120 to < 150 min	≥150 to < 180 min	≥180 to < 210 min	Others
2020 (n=256)	18.0%	19.5%	21.1%	18.4%	5.9%	5.9%	< 4.3%
2022 (n=198)	14.1%	20.7%	23.2%	20.2%	6.1%	3.5%	< 5.6%

^aA total of 524 datasets deposited on the ProteomeXchange repository between June-August 2020 and January-March 2022 were evaluated. The number of items reported for each parameter differs because of the incompleteness of the method specifications in the associated publications. Abbreviations: AcN, acetonitrile; MeOH, methanol; DMSO, dimethyl sulfoxide; TFA, trifluoracetic acid; HFBA, heptafluorobutyric acid; μPACs, micropillar array columns; BEH, bridged ethylene hybrid; PrOH, propanol; ID, inner diameter.

quality of a chromatographic separation cannot be accurately assessed if chromatographic profiles are reconstructed from less than 10 data points. This can be the case for most data-dependent as well as data-independent proteomic analyses.

Chromatographers are used to saying that the separation column is the most crucial part of each liquid chromatographic system. Nevertheless, practitioners can readily deduct from the theory of extra-column dispersion that even a state-of-the-art

column does not produce expected separation performance if the other parts of the system are not carefully adjusted.²²¹ Paradoxically, as we demonstrated in our experiments (Figure 15), the component hindering superior separation can sometimes be just the outlet capillary, i.e., a component worth a few US dollars. By following recommendations derived from the theory of extra-column dispersion, Lenčo et al.⁶⁷

managed to optimize a conventional-flow chromatograph for high-efficiency microflow RPLC-MS proteomic analyses.

RPLC METHODS FOR BOTTOM-UP PROTEOMIC ANALYSES

A number of parameters must be considered during RPLC methods development for bottom-up proteomic analyses to get superior results in a no-longer-than-necessary LC-MS instrument time. We extracted details from more than five hundred data sets deposited on the ProteomeXchange repository to obtain a solid overview of parameters commonly used in current bottom-up proteomic analyses and how they correspond to the current knowledge in RPLC of peptides (Table 2). The data sets are from two distinct periods: June–August 2020 and January–March 2022. A significant portion of the parameters did not change over that period significantly. Therefore, the tabulated settings for most parameters can be interpolated with a certain degree of confidence over 7,114 data sets deposited in the repository between June 2020 and March 2022.

Columns for RPLC Peptide Separation

In contrast to the early days of chromatography, columns varying in diverse parameters have been designed and are commercially available nowadays for peptide RPLC separation. Alternatively, they can be prepared in-house by packing particles into fused silica capillaries or via casting monoliths. Each year, numerous columns packed with new stationary phases are marketed.^{222–224}

The column characteristics should correspond with the particular bottom-up proteomic applications and their aim, with important factors to be considered being sample amount and its complexity, sample throughput, and peptides and proteins properties. Obviously, the column must be compatible with the available instrumentation. Regardless of the particular column characteristics, practitioners should condition each new column with a few injections of a complex peptide sample to load slowly equilibrating active sites and obtain anticipated and reproducible peptide separation without sample losses (Figure 21).²²⁵ The relative quantity of these active sites correlate with the amount of the stationary phase in the column, i.e., with column dimensions.

Particulate Columns. With some exceptions, separation columns currently employed in bottom-up proteomics studies are filled with the particulate stationary phase (Table 2). Particles are easily handled, have excellent mechanical and good chemical stability, and a broad palette of chemistries and sizes is available for LC-MS method tailoring. Particles can be readily packed into capillaries to produce economic alternatives to commercial nanoflow columns.^{226,227} The outlet of such in-house packed columns can directly work as nanoESI emitters, eliminating the need to install an outlet frit and creating additional connections that represent potential sources of band dispersion.¹⁷⁸ A typical column used in proteomics research is still packed using traditional, fully porous particles in which analytes can diffuse in their entire volume. However, particles with constrained diffusion space, such as superficially porous particles, provide significant benefits for the separations of peptides and, particularly, proteins, i.e., analytes with slow diffusivity.

Superficially Porous Particles. Superficially porous particles (SPPs), often referred to as core–shell, fused-core, porous shell, or solid core particles, are formed by solid silica cores

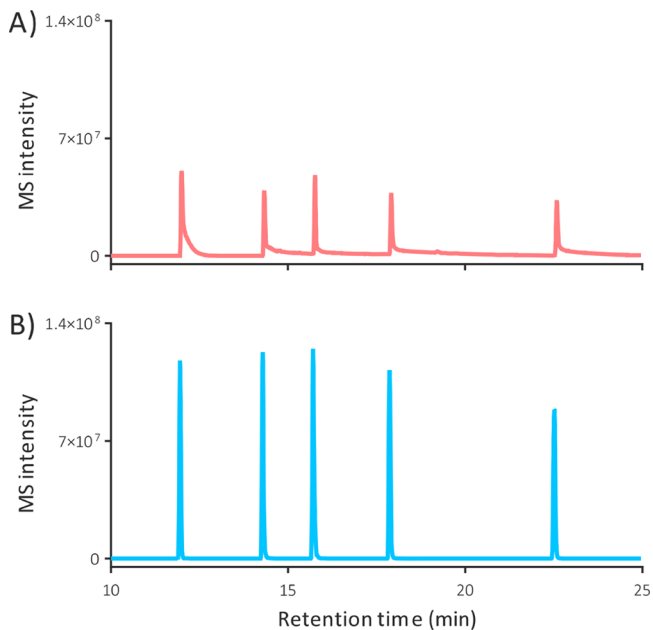


Figure 21. Importance of column conditioning. Five standard peptides were separated using a 30 min linear gradient from 2 to 38% acetonitrile with 0.1% FA in a 1.0 × 150 mm Acuity UPLC CSH C₁₈ 1.7 μm, 130 Å column (Waters). The column temperature was 60 °C, and the flow rate was 50 μL/min. LC-MS chromatograms show the separation of the standard peptides before (A) and after the column was conditioned with three consecutive injections of a whole-cell tryptic digest of eukaryotic cells (B).

surrounded by an outer porous layer having essentially the properties of fully porous particles (for reviews, see refs 228, 229). This particle architecture has been known for more than 50 years.²³⁰ However, the real success of these particles is related to their resurrection by Kirkland a few decades later.^{10,231,232} Indeed, shortly after Advanced Materials Technology commercialized columns packed with 2.7 μm SPPs in 2006, these particles received considerable attention because they allowed separation similar to that of sub-2 μm totally porous particles using instrumentation operating at a maximum pressure of 400 bar.²³³ SPPs can provide a reduced theoretical plate height *h* roughly 25% lower than traditional fully porous particles of the same diameter.²³⁴

SPPs were initially developed with a desire to produce a stationary phase support that would enable high-efficiency separation of larger analytes featuring slow diffusion via shortening their intraparticle diffusion path.¹⁰ Yet, their increased efficiency might not necessarily be attributed only to factors anticipated during their development. Most importantly, SPPs pack denser and more regularly than fully porous particles, reducing the eddy dispersion due to flow path inhomogeneities (A term).¹⁷⁶ The tighter packing can be attributed to their density, surface roughness, and shape. The reduced A term was previously also suggested to be associated with their narrow particle size distribution.¹⁷⁴ However, this theory was experimentally and computationally contested.^{175,177,235} The presence of a solid core inside the SPPs reduces the volume accessible for analytes to diffuse. Hence, the longitudinal broadening (B term) decreases in columns packed with superficially porous particles.¹⁷⁴ Nonetheless, this effect was observed primarily in the isocratic elution of small analytes with fast diffusion, while it is negligible in the gradient

elution of peptides. The positive impact of the particle architecture on the resistance to the mass transfer (C term) is the opposite. It is most significant for larger analytes because of their low diffusivity.^{174,236,237} This feature is successfully utilized in developing modern particulate stationary phases for the analysis of intact proteins and their large parts, with the current primary application being quality control of antibody biopharmaceuticals.^{123,238,239} Indeed, while SPPs represent an appealing benefit for peptide separation, they seem to be indispensable for the efficient separation of proteins (for a recent review, see ref 240).

SPPs are still frequently blamed for having lower loading capacity than their totally porous counterparts. However, this was true only for the first generation particles with a very thin, porous shell produced in the 1960s. Although it is not evident at first glance from the illustrations and electron microscopy photographs, the solid core of current SPPs occupies only between 25 and 39% of the particle volume (calculated for 2.7 μm particles with a 0.5 μm porous shell and 2.6 μm particles with a 0.35 μm shell, respectively). Hence, even if peptides could penetrate to the very center of totally porous particles, which is not very likely, the loading capacity of superficially porous equivalents of the same diameter should not be drastically compromised. Indeed, the loading capacity of SPPs was demonstrated to be not greatly reduced compared with totally porous particles.²⁴¹

Surprisingly, despite their indisputable advantages for the chromatographic separation of peptides and a demonstration of their efficient packing into fused silica capillaries,¹⁷⁶ SPPs are used rather seldomly in bottom-up proteomics (Table 2). Aside from their benefits for separating larger molecules, columns packed with SPPs could at least replace UHPLC columns of the same length where lower pressure is needed or where longer columns will be significantly beneficial, but the pressure limits are a constraining factor. The higher permeability of columns packed with 2.7 μm SPPs versus columns packed with fully porous sub-2 μm particles can also be utilized to increase the flow rate outside the effective elution window of the gradient program to deliver a sample from the autosampler to the column faster or to flush and equilibrate the column in a shorter time.

Nonporous Particles. Nonporous particles are solid spheres covered by chromatographic ligands only on their surface. As a result, these particles do not suffer from the resistance to mass transfer due to diffusion within the pores of the stationary phase support, thereby providing chromatographic separation of peptides less dependent on the flow rate.²⁴² On the other hand, the surface area is reduced to a few m^2/g , corresponding roughly to 1% or less of the surface area of totally porous particles of the same diameter. The small surface area reduces the loading capacity and retention. Hence, the applications of columns packed with nonporous particles are restricted to analyses of low-quantity proteomic samples where they performed better than fully porous particles in terms of peak capacity, mirroring in a larger number of identifications.²⁴³ Nonporous particles are dedicated to very specific applications, and it is thus not surprising that we found no record of using a column packed with these particles within the list of evaluated bottom-up proteomics studies (Table 2). Because of the features mentioned above, nonporous particles can be particularly beneficial for the ultrafast separation of samples with very low protein quantities.²⁴⁴

Properties of Chromatographic Particles. Particle Size.

The column efficiency is proportional to the particle diameter, and therefore, particle downsizing has a long tradition in improving separations in liquid chromatography.²⁴⁵ Martin and Syngue visionary predicted in 1941 that "... the smallest HETP should be obtainable by using very small particles and a high pressure difference across the length of the column".⁶⁸ In 1997, Jorgenson's group demonstrated the efficiency of a column packed with 1.5 μm particles, and by this, they launched the era of UHPLC.⁹ The primary benefit of sub-2 μm particles is shortening interparticle and intraparticle diffusion distances. Subsequently, analytes spend less time diffusing from the mobile phase stream to the particles and need less time to diffuse in and out of the particle pores filled with the stagnant mobile phase. These constraints on the diffusion space vastly reduce the resistance to mass transfer, particularly for slowly diffusing analytes. Hence, the slope of the C term in the separation of peptides significantly decreases with smaller particle sizes, which manifests itself as narrower peaks of peptides eluted at flow rates commonly used in bottom-up proteomics.

The increased efficiency of sub-2 μm particles comes with a penalty of a higher backpressure. Waters commercialized the first ultraperformance liquid chromatography (UPLC) system capable of operating pressures of up to 1000 bar in 2004.²⁴⁶ Since then, numerous other UHPLC instruments, nanoLC systems, and fitting systems compatible with columns packed with sub-2 μm particles have been marketed.^{247,248} A chromatograph able to operate nanoflow, capillary, and microbore columns at pressures of up to 1500 bar was introduced recently (Vanquish Neo UHPLC, Thermo Fisher Scientific).

Because of their intrinsic efficiency, sub-2 μm particles have become very popular in various applications of liquid chromatography, including bottom-up proteomics. It was perhaps their outstanding efficiency that inspired some authors to forecast that the separation performance in bottom-up proteomics can be pushed further by reducing the particle diameter to 1 μm or less.²⁴⁹ However, it must be emphasized that for a fixed N , the column separation efficiency increases proportionally only to the inverse particle size $\left(\frac{1}{d_p}\right)$ (eqs 16, 17, and 18), while the backpressure rises inversely to the square of the particle size $\left(\frac{1}{d_p^2}\right)$ as can be inferred from the Kozeny–Carman equation. This equation is usually used in a simplified form for practical use (eq 36).^{96,250}

$$P \approx \frac{2500 \cdot L \cdot \eta \cdot F}{d_p^2 \cdot d_c^2} \quad (36)$$

The equation considers only the particle bed without additional column hardware and extra-column sources. As a result, the observed pressure is closer to 150% of the calculated pressure.²⁵¹

The theoretical column efficiency gain is 2-fold from reducing the particle diameter to half (eq 18), whereas the backpressure increases 4-fold (eq 36). In other words, a higher number of theoretical plates per one bar of pressure can be obtained using larger particles.²⁵² It should be further noted that doubling the theoretical plate number increases the peak capacity only by a factor of $\sqrt{2}$ (eq 22). For instance, downsizing the particle diameter in a 50 cm long column from

3 to 1 μm increases the backpressure from 333 to 3000 bar while the peak capacity theoretically increases only \sim 1.7-fold (Figure 22, A). For curiosity, a backpressure of 3000 bar

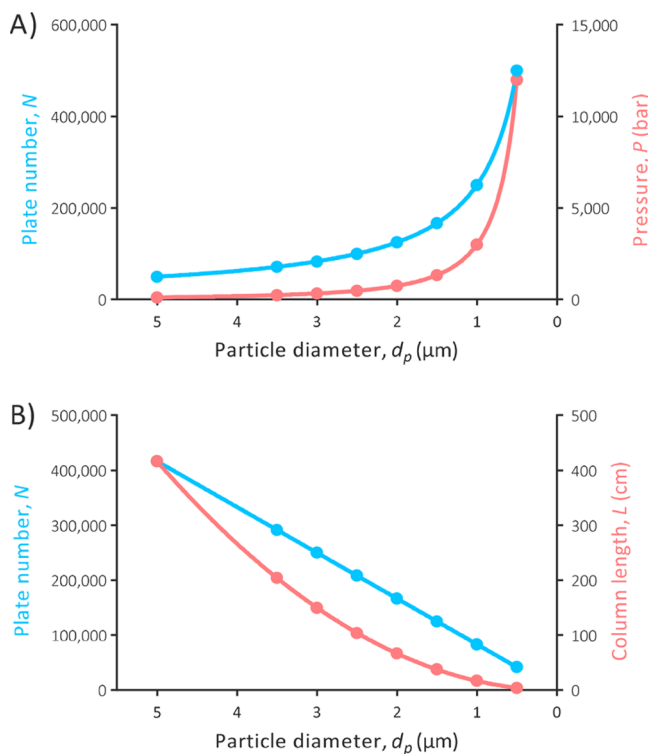


Figure 22. Separation efficiency of 50 cm long columns packed with particles having a diameter between 0.5 and 5 μm (A) and particles packed in a column of a length that produces maximum backpressure of 1000 bar (B). The theoretical plate number N was estimated based on eqs 17 and 18 with an assumption $h = 2 \cdot d_p$. Backpressure of 50 cm long columns varying in the packing particle size and column lengths producing backpressure of 1000 bar were predicted using the Kozeny–Carman equation (eq 36). The simplified projections did not consider that the selected flow rate of 250 nL/min is not optimal for all particle sizes. The column inner diameter was 75 μm , and the mobile phase with a viscosity of 0.75 cP was used.

represents a pressure of 30 km underwater. Such high pressures naturally represent extreme demands on materials and components inside liquid chromatographs. Although some prototype instruments able to deliver the pressures of 4–7 kbar have been developed in academic laboratories, they are not simple to operate.^{253,254} Besides, their robustness in everyday routine would be questionable.

Even if commercial systems capable of delivering pressures of 2000 bar and higher were available in the future, the practitioners in proteomics should not be obsessed with downsizing the particles. It may sound paradoxical, but providing that separation performance is the primary focus, larger particles can afford better performance than sub-2 μm particles in single-shot bottom-up proteomics that relies on long gradient methods. Because of the better permeability of larger particles, they can be packed into longer columns. The maximum column length at a certain pressure limit increases proportionally with the second power of particle diameter (d_p^2). Therefore, larger particles packed in long columns provide more efficient separation at the instrument pressure limit (Figure 22, B).^{255–257} Naturally, longer columns have larger

void volumes, protracting the total method time. Kinetic plots predict that longer columns packed with larger particles provide higher peak capacity per unit of gradient time than UHPLC columns above a particular gradient time, while UHPLC columns are attractive for fast separations using short columns operated at high flow rates.²⁵⁸ Kinetics plots are graphical tools for comparing the separation performance of various columns operated at their optima when the instrument is used at its pressure limit. The explanation of how kinetics plots are constructed is beyond the scope of this tutorial, and instead, we refer interested readers to respective literature,^{259–262} including a short guide for beginners²⁶³ and a recent series of three articles published in LCGC magazine.^{264–266}

Pore Size. In order to provide a sizable chromatographic surface in a constrained volume of the column, the particles need to be porous. Depending on their architecture, the surface area of state-of-the-art particles ranges between 100 and 400 m^2/g and is inversely proportional to the pore size. A larger surface area provided by small pores offers more sites for chromatographic interactions, which is advantageous for column separation performance, including column retentivity and capacity. However, the accessibility of the surface area in the pores diminishes with the hydrodynamic diameter of molecules (see the section **Hydrodynamic Diameter**).²⁶⁷ For instance, insulin ($M_w = 5777$ Da) was shown to have access to only 40% of the surface area in particles with a pore size of 90 \AA .¹²⁸ Consequently, peptides generally utilize a greater surface area of particles with larger pores, even though they have an intrinsically lower surface area, than if separated using particles with the large surface area provided by small pores.^{119,250} In addition, if the pore size is not selected adequately to the analyte size, a secondary size-exclusion effect burdens the separation, further aggravating the peak shape (Figure 12). In an extreme case, when the analyte is much larger than the pores, it can interact only with chromatographic sites localized on the outer surface of the particles that represent only a minute portion of the total chromatographic surface. Such a disbalance in analyte and pore size leads to a dramatic decrease in their retention, as has been exemplified on ipilimumab chromatographed using particles with a pore size of 100 \AA .²⁶⁸

The pore size also impacts how fast analytes diffuse in the stagnant mobile phase inside the pores. Due to the steric hindrance and tortuous pathways, the pore diffusivity is much slower than in bulk solvents.^{187,188} The hindered diffusion subsequently increases the band broadening due to the greater resistance to mass transfer. The diffusion inside the porous particle can be enhanced by increasing the ratio between pore size and molecule size.^{123,269} Therefore, larger pores not only allow peptides to interact with a greater portion of the chromatographic surface, but they also improve the in-column band dispersion by reducing the C term of the van Deemter equation (eq 27). Indeed, even such a small peptide as bradykinin ($M_w = 1060$ Da) can profit from enlarging the average pore size from 80 to 120 \AA .¹¹⁹ Several column producers have developed chromatographic particles with a pore size in a range of >100 \AA and ≤ 160 \AA that are particularly suited for bottom-up proteomic applications. Columns packed with particles with a pore size less than 100 \AA should be used rather cautiously, particularly if larger peptides are present in the sample.

While using larger pore sizes for bottom-up proteomic applications is beneficial, it is an absolute necessity for the

separation of intact proteins because of their substantial hydrodynamic diameter and exceptionally slow diffusion. As a rule of thumb, 300 Å pores were recommended in the past as a standard pore size for protein separations. However, even larger pores can yield more efficient protein separation via unrestricted diffusion and access to the bonded phase. Stationary phases with a pore size in a range of 300–1000 Å are now commercially available for RPLC of proteins.^{123,238,270} The physical stability of particles with such porosity is sometimes questioned. However, particles with a pore size of >300 Å usually have a superficially porous architecture with a rigid core. As a result, depending on the particular preparation method (for a review, see ref.²²⁹), modern wide-pore particles can withstand a pressure of 689 bar (BioResolve RP mAb Polyphenyl 2.7 μm, 450 Å, Waters), or even 1000 bar (Halo C₄ 2.7 μm, 1000 Å, Advanced Materials Technology).

The column pressure preventing stationary phase dewetting (see the section [Chemistry of Bonded Ligands](#)) is inversely proportional to the pore size.²⁷¹ Therefore, columns packed with particles with larger pores are better compatible with the completely aqueous mobile phase.^{272,273} No measurable loss of retention was observed after 150 Å C₁₈-bonded particles were kept in a 100% aqueous environment, whereas 80 Å particles exhibited 80% loss in retention.²⁷⁴ As a result, particles with larger pore sizes can be used to analyze hydrophilic peptides without worries due to percolating columns using an entirely aqueous mobile phase.

Chemistry of Bonded Ligands. Silica-based particles are still by far the preferred material for RPLC separation of peptides for bottom-up proteomic analyses ([Table 2](#)). Their long-term popularity can be attributed, among other reasons, to a very good understanding of bonding chemistry. The chemical and thermal stability of the silica support and bonded ligands have been substantially increased using various means over the years. Because RPLC separation of peptides for LC-MS bottom-up analyses usually does not involve harsh chromatographic conditions (0.1% formic acid gives a theoretical pH of 2.68, and temperatures over 60 °C are used still very scarcely), we do not cover this topic in this tutorial. Instead, we refer interested readers to a comprehensive review of Claessens et al.²⁷⁵ and a more recent review by Borges et al.²⁷⁶

A significant portion of surface Si-OH groups remains unreacted after functionalizing particles with chloroalkyl- or alkoxy-silanes. The residual silanols are acidic and can dissociate at the pH of the mobile phase acidified using a low concentration of a weak acid such as formic acid. Dissociated silanols can subsequently create sites participating in ionic interactions with protonated analytes. The slow kinetics of these secondary interactions result in peak distortions. In an acidic environment, tryptic peptides usually have at least two protonated sites, the amino group at the N-terminus and a basic functional group in the Lys or Arg side chain at the C-terminus. Tryptic peptides thus belong to analytes whose peak shape and loadability can be significantly deteriorated by residual silanol activity of the stationary phase. Although the secondary interactions of dissociated silanols are not the only reason for the tailing of protonated analytes,^{114,277,278} practitioners should use only columns packed with particles designed to significantly reduce silanol activity for highly efficient peptide separation in bottom-up proteomic analyses.

The unwanted silanol activity of silica-based particles can be reduced via numerous strategies (for a review, see ref 279). Moreover, sorbents with no measurable residual silanol activity at low pH values were developed.²⁸⁰ The most recent strategy based on positioning positive charges at the particle surface was demonstrated to be extraordinarily effective for suppressing the tailing of peptides in the LC-MS analyses carried out using the low-ionic-strength mobile phase. This particle chemistry was introduced by Waters in 2010 under a trademark CSH (Charged Surface Hybrid).²⁸¹ CSH particles are covered by a low amount of ionizable pyridyl groups before they are functionalized by ligands for RPLC.²⁸² At a pH < 6, the pyridyl ligands are positively charged.²⁸³ Therefore, positively charged peptides are repelled from the proximity of residual silanols by electrostatic repulsion under acidic pH, improving their peak shape and loadability in the low-ionic-strength mobile phase.¹¹⁶ In combination with this stationary phase, 0.1% formic acid in the mobile phase provides separation performance of high mass loads of peptides even slightly better than that produced with 0.1% TFA using the same stationary phase but the modified surface. Even though it was not the manufacturer's intention, some authors include this particle chemistry among mixed-mode stationary phases because of the positive charge. Currently, similar particle chemistries are available from Agilent (Plus C₁₈) and Phenomenex (PS C₁₈). Surprisingly enough, this type of stationary phase is still used for proteomic applications only sporadically ([Table 2](#)), although it was launched commercially more than a decade ago.²⁸¹

The outstanding performance of CSH C₁₈ particles comes with a small compromise to retentivity. Peptides elute in the mobile phase containing 2–4% less acetonitrile compared to the same particles without the superficial pyridyl groups. Therefore, if a separation column packed with CSH C₁₈ particles is used in a trap-elute configuration, conditions for trapping need to be thoroughly optimized to fully exploit the unique attributes of the column.²¹⁵

Practitioners are traditionally discouraged from using RPLC columns with a completely aqueous mobile phase to avoid so-called phase collapse. It is worth noting here that the phase collapse in the aqueous environment, i.e., change in C₁₈ chains conformation from perpendicular to the silica support to ones that lie flat on the pore surface and themselves, is one of the top 10 chromatographic myths.²⁸⁴ The gradual or sudden decrease in retention when operating the column in an aqueous environment is not because of the change in conformation of the C₁₈ ligands but because of stationary phase dewetting.²⁸⁵ The aqueous solvent can spontaneously extrude from the pores covered by highly hydrophobic water-unfriendly ligands. However, this develops only if the mobile phase flow through the column is stopped or decreased to minimal values. Otherwise, the mobile phase flow produces sufficient pressure that forces the solvent to remain confined within the pores.²⁷² The Young–Laplace law for the behavior of liquids in capillaries determines that the threshold pressure depends on the contact angle of water and the pore radius.^{271–274}

The pore environment must become more water-friendly so that the contact angle decreases. In C₁₈-bonded stationary phases, this can be achieved by keeping the residual silanols non-end-capped. However, this inherently brings issues related to their secondary interactions with positively charged analytes. Therefore, dedicated stationary phases have been developed by

end-capping residual silanols using polar functionalities or embedding polar groups directly to bonded ligands.^{286,287} End-capped silanols or embedded polar groups also contribute to silanol activity reduction.²⁷⁹ Reciprocally, at least a partial effect on decreasing the contact angle of water can be expected from stationary phases with a positively charged surface developed initially for highly efficient separation of basic analytes in the low-ionic-strength mobile phases.¹¹⁶ The effect of pore size on dewetting was discussed in the section above (see the section **Pore Size**). To summarize, many stationary phases that considerably reduce or even eliminate water dewetting from pores are currently available, allowing practitioners to start gradients at very low or even zero acetonitrile concentrations to promote retention of very hydrophilic peptides in columns upon injection.

The typical bonded alkyl chain for separating peptides for bottom-up proteomics studies is C₁₈ (Table 2). Particles functionalized with shorter chains, such as C₄, are typically preferred for RPLC of proteins to mitigate their strong adsorption that contributes to peak broadening, peak tailing, and limited recovery.²⁸⁸ Short alkyl ligands are postulated to provide weaker hydrophobic interactions. Nevertheless, C₄-based sorbents can provide even higher protein retentivity than C₁₈, arguably because large proteins cannot penetrate the alkyl chains layer and interact only with their top part. Also, functionalization with shorter alkyl chains yields a denser bonding.^{288,289} Due to their denser silica surface coverage, shorter ligands reduce secondary interactions of proteins with the residual silanols. Both the lower retentivity and higher density of shorter ligands probably contribute to the more efficient protein separation using these sorbents. The same benefits can be achieved using sorbents bonded with phenyl-based ligands. Among those, the polyphenyl-bonded stationary phase occupies quite a unique position in the RPLC of proteins. This stationary phase is highly bonded, and the ligands are very rigid, limiting secondary interactions and conformational heterogeneity of protein adsorption.²³⁹ Its qualities were demonstrated in LC-MS analyses of antibody biopharmaceuticals that involved a low or even zero concentration of TFA in the mobile phase and a mild column temperature.^{290,291} Despite the extraordinary qualities of particle chemistries developed to respond to the demands of the pharmaceutical industry for columns for quality control of modern protein drugs,^{123,290,292} poly(styrene-*co*-divinylbenzene) macroporous polymeric particles, which were introduced more than three decades ago, are still customary for protein separations in top-down proteomic studies.^{293,294} We anticipate that top-down proteomics will largely benefit from stationary phase developments driven by the need for quality control of protein biopharmaceuticals.

Nonparticulate Columns

Monolithic Columns. Monolithic columns are characterized by a continuous, highly porous sorbent prepared *in situ* within the confines of a column. Two major types of monoliths utilizable as stationary phases for liquid chromatography have been developed. In the 1990s, Švec and Frechét prepared rigid polymer monolithic structures based on poly(methacrylate esters) and poly(styrene-*co*-divinylbenzene).^{295,296} A few years later, Tanaka's group presented inorganic monoliths made of porous silica.²⁹⁷ These two types of monoliths have different bed morphologies. Silica-based monoliths have a bimodal pore structure as they contain flow-through macropores that confer

high permeability and diffusive mesopores. The mesopores are not present in organic monoliths. As a result, the mass transfer of analytes in organic monoliths is dominantly realized by convection, while diffusion plays a marginal role. This feature predetermines their dominant utilization in the fast separation of slowly diffusing analytes at higher mobile phase velocities.^{298–300}

Monolithic columns for nanoLC can be easily prepared, and their high porosity allows the casting of monoliths with effective lengths up to several meters, being beneficial for long single-shot bottom-up analyses.³⁰¹ The monolith bed is covalently anchored to the walls of the fused silica capillary, eliminating the need for frits at both ends of the column. This feature reduces in-column band dispersion and the risk of column clogging by microparticulates. Monoliths can be percolated from both ends at high flow rates, which alongside the ease of casting the monoliths and the features mentioned above, made them a good option for trap columns in the back-flush configuration of the trap-elute setup in nanoLC. However, practitioners should be aware of their lower retentivity compared to C₁₈-functionalized particles, potentially resulting in losing hydrophilic peptides during sample injection.

Many review papers have discussed the potential benefits of monolithic columns and their comparison with particulate columns.^{302–305} Their conclusions are diverse, and since fans of monoliths typically wrote them, they may be somewhat biased. The merit of monolithic columns over particulate columns in bottom-up proteomics is difficult to generalize as the results are influenced by separation conditions, detection conditions, and, critically, the level of compatibility of both steps.¹⁷³ The head-to-head comparison of the performance of equivalent columns for peptide separation is still missing. Overall, it does not seem that the organic monolithic columns can compete with the performance of columns efficiently packed with state-of-the-art particles in bottom-up proteomics. The situation in silica-based monoliths is more promising as their third generation with a domain size and through-pore size reduced to 1–1.5 μm and 0.5–1 μm, respectively, provided a 30–40% higher peak capacity for peptide separation than a commercial nanoflow column packed with 2 μm particles.³⁰⁶ Unfortunately, preparing these columns is not easy, and commercial products are currently not available to practitioners.

In general, monolithic columns can be very beneficial for some niche applications, such as LC-MS analyses relying on steep and fast gradients at high flow rates or long gradient separations of peptides using very long columns. However, the dominance of particulate columns over monoliths in bottom-up proteomics is indisputable (Table 2).

Open-Tubular Columns. Open-tubular (OT) columns represent a specific subgroup of monolithic columns. Typical OT columns used in liquid chromatography are narrow capillaries with a thin layer of porous stationary phase anchored to walls, whereas capillaries with walls physically coated using a nonporous stationary phase dominate in gas chromatography (for recent reviews, see refs 307, 308). Their superior performance in gas chromatography is given by several orders of magnitude faster diffusion of analytes in the gas. In liquid chromatography, the maximum diffusion distance in these columns, i.e., the distance equal to the diameter of the inner space, must be reduced to eliminate the negative effects of slow diffusion in liquids and unlock their full potential.

Indeed, OT columns with a diameter of a few μm were predicted to be needed for optimum results.^{309,310}

The eddy dispersion in these columns is avoided because the flow homogeneity is physically not disrupted by the presence of particles, and the mass transfer is limited only to a homogeneous thin porous layer,³¹¹ contributing further to the superior performance of OT columns when their diameter is optimized. Moreover, OT columns with a length greater than 1 m can be operated under HPLC pressures because of their very high permeability.³¹² The excellent performance of OT columns for bottom-up proteomic applications can be illustrated in recent studies by Liu's group. A 75 cm long OT column with a diameter of 2 μm achieved a peak capacity of around 2000 in 3 h gradient separation of tryptic peptides⁷⁷ and a peak capacity of 700 in 20 min gradient when the column was maintained at 70 °C.⁷⁸ The sensitivity increase gain against a standard 75 μm column allowed to identify around 1000 proteins from a mere 75 pg of a tryptic digest of a bacterium.³¹³

Because of their ultimate sensitivity due to a minimized inner diameter, OT columns should be of high interest for practitioners focused on analyses of samples with highly limited availability. Along with the rapidly growing area of proteomics focused on proteomes of single cells, the OT columns can finally find their "killer application," as stated recently by Roberg-Larsen et al.³¹⁴ Interestingly, an OT column was used for a single-cell proteomic analysis already in 1989.³¹⁵ In this area of applications, their limited loadability does not represent an issue. We presume, however, that until commercial columns and, chiefly, commercial instruments that can operate them on a routine basis at sub-nL/min flow rates with minimum extra-column dispersion are available, the interest in this type of columns will remain a domain of academic laboratories focused on research in separation science with only proof-of-concept applications.

Micropillar Array Columns. Micropillar array columns (μPACs) represent the latest generation of commercial columns. The design was conceptualized based on the fundamental understanding of in-column band broadening by Knox already in 2002.¹⁷⁹ Desmet, De Malsche, and their colleagues subsequently transformed step-by-step the initial idea into an innovative commercial product marketed in 2017 by PharmaFluidics.^{182,183} These *de facto* monolithic columns are fabricated using microlithographic etching of a silicon wafer,³¹⁶ resulting in perfectly ordered support for generating a 0.3 μm porous layer of a C₁₈-bonded stationary phase. The pore size of μPACs ranges between 100 and 300 Å. The strictly ordered bed eliminates the dispersion due to flow path inequalities (A term), i.e., the primary source of in-column band broadening at an optimal flow rate.¹⁵⁷ The regular inter pillar distance of 2.5 μm confers μPACs very high permeability. As a result, much more efficient peptide separation can be achieved using a micropillar array column under significantly reduced backpressure compared to a packed bed column with the same length. The very high permeability of the structured bed allows fabrication of up to 200 cm long μPACs . The improved separation is vastly translated into an increased number of identified peptides and proteins. The exceptional reproducibility of retention times is another appealing benefit of these columns.^{317–319} They are also compelling for long single-shot analyses because the peak widths of peptides increase much more slowly with the gradient time than in a packed bed column.³¹⁷ On the other hand, it should be noted

that the excellent performance of these columns creates much higher demands on the reduction of extra-column dispersion so that their excellent efficiency can be indeed transformed to a longer list of identified peptides and proteins. Although direct evidence is missing, we speculate that the extra-column dispersion was likely the reason why a 200 cm long μPAC produced a lower peak capacity in one of the earliest studies than a 50 cm long equivalent in a later study (240 versus 322).^{11,318}

μPACs are currently available in two basic cross sections with an equivalent inner diameter of 85 μm (in the length of 50 and 200 cm) and 189 μm , corresponding to a nanoflow column and a capillary column, respectively.³²⁰ Recently, the second-generation μPAC with an equivalent inner diameter of 62 μm and an optimized bed structure dedicated for analyses of limited sample loads was introduced.⁹⁴ Currently, there are already four fit-for-purpose formats of separation μPACs . Yet, they still have not found a path to many proteomic laboratories (Table 2). The reason for that is likely their price. These columns are 3–5× more expensive than traditional commercial nanoflow columns. By nature, μPACs do not need frits that are the sites of column blockage with microparticulates (in packed bed columns without the inlet frit, such material is captured by a few first layers of particles without any possibility of being flushed out). Also, the interstitial space between micropillars is large, and the microparticulates can pass through. The assumed lower frequency of μPACs column replacement should compensate for their higher price. Therefore, we expect that the number of studies employing this type of column will further follow the increasing trend that we observed between 2020 and recent data sets (Table 2). We also anticipate that the development in this area will continue, and additional fit-for-purpose columns will be marketed. Readers interested in the concepts behind μPACs , their history, performance, and characteristics are referred to the recent review by Rozing.³²¹

Column Inner Diameter

The nomenclature of columns based on their inner diameter and the terminology of related flow regimes has not been unified.^{322–325} The question is if this is even possible, considering the existence of gray zones between column diameters and wide ranges of flow rates at which a column with a particular diameter can be operated. We do not want to contribute to this debate more than necessary, but for the sake of this tutorial, we define the columns based on the flow rates calculated so that the same mobile phase flow velocity provided by a flow rate of 250 $\mu\text{L}/\text{min}$ in a 2.1 mm column is maintained (Figure 23).

The inner diameter of the column is perhaps the most important parameter that users have to opt for. It dictates the volumetric characteristics of all other components of the LC-MS system. More importantly, it is the critical denominator of the overall MS signal intensity because, to a first approximation, the concentration of peptides in eluting peaks is proportional to the inverse square of the column inner diameter, and MS with electrospray ionization in commonly used flow regimes usually behaves as a concentration-dependent detector.³²⁶ Most samples for proteomic analyses are available in microgram to milligram quantities of the starting material, but the protein mass is distributed over tens to hundreds of thousands of peptides that span a wide concentration range.³²⁷ Furthermore, practitioners usually resist processing the entire available sample, likely due to the

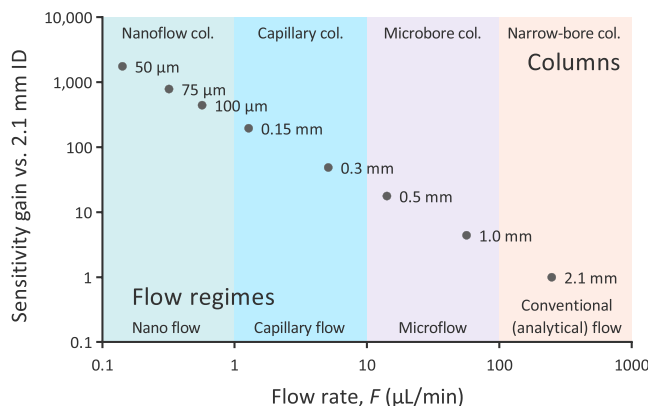


Figure 23. Nomenclature of flow regimes and columns based on the typical column inner diameters (IDs). The flow rates for each column were calculated proportionally to a flow rate of 250 $\mu\text{L}/\text{min}$ for a 2.1 mm ID column.

price of enzymes as other chemicals are not expensive, and the same quantity of consumables (tubes, tips, extraction cartridges, HPLC vials, etc.) must be spent regardless the protein amount. More importantly, some proteomic studies focus only on a defined segment of the total protein mass, such as proteins localized in a particular organelle or cell site, peptides bearing a specific post-translational modification, endogenously generated peptides, etc. Because of these reasons and likely because of the sensitivity of mass spectrometers at the time when the first bottom-up studies emerged, proteomics is traditionally and perhaps kind of dogmatically linked to nanoflow columns.

Nowadays, a typical nanoflow column for bottom-up analyses has an inner diameter of 75 μm (Table 2). This diameter theoretically enhances the MS signal 784-fold versus a 2.1 mm column that currently is the dominating column diameter in LC-MS analyses of small molecules where samples are usually available in larger quantities and/or the concentration of analytes is sufficient.³²⁸ A column diameter of 75 μm is well suited for most proteomic studies. However, this diameter cannot provide the ultimate sensitivity needed to analyze extremely limited samples comprehensively, such as in analyses of individual cells, where more sensitive alternatives with narrower inner diameters are required. For instance, replacing a 75 μm column with a 30 μm column increased the signal intensity approximately 3-fold, leading to a 32% increase in the number of identified peptides from 10 ng of a complex sample.³²⁹ Some manufacturers, such as CoAnn Technologies, have responded to the needs of this thriving area and commercialized columns with inner diameters of 10–30 μm for single-cell proteomics studies. Aside from packed bed columns, open-tubular columns hold great promise in single-cell proteomics because columns as narrow as 2 μm can be readily produced (see the section Open-Tubular Columns). Such a diameter should theoretically enhance the MS signal intensity by a factor of 1406 versus a 75 μm column.³¹³ Hence, liquid chromatography is very likely the critical component for achieving proteome coverage in single-cell proteomic studies similar to those we are used to seeing from analyses of standard samples. We refer interested readers to a recent review of Roberg-Larsen et al.³¹⁴ for further reading on the important aspects of liquid chromatography in single-cell proteomics.

The drawback of nanoLC is markedly lower robustness and sample throughput. Nanoflow columns usually suffer from

shorter lifetimes. In one of the world-leading laboratories, a turnover time of nanoflow columns of 10–14 days motivated their members to build a station for multiplexed column packing.²²⁶ Moreover, specific technical solutions in the hardware are linked to nanoLC to deliver accurate gradients at sub $\mu\text{L}/\text{min}$ flow rates and enable the injection of volumes several times exceeding the nanoflow column volumes (for a review, see ref 248). A higher level of expertise relative to conventional-flow systems is required to operate such instruments. Furthermore, troubleshooting in nanoLC is more challenging than in conventional-flow regimes because of its slow responsiveness.

Where one prefers robustness and sample throughput to the absolute sensitivity and samples are available in sufficient quantities, capillary, microbore, and narrow-bore columns can efficiently replace nanoflow columns. Interestingly, the higher sample quantity predicted in proportion to the square of column diameter does not correspond to reality because more aspects contribute to the final picture, such as ionization efficiency and ions sampling on the site of MS and more efficient chromatographic performance of columns with larger diameters. Lenčo et al.⁶⁷ demonstrated that a column with an inner diameter of 1.0 mm under systematically optimized conditions provided a number of identifications comparable to a nanoflow column when a mere 5.3-fold more sample amount was analyzed. This extra sample amount is far from the predicted 178-fold greater burden. The full merit of 1.0 mm microbore columns in terms of sample throughput and robustness in bottom-up proteomics was subsequently reported by Bian et al.^{330,331} Nevertheless, both authors also demonstrated that the microflow regime lags behind the nanoflow LC-MS in the number of identified phosphopeptides. Thus, it is very likely that the application of supra-nanoflow regimes will be constrained only for analyses of whole-proteome samples.

The utilization of columns with an inner diameter of 2.1 mm for data-dependent analyses is somewhat questionable because the results of studies are contradictory.^{67,332–334} No doubt, narrow-bore columns can be successfully applied in analyses where the absolute sensitivity is boosted by targeting the peptides of interest using extraordinarily sensitive triple quadrupole MS instruments. The seminal work by Percy et al.³³⁵ demonstrated the performance merits of narrow-bore columns operated at a conventional flow rate relative to a nanoflow LC-MS platform for quantifying proteins in human plasma.

Column Length

The relationships between the column length, the quality of peptide separation, and the number of identified peptides in bottom-up studies are well-known.^{12,75,336,337} Column length belongs among the method parameters enabling coping with the enormous complexity of unfractionated proteomic samples. Nowadays, bed-packed columns are commercially available for single-shot proteomic analyses with a length of 75 cm (Thermo Fisher Scientific), and even 200 cm monolithic (GL Sciences) and micropillar array columns have been commercialized (PharmaFluidics/Thermo Fisher Scientific).

Equation 22 predicts that peak capacity grows with the square root of N^* that correlates linearly with the column length. The practical gain in the separation performance of longer columns is usually slightly lower than theoretically predicted. The packing is less homogeneous in the longer

columns because particles do not experience the same packing conditions across the column length.^{164,170,171,338} Interestingly, the axial bed heterogeneity seems unavoidable even for *in situ* prepared monolithic columns.³³⁹

Equation 22 further foresees that longer columns are particularly effective for long gradients. On the other hand, they are disadvantageous for very short gradient methods as they produce smaller peak capacity than shorter columns (Figure 24). Moreover, longer column lengths increase t_0 and

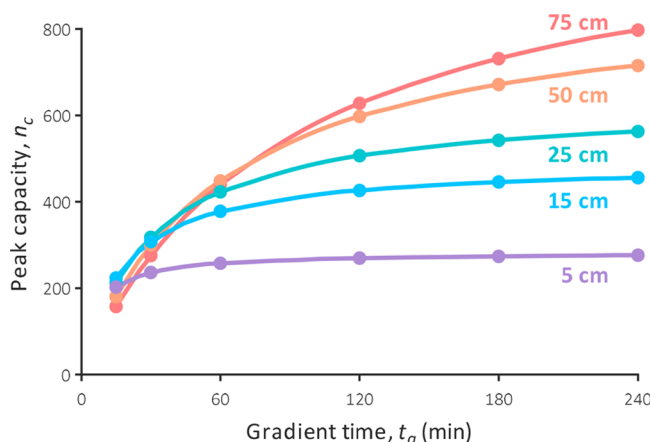


Figure 24. A prediction of peak capacity at various gradient times and column lengths using eq 22. The remaining parameters were identical to the prediction presented in Figure 14.

delay the retention time of all peaks. They also need more time for column equilibration to initial gradient conditions. These two negative effects of using longer columns collectively diminish the sample throughput and the peak capacity per total analysis time.⁷⁵ Therefore, despite being very popular, longer columns should not be perceived as a universal optimal solution for all bottom-up analyses, and their length should be selected based on the gradient time that best accommodates the sample complexity. The accompanying negative effect of longer columns is the higher backpressure, as it is linearly proportional to the column length (eq 36). However, if the generated backpressure approaches the pressure limits of the chromatographic system, the column can be operated under a higher temperature or reduced flow rate, both being beneficial for the number of identified components from a proteomic sample.

Changing a column is a simple procedure in supra nanoflow regimes. However, due to the slow responsiveness of nanoLC, practitioners often balance the time needed to establish stable conditions on the newly installed nanoflow column and possible gains in its proteomic performance. Therefore, running nanoLC-MS analyses using gradients of different times on the same column is customary.

Flow Rate

The flow rate is determined primarily by the inner diameter of the column (Figure 23). Replacing a column with another one of a different inner diameter requires adjusting the flow rate proportionally to the ratio of squared inner diameters.

Peptides are analytes with slow diffusion. Therefore, they require slower flow rates than small molecules to compensate for the mass transfer resistance. Chromatographically optimal flow rate for gradient elution of peptides can be found using pseudo van Deemter plots (Figure 13).¹⁵⁴ However, such flow

rate optimum is extremely low under typical conditions, resulting in concentrated but broad peaks with possible negative consequences on the analysis outputs (see the section **Benefits of Efficient and Reproducible Chromatography in Bottom-Up Proteomics**). Moreover, methods running at a flow rate at the chromatographic optimum would be very long and, thus, highly unpractical. The optimum flow rate can be significantly increased to more practical levels by keeping the column at an elevated temperature (Figure 13).^{107,340}

Flow rate is a parameter that can substantially increase the peak capacity in peptide separation, notably if the stationary phase support has a reduced diffusion path.^{105,154,340,341} For example, if the flow rate increases from 0.250 $\mu\text{L}/\text{min}$ to 0.500 $\mu\text{L}/\text{min}$ in a 15 min model gradient presented in Figure 14, the peak width at half-height w_h theoretically decreases from 2.50 to 1.67 s, and correspondingly, the peak capacity increases from 213 to 318 (the effect of extra-column dispersion was not considered). Although a faster flow rate improves the separation of complex mixtures and diminishes the ion suppression, peptides become more diluted in the mobile phase, decreasing LC-MS analysis sensitivity because MS generally works as a concentration-dependent detector.³²⁶ The latter effect prevails in the analysis of complex mixtures, leading to fewer identified peptides at higher flow rates.⁶⁷ If the uppermost importance is identifying a maximum number of peptides, particularly from a limited sample amount, the flow rate should be decreased to the proteomic optimum level.^{342,343} Proteomic optimum flow rate is the flow rate that provides the maximum number of identified peptides within a given method time. This flow rate is sought only scarcely during method development,³⁴² and usually, a higher final flow rate is applied, likely based on previous experience or information from the literature.

The flow rate shall be kept constant during the effective elution window of the gradient program. However, if the backpressure is far below the tolerated maximum and the method throughput needs to be increased, sample loading, column wash, and the equilibration step can be carried out at higher flow rates.³³¹ Such method tailoring is possible only when pumps can quickly adjust the compression factors of solvents delivered at different pressures caused by the changes in the flow rate.

Gradient Program and Gradient Time

To gradually elute peptides with various hydrophobicities from a reversed-phase column, the concentration of the strong solvent in the mobile phase must progressively increase. The difference in the volume fraction of the strong solvent during the binary gradient $\Delta\phi$ should be optimized so that the peptides elute in a window spanning a maximum range of the programmed elution gradient. Such optimization reduces empty edges in chromatograms, utilizing the instrument time at maximum. Following the effective elution window, a wash step at a high concentration of the strong solvent follows to elute hydrophobic contaminants from the sample, the mobile phase, or the column. If column carryover is significant, fast cycling between the strong and weak solvent instead of a single wash step can be carried out, similarly to LC-MS analysis of small molecules.³⁴⁴

An equilibration step prepares the column for the next injection. Full and repeatable column equilibration can be achieved.³⁴⁵ Repeatable equilibrium level secures run-to-run repeatability even though the full equilibration is not reached.

Repeatable equilibration is sufficient for bottom-up proteomics analyses, increasing the throughput of the method because it can be achieved by percolating mere two column volumes of the mobile phase with the starting composition.³⁴⁶ Because of their high value of the *S* parameter, peptides are virtually trapped at the head of the column upon injection. Therefore, providing that the column inlet is equilibrated independently of the rest of the column, the volume of injected sample dissolved in a weak solvent and the mobile phase filling the gradient delay volume all contribute to the equilibration of the column.¹⁰⁵

The gradient delay volume (V_D) represents the volume of the mobile phase from the point of solvent mixing to the head of the column. It causes a delay between the programmed gradient and the mobile phase composition at the head of the column. The delay volume can be calculated based on the gradient delay time (t_D) using a UV detector from a linear gradient of water versus 0.1% aqueous acetone.³⁴⁷ However, proteomics instrumentation rarely involves a UV detector. The viscosity, and thus the backpressure, is governed by the composition of the mobile phase. Its value ideally does not depend on the direction of the gradient. Based on the assumption that this is also valid for the mobile phase flowing through the tubing of a chromatograph, we propose that the gradient delay volume can be estimated from the pressure readout of a linear increase and decrease of volume fraction of solvents with different viscosities using a detector-free technique (Figure 25). Some practitioners prepend a short isocratic step before the gradient commences. Due to the presence of the gradient delay volume, inserting such a step into the gradient program is usually unnecessary.

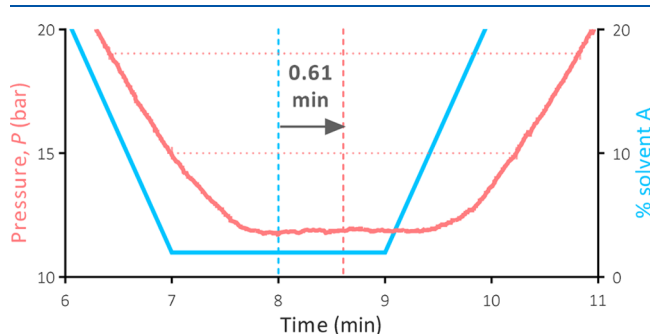


Figure 25. A proposed detector-free technique for estimating the gradient delay volume V_D based on the pressure profile from a linear up and down change in the volume fraction of acetonitrile in the mobile phase. The column was replaced with a zero-dead volume union. The program was: linear increase of solvent B from 2% to 98% between 2 and 7 min followed by an isocratic step of solvent B at 98% for 2 min and linear decrease in solvent B from 98% to 2% between 9 and 14 min. Solvent A and solvent B were aqueous 0.1% formic acid and 0.1% formic acid in acetonitrile, respectively. First, two parallel horizontal lines connecting the same pressure values on the decreasing and increasing arm of the pressure profile were drawn (red dotted lines). Next, a midpoint was found on both lines, and a line intersecting these two points was drawn (red dashed line). If the midpoints are determined accurately, this line is perpendicular to the horizontal lines. The time when the vertical line intersects the y-axis on the extrapolation is readout. This time is subtracted from where the intermediate isocratic step is at its half (8 min) to get the gradient delay time t_D . By multiplying the delay time of 0.61 min by a flow rate of 250 $\mu\text{L}/\text{min}$, the delay volume V_D was determined to be 152 μL .

Typically, the increase in the strong solvent in the mobile phase during the gradient follows a linear function. The linear gradients do not distribute the peptides from complex tryptic digests evenly over the effective elution window of the gradient program.³⁴⁸ Therefore, tools for nonlinear gradient design have been developed to equalize the elution density and maximize the number of peptides identified in an experiment.^{349,350} However, transcribing predicted nonlinear gradient programs to an LC method can be very laborious because such programs have a high number of short segments. Besides, calculations of chromatographic parameters and their predictions from nonlinear gradients using equations derived based on the linear-solvent-strength model are complicated, if not impossible. These drawbacks are arguably behind the fact that these tools have not found broader acceptance among practitioners (Table 2).

A compromise between a full-range linear gradient and a nonlinear gradient is a segmented linear gradient with one main segment and one or two additional short segments at the beginning and/or at the end of the effective elution window. In the main segment, peptides are eluted with a flatter gradient, and in the short segments at the edges, peptides are eluted using steeper gradients. This simple gradient adjustment allows for the distribution of the elution density of peptides across the whole gradient to be more evenly. Moreover, as long as an overwhelming number of peptides elute in the main segment, chromatographic predictions can still be made for most peptides with acceptable extrapolating validity. These gradient programs are becoming very popular (Table 2). Some authors include even more segments, but chromatographic calculations and predictions become challenging again if the main effective elution window is divided into several segments.

Gradient time should primarily correspond to peptide sample complexity. Longer gradients provide greater peak capacity, being beneficial for single-shot analysis of complex samples. Nevertheless, the equation for peak capacity (eq 22) predicts that the relationship between gradient time and peak capacity is not linear, with each additional unit of the peak capacity requiring more time (Figure 24). Experiments confirmed that the peak capacity increases only slowly after a certain gradient time. The moment where the increase in peak capacity with the gradient time starts slowing down depends primarily on the column length.^{105,154,257,337} From this point of view, running long gradients using short columns is not practical. Too long gradients not only increase peak capacity very slowly but also broaden the peaks and lower their heights (Figure 14).³³⁶ Due to this effect, an additional extension of gradients after a certain gradient time can result in fewer identified peptides than a shorter gradient provides despite the higher peak capacity.³⁵¹ Therefore, at a certain point, running multiple short gradients of a fractionated sample using a shorter column provides a higher total peak capacity with sharper peaks than running a lengthy single-shot analysis using a longer column within a restricted instrument time (Figure 26).

The maximum backpressure during a gradient is produced when the typical mobile phase contains around 20% acetonitrile. That is because 20% aqueous acetonitrile has the maximum viscosity out of various volume fractions of acetonitrile in its mixture with water.¹²⁷ In case of the need to experimentally determine the maximum flow rate for a gradient that would produce backpressure still below the pressure limit of the column or the instrument, this must be tested with 20%

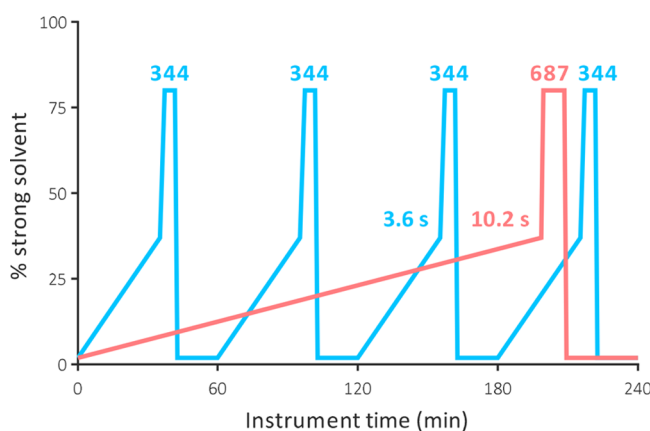


Figure 26. A prediction of the total peak capacity achievable within a total instrument time of 240 min. A peak capacity of 687 with w_h of 10.2 s can be theoretically obtained using single-shot analysis on a 50 cm column. A total peak capacity of 1376 with w_h of 3.6 s can be theoretically obtained by running four gradient analyses of a fractionated sample using a 25 cm column. The time for a wash step was calculated so that one column volume of the mobile phase percolates through each column. Ramping the strong solvent to and from the wash step at 80% of the strong solvent took 1 min. Time for the column equilibration was considered so that three column volumes of mobile phase percolate through each column. A gradient delay volume of 1 μL was assumed. A time of 1 min was reserved for each loading and injection cycle. The remaining parameters were identical to the predictions in Figure 14.

acetonitrile in the mobile phase. Alternatively, the backpressure during the gradient can be estimated from the Kozeny–Carman equation (eq 36).

Mobile Phase Composition

Weak and Strong Solvents. The binary mobile phase for bottom-up analyses is formed from water as the weak solvent and almost exclusively from acetonitrile as the strong solvent (Table 2). Acetonitrile is miscible with water at any ratio, has minimal chemical reactivity, and has a very low viscosity. The last ensures low backpressures and enhances diffusion (eq 23). Acetonitrile is fully compatible with electrospray ionization. In addition, it is reasonably priced except for a short period of the Great Acetonitrile Shortage in 2008–2009.³⁵² These characteristics make acetonitrile the most popular choice for the strong solvent in the RPLC of peptides. A certain amount of water can be added to the strong solvent, for instance, 20%. This is particularly useful when systems without online degassers or systems with low-pressure mixing are used because much less gas can be dissolved in the mixture than in individual components.^{353,354} Adding water to the strong solvent can also smoothen the gradient and pressure profile because the difference in viscosities of the weak and strong components of the mobile phase is lower.

Possible alternatives to acetonitrile represent methanol, ethanol, propanol, and acetone. These solvents provide alternative selectivity and are associated with certain preferences in peptide ionization using electrospray.^{51,355,356} The slightly distinct selectivity has somewhat limited applicability in bottom-up analyses of complex proteomic samples. On the other hand, the substitution of acetonitrile with methanol was previously demonstrated to increase the MS signal of peptides.^{357,358} Methanol thus seems to represent an appealing yet still not fully recognized alternative for analyses of samples with limited protein quantity. The higher

viscosity of methanol with the consequences on backpressure and diffusion of peptides can be compensated by increasing the column temperature by 20 °C.¹²⁷ Another feature currently valued is the “greener” character of the solvent compared to acetonitrile.

Additives for pH Adjustments. The pH of the mobile phase for bottom-up proteomic analyses is traditionally acidic because it did not hydrolyze the silica support of the particulate stationary phase and has positive effects on residual silanols (Table 2). Moreover, acidic pH facilitates protonation of the analytes during electrospray ionization, making it ideal for the downstream MS analysis of peptides and proteins with basic functional groups in the positive mode.³⁵⁹

The pH of the mobile phase should keep peptides at certain dissociation states across analyses. The rule of thumb says that the pH must be at least 1.5 pH units below the lowest $\text{p}K_a$ to achieve stability in retention times across analyses carried out using different batches of weak and strong components of the mobile phase. A secondary function of acidifiers of the mobile phase is to keep residual acidic silanols in the undissociated state to avoid ionic interactions between them and peptides protonated at basic moieties. In addition, by keeping carboxyl groups fully undissociated, the acidifier shall mitigate the chelating tendencies of peptides with multiple acidic residues toward traces of metals present in both the stationary phase and/or the chromatographic system (Figure 27).

Trifluoroacetic acid is a strong, volatile acid with a $\text{p}K_a$ of 0.3. It is a powerful solvent for the solubilization of polypeptides with a low UV cutoff.^{360–362} At the most favorite

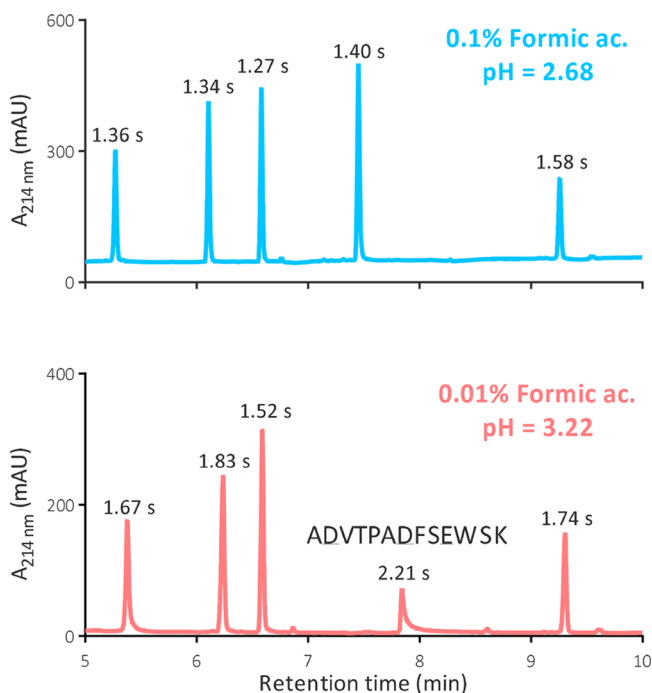


Figure 27. Chelating tendencies of an acidic peptide ADVTPADFS-EWSK with two Asp residues and one Glu residue in the mobile phases acidified with 0.1% formic acid ($\text{pH} = 2.68$) and 0.01% formic acid ($\text{pH} = 3.22$). The values of w_h in seconds are shown above each peak. Averaged values from three consecutive analyses are presented. Peptides were separated using a 12 min linear gradient from 1 to 45% acetonitrile with 0.1% formic acid in a 2.1 × 150 mm Acquity UPLC CSH C₁₈ 1.7 μm , 130 Å column (Waters). The column temperature was 60 °C, and the flow rate was 250 $\mu\text{L}/\text{min}$.

concentration of 0.1% (~ 13 mmol/L), it adjusts the pH theoretically to 1.89. This pH is quite far from the pK_a values of the majority of acidic functional groups on peptides and silanols. Moreover, TFA is 97% dissociated at that pH. The trifluoroacetate anion present at a concentration of 12.7 mmol/L can readily form ion pairs with protonated peptide functionalities, increasing their retentivity and masking them from interacting with high-energy sites. These properties, together with its availability and price, make TFA the preferred acidifier for RPLC of peptides and particularly proteins since its first use by Bennett et al.³⁶³ in 1977. As TFA increases the retention of peptides via forming more hydrophobic ion pairs, it is favored for acidifying the loading solvent that delivers samples from an autosampler in a trap column in nanoLC-MS systems to enhance retention of the least hydrophobic peptides (Table 2).²¹³

When liquid chromatography is online hyphenated to mass spectrometry, the advantages of using TFA for peptide separation quickly become significant disadvantages since the stable ion pairs and the increased surface tension of solutions with TFA prevent efficient ionization using electrospray.^{364,365} Much effort has been spent on keeping TFA usable for LC-MS of peptides and proteins because of its superior chromatographic properties, particularly in RPLC of proteins, where it dramatically limits undesirable secondary interactions and maintain the compact structure of the analytes.^{366–372} While the superior chromatographic performance of TFA, or recently its less fluorinated alternative difluoroacetic acid, added to the mobile phase at least in some percentage, may still predominate the signal suppression in protein LC-MS analyses,^{290,373–375} modern stationary phases with reduced silanol activity and positive surface charge enable efficient separation of peptides only with formic acid.

Formic acid is a volatile acid and, together with TFA, belongs among the most potent solvents for the solubilization of proteins.^{376,377} Its pK_a is 3.75, and, therefore, it theoretically gives a pH of 2.68 at the commonly used concentration of 0.1% (~ 27 mmol/L). At this concentration, only around 8% of the acid is dissociated, yielding a concentration of the formate anion of 2.1 mmol/L. As a result, its ability to form ion pairs with protonated moieties on peptides is reduced. Formic acid currently represents the first choice as the mobile phase acidifier in LC-MS-based proteomics (Table 2). The pH of 2.68 is closer to the pK_a for certain peptides than the required 1.5 units. Therefore, components for the mobile phase acidified by 0.1% formic acid and weak acids, in general, should be mixed with the highest possible accuracy for the best reproducibility of retention times of dissociable analytes across analyses carried out with different batches of weak and strong components of the mobile phase (see the section Acid–Base Properties).

In combination with the current stationary phases featuring dramatically reduced or even eliminated silanol activity, 0.1% formic acid can provide efficient separation of peptides while the electrospray ionization efficiency is not considerably suppressed. However, peak shapes of peptides in such a low-ionic-strength mobile phase exhibit signs of overloading at loads dramatically smaller than when separated in the presence of 0.1% TFA.^{114–116} The cause of this problem is not entirely understood. Interactions between active silanols and positively charged peptides were thought to be the primary underlying phenomenon. However, this explanation was refused to be the only one after introducing stationary phases with practically no

residual silanol activity and purely organic polymer-based stationary phases. Other theories explain the peak distortions of ionic analytes in the low-ionic-strength mobile phase by the mutual repulsion effect of like-charged analytes and/or preferential interactions with high-energy sites in the stationary phase.^{114,277,278} The peak distortions of peptides due to the overloading effect in the low-ionic-strength acidic mobile phase compatible with MS detection motivated column manufacturers to develop stationary phases with a positively charged surface (see the section Chemistry of Bonded Ligands).¹¹⁶

The mobile phase with 0.1% formic acid alone cannot cope with the challenges associated with protein separation. If one is restrained from adding a small amount of TFA or difluoroacetic acid to the mobile phase for LC-MS analyses of proteins, adding a small percentage of 1-butanol can enhance the performance of the low-ionic-strength mobile phase when used with state-of-the-art stationary phases dedicated to the analysis of large proteins.^{193,290}

Some practitioners prefer acidifying the mobile phase using acetic acid rather than formic acid (for recent examples, see refs 378, 379). Acetic acid has a pK_a of 4.75, and at a concentration of 0.1%, it provides a pH of 3.78. The acetate anion is present in a concentration of a mere 0.2 mmol/L in 0.1% acetic acid. Such a meager ionic strength of the mobile phase enhances the overloading of protonated peptides, resulting in the elution of peptides as broader peaks compared to 0.1% formic acid.⁶⁷ Hence, acetic acid must be used at higher concentrations to achieve more efficient peptide separation. For instance, the concentration of 0.5% yields a pH of 2.91, and the concentration of acetate anion increases to 1.2 mmol/L. Such an ionic strength provides separation performance very close to that achievable using 0.1% formic acid. The benefit of using 0.5% acetic acid lies in increased MS signal and, in turn, a higher number of identified peptides versus 0.1% formic acid.⁶⁷ Because of its effect on the MS signal, acetic acid represents an acidifier with very promising potential for analyses of samples with restricted availability. Surprisingly, its use in current bottom-up proteomic analyses is rare (Table 2).

Independently of what particular acid is used to acidify the mobile phase, these diluted solutions have no buffering capacity. Therefore, it is inappropriate to refer to acidified mobile phase components as buffers. Buffer solutions as the mobile phases in proteomics are dominantly used for peptide prefractionation using RPLC at alkaline pH to achieve orthogonal selectivity before final-stage RPLC using an acidic mobile phase hyphenated to a mass spectrometer.^{43,44,113}

Adding a small amount of a base to the acidified mobile phase can create a volatile MS-compatible buffer. The ionic strength of buffers is significantly larger than the ionic strength of solutions containing the same concentration of the acid alone. Increased ionic strength subsequently alleviates the peak distortions due to the overloading effect of positively charged peptides. Ammonium formate-containing mobile phases can provide separation characteristics common for the mobile phase acidified using 0.1% TFA.^{115,117} Using this kind of volatile mobile phase with a stationary phase vulnerable to overloading increases the number of identified peptides and proteins.¹¹⁸ So, aside from the application of stationary phases with the positively charged surface, adding a small amount of ammonia is another powerful approach to handling the overloading problem while keeping the mobile phase still MS-friendly.

Other Additives. Besides the major components, the mobile phase can contain auxiliary additives with specific roles. Among those belong the additives that (i) increase MS sensitivity, (ii) decrease carry-over of peptides, and (iii) reduce chelation of peptides to traces of metals.

Dimethyl sulfoxide (DMSO) in a concentration of 3%^{67,331} or 5%^{380,381} was demonstrated to enhance the MS signal of peptides. Depending on the instrumentation and experimental settings, the MS detection of peptides is increased via charge-state coalescence^{67,381} and/or by more efficient ionization.³⁸⁰ Hahne reported that other solvents with similar physicochemical properties, such as ethylene glycol, can act similarly.³⁸² So, DMSO and similar low volatile liquids can remarkably improve LC-MS proteomic analysis outputs. However, these liquids with low vapor pressure can contaminate the MS instrumentation with a long-surviving memory effect. For instance, DMSO peaks of m/z 79.021 ($\text{DMSO} + \text{H}^+$) and 157.035 (($\text{DMSO}_2 + \text{H}^+$) were detected in the Q Exactive HF-X instrument installed at the Faculty of Pharmacy in Hradec Králové even a few months after the mobile phase containing DMSO was abandoned. In addition, one research group reported instrument fouling because of using DMSO.³⁸³ On the other hand, Küster's group has been using DMSO to boost MS sensitivity for almost a decade without reporting any issues.

An important benefit of adding DMSO to the mobile phase is that it dramatically reduces the carry-over.³⁸⁰ A similar positive effect on the carry-over can be gained without the memory effect of DMSO by replacing a portion of acetonitrile in the strong component of the mobile phase with a more potent solvent. Peptides bound strongly to a reversed-phase stationary phase can be removed by adding trifluoroethanol to the strong solvent. In nanoLC-MS realized using the trap-elute setup, the loading solvent line deserves particular attention in terms of the carry-over.³⁸⁴ For a comprehensive work concerning unwanted adsorption of peptides in LC-MS analyses that also covers the carry-over problem, we refer the readers to the review by Maes et al.³⁸⁵

At the typically used concentration of 0.1%, formic acid adjusts pH to 2.68. This pH may not completely dedissociate all acidic residues on peptides, exacerbating their chelating tendencies.³⁸⁶ Chelating additives, such as acetylacetone, citrate, and medronic acid, can be added in low $\mu\text{mol/L}$ or mmol/L concentrations to the mobile phase to improve the recovery and peak shape of peptides with strong chelating properties, including phosphopeptides (see the section **Amino Acids with Chelating Properties**).^{140,386–388} Chelating additives also reduce in-column Met oxidation associated with the traces of metals.¹⁴⁴

Loading Solvent. The solvent for loading peptides into the trap column should have minimum elution strength to retain even the most hydrophilic peptides, particularly if the stationary phase has lower retentivity than the stationary phase in the separation column. It is not uncommon that the loading phase contains no strong solvent (Table 2). The desired retention of peptides can be further enhanced using stronger ion-pairing acidifiers with more hydrophobic counteranions because peptide retention increases in the order 0.5% acetic acid < 0.1% formic acid < 0.1% trifluoroacetic acid < 0.1% heptafluorobutyric acid. Compared to acetic acid, the solvents in the increased order of ion-pairing properties retain peptides by 0.7, 6.29, and 12.28% acetonitrile per average tryptic peptide and 0.28, 2.37, and 4.62% acetonitrile per each positively charged group. Alternatively, manipulation with trap

column temperature and temperature of the loading solvent can increase the retention of peptides in the trap column during sample loading.^{389,390}

Column Temperature

The column temperature represents an exceptionally cost-effective and powerful means that can substantially improve RPLC peptide separation. Unfortunately, its benefits are generally overlooked in bottom-up proteomics, perhaps due to the requirement of additional LC accessories. Indeed, to obtain 50 records regarding the column temperature for each of the two distinct periods, we had to investigate the details of 315 proteomic data sets deposited at the ProteomeXchange repository in 2020 and 209 studies deposited in 2022 (Table 2).

The most noticeable effects of elevated column temperature are undoubtedly decreased retention and lower backpressure. An increment of 5 °C in column temperature has an effect analogous to increasing acetonitrile concentration in the mobile phase by 1%.¹⁰⁶ The lower backpressure results from the decreased viscosity of the mobile phase passing the packed bed column, as can be inferred from the Kozeny–Carman equation (eq 36). The viscosity of acetonitrile–water mixture at temperatures up to 60 °C was tabulated by Colin et al.³⁹¹ For precise calculations, the viscosity of acetonitrile–water mixture at temperatures between 20 and 100 °C corrected for pressure can be applied.¹²⁷

The lower backpressure is a typical motivation for using an elevated temperature in proteomic analyses, particularly when long columns packed with sub-2 μm particles are used. Its effect on the peptide diffusivity and their adsorption–desorption kinetics is less recognized by the practitioners yet more important. Slow diffusion and lower adsorption–desorption rate of peptides cause that flow rates typically used in proteomic LC-MS analyses are far above the van Deemter optimum, i.e., in the range where the resistance to mass transfer (C term) is the dominant contributor to the in-column band broadening. According to the empirical equation proposed by Young et al.,¹²⁵ the peptide diffusivity can be enhanced by elevated temperature directly and indirectly via the decreased solvent viscosity (eq 23). Elevated temperature also enhances the rate constant of adsorption, k_{ads} .¹⁴⁹ In turn, faster diffusion and an enhanced sorption rate improve the mass transfer of peptides between the mobile and stationary phases.³⁹² As a result, the van Deemter minimum shifts to higher flow rates, and the van Deemter plot flattens at higher column temperatures. In the bottom-up proteomics analyses, this manifests itself as narrower peaks of peptides eluted at the initial flow rate (Figure 13).¹⁰⁷

The temperature has also been shown to enhance the recovery of peptides, thus minimizing their carry-over.³⁹³ This applies particularly to hydrophobic peptides.^{394,395} Finally, the chromatographic behavior of polypeptides containing Pro–Pro bonds can principally profit from elevated temperature because of their very slow *cis*–*trans* isomerization kinetics.^{142,396} These peptides, in particular, benefit from being separated at temperatures even above 60 °C (see the section **Peptides with Vicinal Prolines**).¹⁰⁷

Compared to tryptic peptides, intact proteins are much larger molecules with exceptionally slow diffusion and many interaction sites, resulting in profound resistance to mass transfer and strong adsorption to the stationary phase. Because these phenomena are temperature-dependent, raising the

column temperature has a 2-fold positive effect. It promotes protein diffusion and accelerates their adsorption–desorption kinetics. Indeed, experiments involving large protein bio-pharmaceuticals demonstrate that efficient separation of intact proteins with high recoveries is difficult to achieve without increasing the column temperature.^{193,194,239,397} The merit of top-down proteomics is the characterization of proteoforms varying in post-translational modifications. Therefore, practitioners must be aware of the thermostability of these modifications to exploit the benefits of elevated column temperature in top-down proteomics wisely.

The temperature mismatch is observed when the incoming mobile phase does not have enough time to heat up to the programmed column temperature. Consequently, the temperature and hence the viscosity along the column wall to where a thermostat delivers heat faster is not the same as in the column center, resulting in band broadening.¹⁹⁷ Due to the short distance from column walls to the center of nanoflow and capillary columns and usually slower mobile phase velocities in the inlet capillary, temperature mismatch is not observed in typical LC-MS proteomic analyses. Mobile phase preconditioning using a passive or active preheater efficiently mitigates the issue of the radial temperature gradient in columns with larger inner diameters.¹⁰⁷ An online metal filter placed ahead of the column in the column thermostat is assumed to provide a similar service.³⁹⁸

A high temperature negatively affects the stability of silica-based stationary phases. However, current columns for reversed-phase chromatography packed with hybrid technology particles, sterically protected silica-based particles, and polydentate silica stationary phases can be operated using the acidified mobile phase at 80 °C and even at 90 °C.^{276,399} Still, operating columns at the maximum tolerated temperature shortens the lifespan of each column. In addition, one should be aware that a column becomes an effective reactor that can lead to a decreased number of identified components from a proteomic sample in long bottom-up analyses because of inducing artificial modifications and cleavage of peptide bonds.^{67,107} Even if the thermal instability of particular samples excludes using column heating, the column should be thermostated at a certain safe temperature to avoid shifts in retention time and backpressure fluctuations owing to room temperature fluctuations, for instance, because of hysteresis of the air conditioning.

Sample Load

The association between the amount of injected sample and the number of identified peptides fits well the plot typical of saturation binding experiments.^{342,351,400,401} The number of identified peptides (p) from an injected amount of sample (m_{inj}) can be predicted using the maximum number of identifiable peptides (p_{max}) and amount of material needed to achieve 50% of p_{max} ($m_{50\%}$) that are the coefficients determining the nonlinear regression model (eq 37).

$$p = \frac{p_{max} \cdot m_{inj}}{m_{50\%} + m_{inj}} \quad (37)$$

The number of identified peptides increases with a steep slope to approximately 80% of p_{max} (Figure 28). Then, the trend slows down, and roughly above 90% of p_{max} an ever-decreasing number of additionally identified peptides requires an even much higher amount of injected material. If practitioners register only a minor increase after, for instance, doubling the

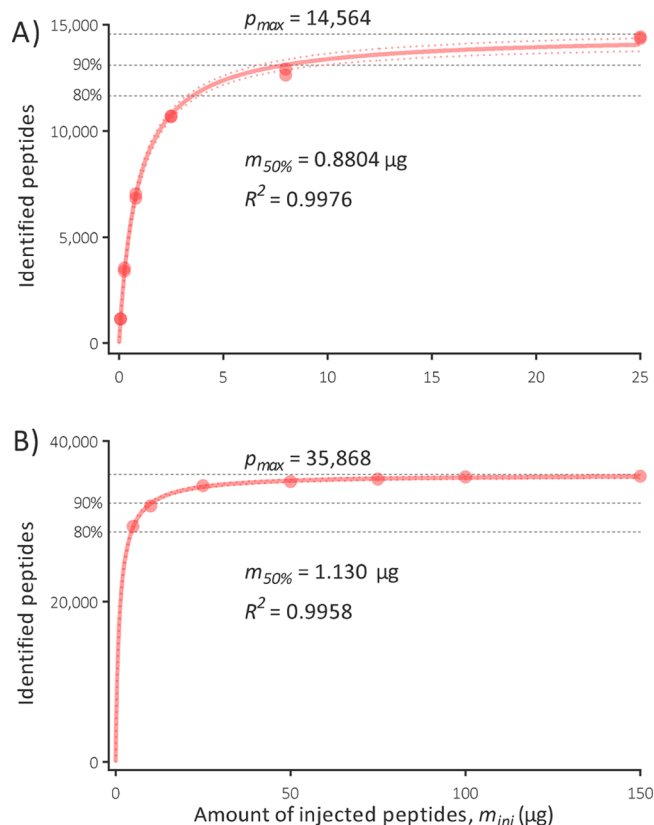


Figure 28. Nonlinear dependency between the quantity of analyzed material and the number of identified peptides in bottom-up analyses. (A) The tryptic peptides of a bacterium *F. tularensis* were separated in a 1.0 × 150 mm Halo Peptide ES-C18, 2.7 μm, 160 Å column (Advanced Materials Technology) using a 32 min gradient. A Top10 data-dependent acquisition setup described earlier was used.¹⁴ Data from duplicates for each injection level are present. (B) LC-MS data previously published by Bian et al.³⁵¹ were used to create the plot. Data from one replicate were available for each injection level. Dot lines define a 95% confidence interval in both plots.

quantity of injected material, they should optimize their RPLC method and/or MS settings rather than continue further increasing the injection.

Practitioners who are unaware of the sudden change in the curve between 80% and 90% of p_{max} sometimes inject more material than the column can tolerate with a desire to expand the list of identified peptides and proteins, leading to mass overloading. Mass overloading results in deterioration of the peak shape^{342,401,402} with all the consequences, and eventually, can have the opposite than the desired effect, the number of identified peptides and proteins decreases.⁴⁰³ In addition, the carry-over of the sample to the subsequent runs can be significant if specific remedies are not taken. Mass overloading is related to many factors, such as analyte, ligand chain length, ligand coverage, surface area, end-capping, pH of the mobile phase, and its ionic strength.^{241,402} However, the most crucial parameter related to mass overloading in the RPLC separation of peptides is the cross-section of the column. In this context, it is worth noting that Chervet et al.⁴⁰⁴ predicted that the maximum injected amount of an isocratically eluted analyte should not exceed 50 ng for a 75 μm × 150 mm column.

Upon injection, peptides are concentrated in a very thin layer of the stationary phase. If the amount of injected peptides exceeds the tolerable level, they can turn into particulate solids

and damage the column, mainly when not completely digested proteins are also present in the sample. Provided that the peptides would focus on, let us say, a 0.25 mm layer of stationary phase, injecting 5 μg of peptides directly in a nanoflow column with a 75 μm inner diameter theoretically creates a local peptide concentration of 4.5 mg/ μL . No study on the particular mechanism was found in the peer-reviewed literature, but the very high concentration of analytes is often linked to creating a secondary stationary phase or inducing peptide aggregation and precipitation accompanied by an increase in backpressure.

The volume overloading concerns primarily isocratic elution or analytes with a small S parameter. In such a case, the injection volume for a 75 $\mu\text{m} \times 150$ mm column should not exceed several nanoliters.⁴⁰⁴ In gradient RPLC, volume overloading affects only a small subset of peptides, i.e., the most hydrophilic ones. Other, more hydrophobic peptides are more or less refocused at the head of the column thanks to high values of the S parameter. Therefore, the injection volume in nanoLC can be far much larger than is the column volume (see also the section [S Parameter](#)).

Increasing the peptide concentration in the sample and injecting a proportionally smaller volume can at least partially mitigate the volume overloading effect of the most hydrophilic peptides. Alternatively, the strength of the sample solvent can be reduced. This is typically not an issue in RPLC of peptides because they are generally well soluble in the aqueous environment. Hence, in contrast to HILIC,⁴⁰⁵ it is easy to deliver the peptides into the column in sample solvent identical to the composition of the mobile phase at the beginning of the gradient. In the trap-elute configuration, the retention of peptides can be readily increased by acidifying the loading solvent with TFA instead of formic acid (see the section [Loading Solvent](#)).

CHROMATOGRAPHIC SYSTEMS

The authors of this tutorial are aware that the theoretical knowledge of liquid chromatography solely cannot provide excellent LC-MS chromatograms. It is mandatory for each user to be thoroughly familiarized with the instrument platforms they operate. The focus of this tutorial does not involve discussion on technical aspects of the chromatography instrumentation commonly used in proteomics. Nevertheless, we would at least like to refer readers who are interested in the technical details of nanoLC to a review by Šesták et al.²⁴⁸ We also recommend reading articles published by John Dolan in 2016^{406–409} and a few recent articles^{410–412} focused on LC instrumentation in general published in LCGC magazine, a precious free source on different topics of chromatography.

CONCLUSION

The performance of the state-of-the-art mass spectrometers in bottom-up proteomics is astonishing. However, it has been demonstrated in several studies and experiments, including those presented in this tutorial, that the performance of the mass spectrometers cannot mirror their full potential when the quality of the peptide separation is not superior. Some proteomics groups have realized the need for excellent peptide chromatography for current LC-MS-based proteomics, and we assume their number will increase. We also anticipate that larger proteomics centers will include experts with a strong background in separation sciences to respond to that need

readily, similarly as they include experts in mass spectrometry, bioinformatics, and statistics.

In this tutorial, we sought to summarize key aspects and basic knowledge of the fundamentals of peptide separation using RPLC for bottom-up proteomic applications. We believe that this tutorial will facilitate users to develop high- and ultrahigh-efficient chromatographic methods and/or help them troubleshoot the issues they may encounter during the RPLC of peptides so that they can fully exploit the potential of their MS instruments. Our ambition was not to write comprehensive guidance that should substitute the essential literature in chromatography. In reality, we hope for the opposite effect, i.e., that this tutorial will stimulate the interest of practitioners focused on proteomics in reading articles and books on the fundamentals of chromatography to boost the performance of their RPLC methods. From the myriad of books written about liquid chromatography, we would like to recommend at least one. The excellent book *Introduction to modern liquid chromatography* by Snyder, Kirkland, and Dolan is perhaps the best starting point for quickly gaining solid knowledge in the area.⁹⁶

ASSOCIATED CONTENT

Data Availability Statement

The LC-MS proteomics data subjected to protein identification have been deposited to the ProteomeXchange Consortium via the PRIDE⁴¹³ partner repository with the dataset identifier PXD036783.

Supporting Information

The Supporting Information is available free of charge at <https://pubs.acs.org/doi/10.1021/acs.jproteome.2c00407>.

Figure S1: One hundred total ion current chromatograms exported from data sets deposited at ProteomeX-change repository from July 27th, 2020 onward ([PDF](#))

AUTHOR INFORMATION

Corresponding Author

Juraj Lenčo – Department of Analytical Chemistry, Faculty of Pharmacy in Hradec Králové, Charles University, 500 05 Hradec Králové, Czech Republic;  orcid.org/0000-0002-8526-9249; Phone: +420 495 067 381; Email: lenco@faf.cuni.cz

Authors

Siddharth Jadeja – Department of Analytical Chemistry, Faculty of Pharmacy in Hradec Králové, Charles University, 500 05 Hradec Králové, Czech Republic

Denis K. Naplekov – Department of Analytical Chemistry, Faculty of Pharmacy in Hradec Králové, Charles University, 500 05 Hradec Králové, Czech Republic

Oleg V. Krokhin – Department of Internal Medicine, Manitoba Centre for Proteomics and Systems Biology, University of Manitoba, Winnipeg R3E 3P4 Manitoba, Canada;  orcid.org/0000-0002-9989-6593

Maria A. Khalikova – Department of Analytical Chemistry, Faculty of Pharmacy in Hradec Králové, Charles University, 500 05 Hradec Králové, Czech Republic

Petr Chocholouš – Department of Analytical Chemistry, Faculty of Pharmacy in Hradec Králové, Charles University, 500 05 Hradec Králové, Czech Republic;  orcid.org/0000-0002-6919-6449

Jiří Urban – Department of Chemistry, Faculty of Science, Masaryk University, 625 00 Brno, Czech Republic; [ORCID iD](https://orcid.org/0000-0002-5169-4327)

Ken Broeckhoven – Department of Chemical Engineering (CHIS), Faculty of Engineering, Vrije Universiteit Brussel, 1050 Brussel, Belgium; [ORCID iD](https://orcid.org/0000-0003-0524-7830)

Lucie Nováková – Department of Analytical Chemistry, Faculty of Pharmacy in Hradec Králové, Charles University, 500 05 Hradec Králové, Czech Republic

František Švec – Department of Analytical Chemistry, Faculty of Pharmacy in Hradec Králové, Charles University, 500 05 Hradec Králové, Czech Republic; [ORCID iD](https://orcid.org/0000-0001-6574-1537)

Complete contact information is available at:
<https://pubs.acs.org/10.1021/acs.jproteome.2c00407>

Notes

The authors declare no competing financial interest.

ACKNOWLEDGMENTS

The authors gratefully acknowledge the financial support of the STARSS project (Reg. No. CZ.02.1.01/0.0/0.0/15_003/0000465) cofunded by ERDF, the Project of the Czech Science Foundation (GAČR No. 22-21620S), the Project of the Charles University Grant Agency (GAUK No. 370522), and the SVV Project No. 260 548. The authors also thank Mykyta Starovoit for acquiring chromatograms simulating the trap-elute setup injections.

REFERENCES

- (1) Meier, F.; Geyer, P. E.; Virreira Winter, S.; Cox, J.; Mann, M. BoxCar acquisition method enables single-shot proteomics at a depth of 10,000 proteins in 100 minutes. *Nat. Methods* **2018**, *15* (6), 440–448.
- (2) Meier, F.; Brunner, A. D.; Koch, S.; Koch, H.; Lubeck, M.; Krause, M.; Goedecke, N.; Decker, J.; Kosinski, T.; Park, M. A.; Bache, N.; Hoerning, O.; Cox, J.; Rather, O.; Mann, M. Online Parallel Accumulation-Serial Fragmentation (PASEF) with a Novel Trapped Ion Mobility Mass Spectrometer. *Mol. Cell Proteomics* **2018**, *17* (12), 2534–2545.
- (3) Muntel, J.; Gandhi, T.; Verbeke, L.; Bernhardt, O. M.; Treiber, T.; Bruderer, R.; Reiter, L. Surpassing 10 000 identified and quantified proteins in a single run by optimizing current LC-MS instrumentation and data analysis strategy. *Mol. Omics* **2019**, *15* (5), 348–360.
- (4) Bekker-Jensen, D. B.; Martinez-Val, A.; Steigerwald, S.; Ruther, P.; Fort, K. L.; Arrey, T. N.; Harder, A.; Makarov, A.; Olsen, J. V. A Compact Quadrupole-Orbitrap Mass Spectrometer with FAIMS Interface Improves Proteome Coverage in Short LC Gradients. *Mol. Cell Proteomics* **2020**, *19* (4), 716–729.
- (5) Meier, F.; Brunner, A. D.; Frank, M.; Ha, A.; Bludau, I.; Voytik, E.; Kaspar-Schoenfeld, S.; Lubeck, M.; Raether, O.; Bache, N.; Aebersold, R.; Collins, B. C.; Rost, H. L.; Mann, M. diaPASEF: parallel accumulation-serial fragmentation combined with data-independent acquisition. *Nat. Methods* **2020**, *17* (12), 1229–1236.
- (6) Meier, F.; Brunner, A. D.; Frank, M.; Ha, A.; Bludau, I.; Voytik, E.; Kaspar-Schoenfeld, S.; Lubeck, M.; Raether, O.; Bache, N.; Aebersold, R.; Collins, B.; Rost, H. L.; Mann, M. diaPASEF: parallel accumulation-serial fragmentation combined with data-independent acquisition. *Nat. Methods* **2020**, *17* (12), 1229–1236.
- (7) Messner, C. B.; Demichev, V.; Bloomfield, N.; Yu, J. S. L.; White, M.; Kreidl, M.; Egger, A. S.; Freiwald, A.; Ivosev, G.; Wasim, F.; Zelezniak, A.; Jurgens, L.; Suttorp, N.; Sander, L. E.; Kurth, F.; Lilley, K. S.; Mülleder, M.; Tate, S.; Ralser, M. Ultra-fast proteomics with Scanning SWATH. *Nat. Biotechnol.* **2021**, *39* (7), 846–854.
- (8) Demichev, V.; Szrywił, L.; Yu, F.; Teo, G. C.; Rosenberger, G.; Niewienda, A.; Ludwig, D.; Decker, J.; Kaspar-Schoenfeld, S.; Lilley, K. S.; Mülleder, M.; Nesvizhskii, A. I.; Ralser, M. dia-PASEF data analysis using FragPipe and DIA-NN for deep proteomics of low sample amounts. *Nat. Commun.* **2022**, *13* (1), 3944.
- (9) MacNair, J. E.; Lewis, K. C.; Jorgenson, J. W. Ultrahigh-pressure reversed-phase liquid chromatography in packed capillary columns. *Anal. Chem.* **1997**, *69* (6), 983–9.
- (10) Kirkland, J. J.; Langlois, T. J.; DeStefano, J. J. Fused core particles for HPLC columns. *Am. Lab.* **2007**, *39* (8), 18–21.
- (11) Koen, S.; Pat, S.; Wim De, M.; Gert, D.; Ruben, t. K.; Jeff Op De, B.; Bo, C.; Jonathan, V. Evaluation of Micro-Pillar Array Columns (μ PAC) Combined with High Resolution Mass Spectrometry for Lipidomics. *Special Issues* **2017**, *30* (6), 6–13.
- (12) Shishkova, E.; Hebert, A. S.; Coon, J. J. Now, More Than Ever, Proteomics Needs Better Chromatography. *Cell Syst* **2016**, *3* (4), 321–324.
- (13) McCormack, A. L.; Schieltz, D. M.; Goode, B.; Yang, S.; Barnes, G.; Drubin, D.; Yates, J. R., 3rd Direct analysis and identification of proteins in mixtures by LC/MS/MS and database searching at the low-femtomole level. *Anal. Chem.* **1997**, *69* (4), 767–76.
- (14) Lenco, J.; Khalikova, M. A.; Švec, F. Dissolving Peptides in 0.1% Formic Acid Brings Risk of Artificial Formylation. *J. Proteome Res.* **2020**, *19* (3), 993–999.
- (15) Vizcaino, J. A.; Deutsch, E. W.; Wang, R.; Csordas, A.; Reisinger, F.; Rios, D.; Dianes, J. A.; Sun, Z.; Farrah, T.; Bandeira, N.; Binz, P. A.; Xenarios, I.; Eisenacher, M.; Mayer, G.; Gatto, L.; Campos, A.; Chalkley, R. J.; Kraus, H. J.; Albar, J. P.; Martinez-Bartolome, S.; Apweiler, R.; Omenn, G. S.; Martens, L.; Jones, A. R.; Hermjakob, H. ProteomeXchange provides globally coordinated proteomics data submission and dissemination. *Nat. Biotechnol.* **2014**, *32* (3), 223–6.
- (16) MacLean, B.; Tomazela, D. M.; Shulman, N.; Chambers, M.; Finney, G. L.; Frewen, B.; Kern, R.; Tabb, D. L.; Liebler, D. C.; MacCoss, M. J. Skyline: an open source document editor for creating and analyzing targeted proteomics experiments. *Bioinformatics* **2010**, *26* (7), 966–8.
- (17) Toby, T. K.; Fornelli, L.; Kelleher, N. L. Progress in Top-Down Proteomics and the Analysis of Proteoforms. *Annu. Rev. Anal. Chem. (Palo Alto Calif.)* **2016**, *9* (1), 499–519.
- (18) Chen, B.; Brown, K. A.; Lin, Z.; Ge, Y. Top-Down Proteomics: Ready for Prime Time? *Anal. Chem.* **2018**, *90* (1), 110–127.
- (19) Nickerson, J. L.; Baghalabadi, V.; Rajendran, S.; Jakubec, P. J.; Said, H.; McMillen, T. S.; Dang, Z.; Doucette, A. A. Recent advances in top-down proteome sample processing ahead of MS analysis. *Mass Spectrom. Rev.* **2021**, 1–39.
- (20) Melby, J. A.; Roberts, D. S.; Larson, E. J.; Brown, K. A.; Bayne, E. F.; Jin, S.; Ge, Y. Novel Strategies to Address the Challenges in Top-Down Proteomics. *J. Am. Soc. Mass Spectrom.* **2021**, *32* (6), 1278–1294.
- (21) Schappler, J.; Nicoli, R.; Nguyen, D.; Rudaz, S.; Veuthey, J. L.; Guillarme, D. Coupling ultra high-pressure liquid chromatography with single quadrupole mass spectrometry for the analysis of a complex drug mixture. *Talanta* **2009**, *78* (2), 377–87.
- (22) Pino, L. K.; Just, S. C.; MacCoss, M. J.; Searle, B. C. Acquiring and Analyzing Data Independent Acquisition Proteomics Experiments without Spectrum Libraries. *Mol. Cell Proteomics* **2020**, *19* (7), 1088–1103.
- (23) Bruderer, R.; Bernhardt, O. M.; Gandhi, T.; Xuan, Y.; Sondermann, J.; Schmidt, M.; Gomez-Varela, D.; Reiter, L. Optimization of Experimental Parameters in Data-Independent Mass Spectrometry Significantly Increases Depth and Reproducibility of Results. *Mol. Cell Proteomics* **2017**, *16* (12), 2296–2309.
- (24) Cai, J. W.; Yan, Z. Y. Re-Examining the Impact of Minimal Scans in Liquid Chromatography-Mass Spectrometry Analysis. *J. Am. Soc. Mass Spectrom.* **2021**, *32* (8), 2110–2122.
- (25) Doellinger, J.; Blumenscheit, C.; Schneider, A.; Lasch, P. Isolation Window Optimization of Data-Independent Acquisition

- Using Predicted Libraries for Deep and Accurate Proteome Profiling. *Anal. Chem.* **2020**, *92* (18), 12185–12192.
- (26) Villalobos Solis, M. I.; Giannone, R. J.; Hettich, R. L.; Abraham, P. E. Exploiting the Dynamic Relationship between Peptide Separation Quality and Peptide Coisolation in a Multiple-Peptide Matches-per-Spectrum Approach Offers a Strategy To Optimize Bottom-Up Proteomics Throughput and Depth. *Anal. Chem.* **2019**, *91* (11), 7273–7279.
- (27) Cox, J.; Neuhauser, N.; Michalski, A.; Scheltema, R. A.; Olsen, J. V.; Mann, M. Andromeda: a peptide search engine integrated into the MaxQuant environment. *J. Proteome Res.* **2011**, *10* (4), 1794–805.
- (28) Zhang, B.; Pirmoradian, M.; Chernobrovkin, A.; Zubarev, R. A. DeMix workflow for efficient identification of cofragmented peptides in high resolution data-dependent tandem mass spectrometry. *Mol. Cell Proteomics* **2014**, *13* (11), 3211–23.
- (29) Shteynberg, D.; Mendoza, L.; Hoopmann, M. R.; Sun, Z.; Schmidt, F.; Deutsch, E. W.; Moritz, R. L. reSpect: software for identification of high and low abundance ion species in chimeric tandem mass spectra. *J. Am. Soc. Mass Spectrom.* **2015**, *26* (11), 1837–47.
- (30) Dorfer, V.; Maltsev, S.; Winkler, S.; Mechtler, K. CharmeRT: Boosting Peptide Identifications by Chimeric Spectra Identification and Retention Time Prediction. *J. Proteome Res.* **2018**, *17* (8), 2581–2589.
- (31) Karp, N. A.; Huber, W.; Sadowski, P. G.; Charles, P. D.; Hester, S. V.; Lilley, K. S. Addressing accuracy and precision issues in iTRAQ quantitation. *Mol. Cell Proteomics* **2010**, *9* (9), 1885–97.
- (32) Ting, L.; Rad, R.; Gygi, S. P.; Haas, W. MS3 eliminates ratio distortion in isobaric multiplexed quantitative proteomics. *Nat. Methods* **2011**, *8* (11), 937–40.
- (33) Savitski, M. M.; Mathieson, T.; Zinn, N.; Sweetman, G.; Doce, C.; Becher, I.; Pachl, F.; Kuster, B.; Bantscheff, M. Measuring and managing ratio compression for accurate iTRAQ/TMT quantification. *J. Proteome Res.* **2013**, *12* (8), 3586–98.
- (34) Strittmatter, E. F.; Kangas, L. J.; Petritis, K.; Mottaz, H. M.; Anderson, G. A.; Shen, Y.; Jacobs, J. M.; Camp, D. G., 2nd; Smith, R. D. Application of peptide LC retention time information in a discriminant function for peptide identification by tandem mass spectrometry. *J. Proteome Res.* **2004**, *3* (4), 760–9.
- (35) Gessulat, S.; Schmidt, T.; Zolg, D. P.; Samaras, P.; Schnatbaum, K.; Zerweck, J.; Knaute, T.; Rechenberger, J.; Delanghe, B.; Huhmer, A.; Reimer, U.; Ehrlich, H. C.; Aiche, S.; Kuster, B.; Wilhelm, M. ProSIT: proteome-wide prediction of peptide tandem mass spectra by deep learning. *Nat. Methods* **2019**, *16* (6), 509–518.
- (36) Chen, A. T.; Franks, A.; Slavov, N. DART-ID increases single-cell proteome coverage. *PLoS Comput. Biol.* **2019**, *15* (7), e1007082.
- (37) Klammer, A. A.; Yi, X.; MacCoss, M. J.; Noble, W. S. Improving tandem mass spectrum identification using peptide retention time prediction across diverse chromatography conditions. *Anal. Chem.* **2007**, *79* (16), 6111–8.
- (38) Pfeifer, N.; Leinenbach, A.; Huber, C. G.; Kohlbacher, O. Improving peptide identification in proteome analysis by a two-dimensional retention time filtering approach. *J. Proteome Res.* **2009**, *8* (8), 4109–15.
- (39) Escher, C.; Reiter, L.; MacLean, B.; Ossola, R.; Herzog, F.; Chilton, J.; MacCoss, M. J.; Rinner, O. Using iRT, a normalized retention time for more targeted measurement of peptides. *Proteomics* **2012**, *12* (8), 1111–21.
- (40) McQueen, P.; Spicer, V.; Rydzak, T.; Sparling, R.; Levin, D.; Wilkins, J. A.; Krokhin, O. Information-dependent LC-MS/MS acquisition with exclusion lists potentially generated on-the-fly: case study using a whole cell digest of Clostridium thermocellum. *Proteomics* **2012**, *12* (8), 1160–9.
- (41) Moruz, L.; Kall, L. Peptide retention time prediction. *Mass Spectrom Rev.* **2017**, *36* (5), 615–623.
- (42) Bern, M.; Kil, Y. J.; Becker, C. Byonic: advanced peptide and protein identification software. *Curr. Protoc Bioinformatics* **2012**, Chapter 13, Unit 13.20. DOI: [10.1002/0471250953.bi1320s40](https://doi.org/10.1002/0471250953.bi1320s40).
- (43) Yeung, D.; Mizero, B.; Gussakovskiy, D.; Klaassen, N.; Lao, Y.; Spicer, V.; Krokhin, O. V. Separation Orthogonality in Liquid Chromatography-Mass Spectrometry for Proteomic Applications: Comparison of 16 Different Two-Dimensional Combinations. *Anal. Chem.* **2020**, *92* (5), 3904–3912.
- (44) Gilar, M.; Olivova, P.; Daly, A. E.; Gebler, J. C. Orthogonality of separation in two-dimensional liquid chromatography. *Anal. Chem.* **2005**, *77* (19), 6426–34.
- (45) Horváth, C.; Melander, W.; Molnár, I. Solvophobic interactions in liquid chromatography with nonpolar stationary phases. *Journal of Chromatography A* **1976**, *125* (1), 129–156.
- (46) Vailaya, A.; Horvath, C. Retention in reversed-phase chromatography: partition or adsorption? *J. Chromatogr A* **1998**, *829* (1–2), 1–27.
- (47) Dill, K. A. The mechanism of solute retention in reversed-phase liquid chromatography. *J. Phys. Chem.* **1987**, *91* (7), 1980–1988.
- (48) Dorsey, J. G.; Dill, K. A. The Molecular Mechanism of Retention in Reversed-Phase Liquid Chromatography. *Chem. Rev.* **1989**, *89* (2), 331–346.
- (49) Regnier, F. E. The role of protein structure in chromatographic behavior. *Science* **1987**, *238* (4825), 319–23.
- (50) Lau, S. Y. M.; Taneja, A. K.; Hodges, R. S. Effects of High-Performance Liquid-Chromatographic Solvents and Hydrophobic Matrices on the Secondary and Quaternary Structure of a Model Protein - Reversed-Phase and Size-Exclusion High-Performance Liquid-Chromatography. *J. Chromatogr.* **1984**, *317* (Dec), 129–140.
- (51) Gilar, M.; Jaworski, A.; McDonald, T. S. Solvent selectivity and strength in reversed-phase liquid chromatography separation of peptides. *J. Chromatogr A* **2014**, *1337*, 140–6.
- (52) Hancock, W. S.; Bishop, C. A.; Prestidge, R. L.; Harding, D. R.; Hearn, M. T. Reversed-phase, high-pressure liquid chromatography of peptides and proteins with ion-pairing reagents. *Science* **1978**, *200* (4346), 1168–70.
- (53) Horvath, C.; Melander, W.; Molnar, I.; Molnar, P. Enhancement of retention by ion-pair formation in liquid chromatography with nonpolar stationary phases. *Anal. Chem.* **1977**, *49* (14), 2295–2305.
- (54) Snyder, L. R.; Dolan, J. W.; Gant, J. R. Gradient elution in high-performance liquid chromatography: I. Theoretical basis for reversed-phase systems. *Journal of Chromatography A* **1979**, *165* (1), 3–30.
- (55) Jandera, P.; Churáček, J. Gradient elution in liquid chromatography: I. The influence of the composition of the mobile phase on the capacity ratio (retention volume, band width, and resolution) in isocratic elution — theoretical considerations. *Journal of Chromatography A* **1974**, *91*, 207–221.
- (56) Fekete, S.; Beck, A.; Veuthey, J. L.; Guillarme, D. Proof of Concept To Achieve Infinite Selectivity for the Chromatographic Separation of Therapeutic Proteins. *Anal. Chem.* **2019**, *91* (20), 12954–12961.
- (57) Neue, U. D. Theory of peak capacity in gradient elution. *J. Chromatogr A* **2005**, *1079* (1–2), 153–61.
- (58) Cabooter, D.; Fanigliulo, A.; Bellazzi, G.; Allieri, B.; Rottigni, A.; Desmet, G. Relationship between the particle size distribution of commercial fully porous and superficially porous high-performance liquid chromatography column packings and their chromatographic performance. *J. Chromatogr A* **2010**, *1217* (45), 7074–81.
- (59) Poppe, H.; Paanakker, J.; Bronckhorst, M. Peak width in solvent-programmed chromatography: I. General description of peak broadening in solvent-programmed elution. *Journal of Chromatography A* **1981**, *204*, 77–84.
- (60) Neue, U. D.; Marchand, D. H.; Snyder, L. R. Peak compression in reversed-phase gradient elution. *Journal of chromatography A* **2006**, *1111* (1), 32–39.
- (61) Snyder, L. R.; Dolan, J. W. *High-performance gradient elution: the practical application of the linear-solvent-strength model*; John Wiley: Hoboken, NJ, 2007; p xxviii, 461 p.
- (62) Jandera, P.; Hájek, T. Possibilities of retention prediction in fast gradient liquid chromatography. Part 3: Short silica monolithic columns. *Journal of Chromatography A* **2015**, *1410*, 76–89.

- (63) Grushka, E., Chromatographic Peak Shape Analysis. In *Methods of Protein Separation*; Catsimoolas, N., Ed.; Springer US: Boston, MA, 1975; pp 161–192.
- (64) Wahab, M. F.; Patel, D. C.; Armstrong, D. W. Peak Shapes and Their Measurements: The Need and the Concept Behind Total Peak Shape Analysis. *LCGC Europe* **2017**, *30* (12), 670–678.
- (65) Ette, L. S. Nomenclature for chromatography (IUPAC Recommendations 1993). *Pure Appl. Chem.* **1993**, *65* (4), 819–872.
- (66) Gritti, F.; Guiuchon, G. Accurate measurements of peak variances: importance of this accuracy in the determination of the true corrected plate heights of chromatographic columns. *J. Chromatogr A* **2011**, *1218* (28), 4452–61.
- (67) Lenco, J.; Vajrychova, M.; Pimkova, K.; Proksova, M.; Benkova, M.; Klimentova, J.; Tambor, V.; Soukup, O. Conventional-Flow Liquid Chromatography-Mass Spectrometry for Exploratory Bottom-Up Proteomic Analyses. *Anal. Chem.* **2018**, *90* (8), 5381–5389.
- (68) Martin, A. J. P.; Syng, R. L. M. A new form of chromatogram employing two liquid phases: A theory of chromatography. 2. Application to the micro-determination of the higher monoamino-acids in proteins. *Biochem. J.* **1941**, *35* (12), 1358–1368.
- (69) van Deemter, J. J.; Zuiderweg, F. J.; Klinkenberg, A. Longitudinal diffusion and resistance to mass transfer as causes of nonideality in chromatography. *Chem. Eng. Sci.* **1956**, *5* (6), 271–289.
- (70) Gritti, F.; Wahab, M. F. Understanding the science behind packing high-efficiency columns and capillaries: Facts, fundamentals, challenges, and future directions. *LCGC Europe* **2018**, *31* (2), 90–101.
- (71) Giddings, J. C. Maximum number of components resolvable by gel filtration and other elution chromatographic methods. *Anal. Chem.* **1967**, *39* (8), 1027–1028.
- (72) Horvath, C. G.; Lipsky, S. R. Peak capacity in chromatography. *Anal. Chem.* **1967**, *39* (14), 1893–1893.
- (73) Neue, U. D. Peak capacity in unidimensional chromatography. *J. Chromatogr A* **2008**, *1184* (1–2), 107–30.
- (74) Dolan, J. W.; Snyder, L. R.; Djordjevic, N. M.; Hill, D. W.; Waeghe, T. J. Reversed-phase liquid chromatographic separation of complex samples by optimizing temperature and gradient time II. Two-run assay procedures. *J. Chromatogr A* **1999**, *857* (1–2), 21–39.
- (75) Eeltink, S.; Dolman, S.; Detobel, F.; Swart, R.; Ursem, M.; Schoenmakers, P. J. High-efficiency liquid chromatography–mass spectrometry separations with 50mm, 250mm, and 1m long polymer-based monolithic capillary columns for the characterization of complex proteolytic digests. *Journal of Chromatography A* **2010**, *1217* (43), 6610–6615.
- (76) Baca, M.; Desmet, G.; Ottevaere, H.; De Malsche, W. Achieving a Peak Capacity of 1800 Using an 8 m Long Pillar Array Column. *Anal. Chem.* **2019**, *91* (17), 10932–10936.
- (77) Xiang, P.; Yang, Y.; Zhao, Z.; Chen, A.; Liu, S. Experimentally Validating Open Tubular Liquid Chromatography for a Peak Capacity of 2000 in 3 h. *Anal. Chem.* **2019**, *91* (16), 10518–10523.
- (78) Yang, Y.; Xiang, P.; Chen, A.; Liu, S. Liquid Chromatographic Separation Using a 2 μ m i.d. Open Tubular Column at Elevated Temperature. *Anal. Chem.* **2021**, *93* (10), 4361–4364.
- (79) Meek, J. L. Prediction of peptide retention times in high-pressure liquid chromatography on the basis of amino acid composition. *Proc. Natl. Acad. Sci. U. S. A.* **1980**, *77* (3), 1632–6.
- (80) Guo, D. C.; Mant, C. T.; Taneja, A. K.; Parker, J. M. R.; Rodges, R. S. Prediction of Peptide Retention Times in Reversed-Phase High-Performance Liquid-Chromatography. 1. Determination of Retention Coefficients of Amino-Acid-Residues of Model Synthetic Peptides. *J. Chromatogr.* **1986**, *359*, 499–517.
- (81) Kovacs, J. M.; Mant, C. T.; Hodges, R. S. Determination of intrinsic hydrophilicity/hydrophobicity of amino acid side chains in peptides in the absence of nearest-neighbor or conformational effects. *Biopolymers* **2006**, *84* (3), 283–97.
- (82) Houghten, R. A.; DeGraw, S. T. Effect of positional environmental domains on the variation of high-performance liquid chromatographic peptide retention coefficients. *J. Chromatogr.* **1987**, *386*, 223–8.
- (83) Mant, C. T.; Burke, T. W.; Black, J. A.; Hodges, R. S. Effect of peptide chain length on peptide retention behaviour in reversed-phase chromatography. *J. Chromatogr.* **1988**, *458*, 193–205.
- (84) Sereda, T. J.; Mant, C. T.; Sonnichsen, F. D.; Hodges, R. S. Reversed-phase chromatography of synthetic amphipathic alpha-helical peptides as a model for ligand/receptor interactions. Effect of changing hydrophobic environment on the relative hydrophilicity/hydrophobicity of amino acid side-chains. *J. Chromatogr A* **1994**, *676* (1), 139–53.
- (85) Spicer, V.; Lao, Y. W.; Shamshurin, D.; Ezzati, P.; Wilkins, J. A.; Krokhin, O. V. N-capping motifs promote interaction of amphipathic helical peptides with hydrophobic surfaces and drastically alter hydrophobicity values of individual amino acids. *Anal. Chem.* **2014**, *86* (23), 11498–502.
- (86) Krokhin, O. V.; Craig, R.; Spicer, V.; Ens, W.; Standing, K. G.; Beavis, R. C.; Wilkins, J. A. An improved model for prediction of retention times of tryptic peptides in ion pair reversed-phase HPLC: its application to protein peptide mapping by off-line HPLC-MALDI MS. *Mol. Cell Proteomics* **2004**, *3* (9), 908–19.
- (87) Shamshurin, D.; Spicer, V.; Krokhin, O. V. Defining intrinsic hydrophobicity of amino acids' side chains in random coil conformation. Reversed-phase liquid chromatography of designed synthetic peptides vs. random peptide data sets. *J. Chromatogr A* **2011**, *1218* (37), 6348–55.
- (88) Krokhin, O. V.; Ying, S.; Cortens, J. P.; Ghosh, D.; Spicer, V.; Ens, W.; Standing, K. G.; Beavis, R. C.; Wilkins, J. A. Use of peptide retention time prediction for protein identification by off-line reversed-phase HPLC-MALDI MS/MS. *Anal. Chem.* **2006**, *78* (17), 6265–9.
- (89) Krokhin, O. V. Sequence-specific retention calculator. Algorithm for peptide retention prediction in ion-pair RP-HPLC: application to 300- and 100-A pore size C18 sorbents. *Anal. Chem.* **2006**, *78* (22), 7785–95.
- (90) Krokhin, O. V.; Spicer, V. Peptide retention standards and hydrophobicity indexes in reversed-phase high-performance liquid chromatography of peptides. *Anal. Chem.* **2009**, *81* (22), 9522–30.
- (91) Stejskal, K.; Potesil, D.; Zdrahal, Z. Suppression of peptide sample losses in autosampler vials. *J. Proteome Res.* **2013**, *12* (6), 3057–62.
- (92) Kovalchuk, S. I.; Anikanov, N. A.; Ivanova, O. M.; Ziganshin, R. H.; Govorun, V. M. Bovine serum albumin as a universal suppressor of non-specific peptide binding in vials prior to nano-chromatography coupled mass-spectrometry analysis. *Anal. Chim. Acta* **2015**, *893*, 57–64.
- (93) Cho, H. R.; Park, J. S.; Wood, T. D.; Choi, Y. S. Longitudinal Assessment of Peptide Recoveries from a Sample Solution in an Autosampler Vial for Proteomics. *Bulletin of the Korean Chemical Society* **2015**, *36* (1), 312–321.
- (94) Stejskal, K.; Op de Beeck, J.; Durnberger, G.; Jacobs, P.; Mechtlar, K. Ultrasensitive NanoLC-MS of Subnanogram Protein Samples Using Second Generation Micropillar Array LC Technology with Orbitrap Exploris 480 and FAIMS PRO. *Anal. Chem.* **2021**, *93* (25), 8704–8710.
- (95) Kyte, J.; Doolittle, R. F. A simple method for displaying the hydrophobic character of a protein. *J. Mol. Biol.* **1982**, *157* (1), 105–32.
- (96) Snyder, L. R.; Kirkland, J. J.; Dolan, J. W. *Introduction to modern liquid chromatography*, 3rd ed.; Wiley: Hoboken, NJ, 2010; p xli, 912 p.
- (97) Terabe, S.; Nishi, H.; Ando, T. Separation of cytochromes c by reversed-phase high-performance liquid chromatography. *J. Chromatogr.* **1981**, *212* (3), 295–304.
- (98) Koyama, J.; Nomura, J.; Shiojima, Y.; Ohtsu, Y.; Horii, I. Effect of Column Length and Elution Mechanism on the Separation of Proteins by Reversed-Phase High-Performance Liquid-Chromatography. *J. Chromatogr.* **1992**, *625* (2), 217–222.
- (99) Vu, H.; Spicer, V.; Gotfrid, A.; Krokhin, O. V. A model for predicting slopes S in the basic equation for the linear-solvent-strength theory of peptide separation by reversed-phase high-

- performance liquid chromatography. *J. Chromatogr A* **2010**, *1217* (4), 489–97.
- (100) Spicer, V.; Grigoryan, M.; Gotfrid, A.; Standing, K. G.; Krokhin, O. V. Predicting retention time shifts associated with variation of the gradient slope in peptide RP-HPLC. *Anal. Chem.* **2010**, *82* (23), 9678–85.
- (101) Eugster, P. J.; Biass, D.; Guillarme, D.; Favreau, P.; Stocklin, R.; Wolfender, J. L. Peak capacity optimization for high resolution peptide profiling in complex mixtures by liquid chromatography coupled to time-of-flight mass spectrometry: application to the Conus consors cone snail venom. *J. Chromatogr A* **2012**, *1259*, 187–99.
- (102) Gritti, F.; Guiochon, G. Optimization of the peak capacity per unit time. *J. Chromatogr A* **2012**, *1263*, 125–40.
- (103) Vaast, A.; Tyteca, E.; Desmet, G.; Schoenmakers, P. J.; Eeltink, S. Gradient-elution parameters in capillary liquid chromatography for high-speed separations of peptides and intact proteins. *J. Chromatogr A* **2014**, *1355*, 149–57.
- (104) Mant, C. T.; Burke, T. W. L.; Hodges, R. S. Optimization of Peptide Separations in Reversed-Phase Hplc - Isocratic Versus Gradient Elution. *Chromatographia* **1987**, *24*, 565–572.
- (105) Liu, H.; Finch, J. W.; Lavallee, M. J.; Collamati, R. A.; Benevides, C. C.; Gebler, J. C. Effects of column length, particle size, gradient length and flow rate on peak capacity of nano-scale liquid chromatography for peptide separations. *J. Chromatogr A* **2007**, *1147* (1), 30–6.
- (106) Chen, M. H.; Horváth, C. Temperature programming and gradient elution in reversed-phase chromatography with packed capillary columns. *J. Chromatography A* **1997**, *788* (1), 51–61.
- (107) Lenco, J.; Semlej, T.; Khalikova, M. A.; Fabrik, I.; Svec, F. Sense and Nonsense of Elevated Column Temperature in Proteomic Bottom-up LC-MS Analyses. *J. Proteome Res.* **2021**, *20* (1), 420–432.
- (108) Dawson, R. M. *C. Data for biochemical research*, 3rd ed.; Clarendon Press: Oxford, 1986; p xii, 580 p.
- (109) Plasson, R.; Cottet, H. Determination and modeling of peptide pKa by capillary zone electrophoresis. *Anal. Chem.* **2006**, *78* (15), 5394–402.
- (110) Thurlkill, R. L.; Grimsley, G. R.; Scholtz, J. M.; Pace, C. N. pK values of the ionizable groups of proteins. *Protein Sci.* **2006**, *15* (5), 1214–8.
- (111) Solinova, V.; Kasicka, V. Determination of acidity constants and ionic mobilities of polyprotic peptide hormones by CZE. *Electrophoresis* **2013**, *34* (18), 2655–65.
- (112) Pahari, S.; Sun, L. X.; Alexov, E. PKAD: a database of experimentally measured pKa values of ionizable groups in proteins. *DATABASE* **2019**, *2019*, baz024.
- (113) Gilar, M.; Olivova, P.; Daly, A. E.; Gebler, J. C. Two-dimensional separation of peptides using RP-RP-HPLC system with different pH in first and second separation dimensions. *J. Sep Sci.* **2005**, *28* (14), 1694–703.
- (114) McCalley, D. V. Overload for ionized solutes in reversed-phase high-performance liquid chromatography. *Anal. Chem.* **2006**, *78* (8), 2532–8.
- (115) McCalley, D. V. Effect of buffer on peak shape of peptides in reversed-phase high performance liquid chromatography. *J. Chromatogr A* **2004**, *1038* (1–2), 77–84.
- (116) Lauber, M. A.; Koza, S. M.; McCall, S. A.; Alden, B. A.; Iraneta, P. C.; Fountain, K. J. High-resolution peptide mapping separations with MS-friendly mobile phases and charge-surface-modified C18. *Anal. Chem.* **2013**, *85* (14), 6936–44.
- (117) Schuster, S. A.; Boyes, B. E.; Wagner, B. M.; Kirkland, J. J. Fast high performance liquid chromatography separations for proteomic applications using Fused-Core(R) silica particles. *J. Chromatogr A* **2012**, *1228*, 232–41.
- (118) Johnson, D.; Boyes, B.; Orlando, R. The use of ammonium formate as a mobile-phase modifier for LC-MS/MS analysis of tryptic digests. *J. Biomol Tech* **2013**, *24* (4), 187–97.
- (119) Gritti, F.; Guiochon, G. The quantitative impact of the mesopore size on the mass transfer mechanism of the new 1.9 μm fully porous Titan-C18 particles II—analysis of biomolecules. *J. Chromatogr A* **2015**, *1392*, 10–9.
- (120) Gritti, F.; Guiochon, G. The rationale for the optimum efficiency of columns packed with new 1.9 μm fully porous Titan-C18 particles—a detailed investigation of the intra-particle diffusivity. *J. Chromatogr A* **2014**, *1355*, 164–78.
- (121) Lambert, N.; Kiss, I.; Felinger, A. Mass-transfer properties of insulin on core-shell and fully porous stationary phases. *Journal of Chromatography A* **2014**, *1366*, 84–91.
- (122) Gritti, F.; Guiochon, G. Mass transfer equation for proteins in very high-pressure liquid chromatography. *Anal. Chem.* **2009**, *81* (7), 2723–36.
- (123) Wagner, B. M.; Schuster, S. A.; Boyes, B. E.; Shields, T. J.; Miles, W. L.; Haynes, M. J.; Moran, R. E.; Kirkland, J. J.; Schure, M. R. Superficially porous particles with 1000A pores for large biomolecule high performance liquid chromatography and polymer size exclusion chromatography. *J. Chromatogr A* **2017**, *1489*, 75–85.
- (124) Wilke, C. R.; Chang, P. Correlation of Diffusion Coefficients in Dilute Solutions. *Aiche Journal* **1955**, *1* (2), 264–270.
- (125) Young, M. E.; Carroad, P. A.; Bell, R. L. Estimation of Diffusion-Coefficients of Proteins. *Biotechnol. Bioeng.* **1980**, *22* (5), 947–955.
- (126) Cavazzini, A.; Gritti, F.; KaczmarSKI, K.; Marchetti, N.; Guiochon, G. Mass-transfer kinetics in a shell packing material for chromatography. *Anal. Chem.* **2007**, *79* (15), 5972–5979.
- (127) Billen, J.; Broeckhoven, K.; Liekens, A.; ChoikhET, K.; Rozing, G.; Desmet, G. Influence of pressure and temperature on the physico-chemical properties of mobile phase mixtures commonly used in high-performance liquid chromatography. *J. Chromatogr A* **2008**, *1210* (1), 30–44.
- (128) Gritti, F.; Guiochon, G. Comparison between the loading capacities of columns packed with partially and totally porous fine particles. What is the effective surface area available for adsorption? *J. Chromatogr A* **2007**, *1176* (1–2), 107–22.
- (129) Gritti, F.; Horvath, K.; Guiochon, G. How changing the particle structure can speed up protein mass transfer kinetics in liquid chromatography. *J. Chromatogr A* **2012**, *1263*, 84–98.
- (130) Wilkins, D. K.; Grimshaw, S. B.; Receveur, V.; Dobson, C. M.; Jones, J. A.; Smith, L. J. Hydrodynamic radii of native and denatured proteins measured by pulse field gradient NMR techniques. *Biochemistry* **1999**, *38* (50), 16424–31.
- (131) Dongré, A. R.; Jones, J. L.; Somogyi, Á.; Wysocki, V. H. Influence of Peptide Composition, Gas-Phase Basicity, and Chemical Modification on Fragmentation Efficiency: Evidence for the Mobile Proton Model. *J. Am. Chem. Soc.* **1996**, *118* (35), 8365–8374.
- (132) Tabb, D. L.; Smith, L. L.; Breci, L. A.; Wysocki, V. H.; Lin, D.; Yates, J. R., 3rd Statistical characterization of ion trap tandem mass spectra from doubly charged tryptic peptides. *Anal. Chem.* **2003**, *75* (5), 1155–63.
- (133) Olsen, J. V.; Ong, S. E.; Mann, M. Trypsin cleaves exclusively C-terminal to arginine and lysine residues. *Mol. Cell Proteomics* **2004**, *3* (6), 608–14.
- (134) Michalski, A.; Neuhauser, N.; Cox, J.; Mann, M. A systematic investigation into the nature of tryptic HCD spectra. *J. Proteome Res.* **2012**, *11* (11), 5479–91.
- (135) Kay, R. G.; Challis, B. G.; Casey, R. T.; Roberts, G. P.; Meek, C. L.; Reimann, F.; Gribble, F. M. Peptidomic analysis of endogenous plasma peptides from patients with pancreatic neuroendocrine tumours. *Rapid Commun. Mass Spectrom.* **2018**, *32* (16), 1414–1424.
- (136) Hochuli, E.; Bannwarth, W.; Dobeli, H.; Gentz, R.; Stuber, D. Genetic Approach to Facilitate Purification of Recombinant Proteins with a Novel Metal Chelate Adsorbent. *Bio-Technology* **1988**, *6* (11), 1321–1325.
- (137) Ruprecht, B.; Koch, H.; Medard, G.; Mundt, M.; Kuster, B.; Lemeer, S. Comprehensive and reproducible phosphopeptide enrichment using iron immobilized metal ion affinity chromatography (Fe-IMAC) columns. *Mol. Cell Proteomics* **2015**, *14* (1), 205–15.

- (138) Engelhardt, H.; Lobert, T. Chromatographic determination of metallic impurities in reversed-phase HPLC columns. *Anal. Chem.* **1999**, *71* (9), 1885–92.
- (139) Seidler, J.; Zinn, N.; Haaf, E.; Boehm, M. E.; Winter, D.; Schlosser, A.; Lehmann, W. D. Metal ion-mobilizing additives for comprehensive detection of femtomole amounts of phosphopeptides by reversed phase LC-MS. *Amino Acids* **2011**, *41* (2), 311–20.
- (140) Hsiao, J. J.; Potter, O. G.; Chu, T. W.; Yin, H. Improved LC/MS Methods for the Analysis of Metal-Sensitive Analytes Using Medronic Acid as a Mobile Phase Additive. *Anal. Chem.* **2018**, *90* (15), 9457–9464.
- (141) Grathwohl, C.; Wuthrich, K. Nmr-Studies of the Rates of Proline Cis-Trans Isomerization in Oligopeptides. *Biopolymers* **1981**, *20* (12), 2623–2633.
- (142) Gesquiere, J. C.; Diesis, E.; Cung, M. T.; Tartar, A. Slow Isomerization of Some Proline-Containing Peptides Inducing Peak Splitting during Reversed-Phase High-Performance Liquid-Chromatography. *J. Chromatogr. A* **1989**, *478* (1), 121–129.
- (143) Denny, P.; Hagen, F. K.; Hardt, M.; Liao, L.; Yan, W.; Arellanno, M.; Bassilian, S.; Bedi, G. S.; Boontheung, P.; Cociorva, D.; Delahunty, C. M.; Denny, T.; Dunsmore, J.; Faull, K. F.; Gilligan, J.; Gonzalez-Begne, M.; Halgand, F.; Hall, S. C.; Han, X.; Henson, B.; Hewel, J.; Hu, S.; Jeffrey, S.; Jiang, J.; Loo, J. A.; Ogorzalek Loo, R. R.; Malamud, D.; Melvin, J. E.; Miroshnychenko, O.; Navazesh, M.; Niles, R.; Park, S. K.; Prakobphol, A.; Ramachandran, P.; Richert, M.; Robinson, S.; Sondej, M.; Souda, P.; Sullivan, M. A.; Takashima, J.; Than, S.; Wang, J.; Whitelegge, J. P.; Witkowska, H. E.; Wolinsky, L.; Xie, Y.; Xu, T.; Yu, W.; Ytterberg, J.; Wong, D. T.; Yates, J. R., 3rd; Fisher, S. J. The proteomes of human parotid and submandibular/sublingual gland salivas collected as the ductal secretions. *J. Proteome Res.* **2008**, *7* (5), 1994–2006.
- (144) Zang, L.; Carlage, T.; Murphy, D.; Frenkel, R.; Bryngelson, P.; Madsen, M.; Lyubarskaya, Y. Residual metals cause variability in methionine oxidation measurements in protein pharmaceuticals using LC-UV/MS peptide mapping. *J. Chromatogr B Analyt Technol Biomed Life Sci.* **2012**, *895*–896, 71–6.
- (145) Geisler, D. J.; Kong, A. T.; Avtonomov, D. M.; Yu, F.; Leprevost, F. D. V.; Nesvizhskii, A. I. PTM-Shepherd: Analysis and Summarization of Post-Translational and Chemical Modifications From Open Search Results. *Mol. Cell Proteomics* **2021**, *20*, 100018.
- (146) Solntsev, S. K.; Shortreed, M. R.; Frey, B. L.; Smith, L. M. Enhanced Global Post-translational Modification Discovery with MetaMorpheus. *J. Proteome Res.* **2018**, *17* (5), 1844–1851.
- (147) Gritti, F.; Guiochon, G. The ultimate band compression factor in gradient elution chromatography. *J. Chromatogr A* **2008**, *1178* (1–2), 79–91.
- (148) Gritti, F.; Guiochon, G. Peak compression factor of proteins. *J. Chromatogr A* **2009**, *1216* (33), 6124–33.
- (149) Gritti, F.; Guiochon, G. The van Deemter equation: assumptions, limits, and adjustment to modern high performance liquid chromatography. *J. Chromatogr A* **2013**, *1302*, 1–13.
- (150) Wicke, E. J. C. Giddings: Dynamics of Chromatography. Part I: Principles and Theory. Marcel Dekker, New York, 1965. XII und 323 Seiten. 39 Abb. Preis:\$ 11.50. *Berichte der Bunsengesellschaft für physikalische Chemie* **1967**, *71* (2), 236–236.
- (151) Horvath, C.; Lin, H.-J. Movement and band spreading of unsorbed solutes in liquid chromatography. *Journal of Chromatography A* **1976**, *126* (Nov3), 401–420.
- (152) Knox, J. H. Practical aspects of LC theory. *Journal of Chromatographic Science* **1977**, *15* (9), 352–364.
- (153) Usher, K. M.; Simmons, C. R.; Dorsey, J. G. Modeling chromatographic dispersion: a comparison of popular equations. *J. Chromatogr A* **2008**, *1200* (2), 122–8.
- (154) Gilar, M.; Neue, U. D. Peak capacity in gradient reversed-phase liquid chromatography of biopolymers. Theoretical and practical implications for the separation of oligonucleotides. *J. Chromatogr A* **2007**, *1169* (1–2), 139–50.
- (155) Petersson, P.; Frank, A.; Heaton, J.; Euerby, M. R. Maximizing peak capacity and separation speed in liquid chromatography. *J. Sep Sci.* **2008**, *31* (13), 2346–57.
- (156) Gritti, F.; Guiochon, G. Effect of the surface coverage of C18-bonded silica particles on the obstructive factor and intraparticle diffusion mechanism. *Chem. Eng. Sci.* **2006**, *61* (23), 7636–7650.
- (157) Gritti, F.; Guiochon, G. Perspectives on the evolution of the column efficiency in liquid chromatography. *Anal. Chem.* **2013**, *85* (6), 3017–35.
- (158) Gritti, F.; Guiochon, G. Relationship between trans-column eddy diffusion and retention in liquid chromatography: theory and experimental evidence. *J. Chromatogr A* **2010**, *1217* (41), 6350–65.
- (159) Reising, A. E.; Schlabach, S.; Baranau, V.; Stoeckel, D.; Tallarek, U. Analysis of packing microstructure and wall effects in a narrow-bore ultrahigh pressure liquid chromatography column using focused ion-beam scanning electron microscopy. *J. Chromatogr A* **2017**, *1513*, 172–182.
- (160) Gritti, F. A stochastic view on column efficiency. *J. Chromatogr A* **2018**, *1540*, 55–67.
- (161) Bruns, S.; Grinias, J. P.; Blue, L. E.; Jorgenson, J. W.; Tallarek, U. Morphology and separation efficiency of low-aspect-ratio capillary ultrahigh pressure liquid chromatography columns. *Anal. Chem.* **2012**, *84* (10), 4496–503.
- (162) Godinho, J. M.; Reising, A. E.; Tallarek, U.; Jorgenson, J. W. Implementation of high slurry concentration and sonication to pack high-efficiency, meter-long capillary ultrahigh pressure liquid chromatography columns. *J. Chromatogr A* **2016**, *1462*, 165–9.
- (163) Gritti, F.; Gilar, M. Impact of frit dispersion on gradient performance in high-throughput liquid chromatography. *J. Chromatogr A* **2019**, *1591*, 110–119.
- (164) Zelenyanszki, D.; Lambert, N.; Gritti, F.; Felinger, A. The effect of column packing procedure on column end efficiency and on bed heterogeneity - Experiments with flow-reversal. *J. Chromatogr A* **2019**, *1603*, 412–416.
- (165) Gritti, F.; McDonald, T.; Gilar, M. Impact of the column hardware volume on resolution in very high pressure liquid chromatography non-invasive investigations. *J. Chromatogr A* **2015**, *1420*, 54–65.
- (166) Cheong, W. J. Fritting techniques in chromatography. *J. Sep. Sci.* **2014**, *37* (6), 603–617.
- (167) Franc, M.; Sobotnikova, J.; Coufal, P.; Bosakova, Z. Comparison of different types of outlet frits in slurry-packed capillary columns. *J. Sep Sci.* **2014**, *37* (17), 2278–83.
- (168) Bruns, S.; Franklin, E. G.; Grinias, J. P.; Godinho, J. M.; Jorgenson, J. W.; Tallarek, U. Slurry concentration effects on the bed morphology and separation efficiency of capillaries packed with sub-2 μ m particles. *J. Chromatogr A* **2013**, *1318*, 189–97.
- (169) Reising, A. E.; Godinho, J. M.; Hormann, K.; Jorgenson, J. W.; Tallarek, U. Larger voids in mechanically stable, loose packings of 1.3 μ m frictional, cohesive particles: Their reconstruction, statistical analysis, and impact on separation efficiency. *J. Chromatogr A* **2016**, *1436*, 118–32.
- (170) Wahab, M. F.; Patel, D. C.; Wimalasinghe, R. M.; Armstrong, D. W. Fundamental and Practical Insights on the Packing of Modern High-Efficiency Analytical and Capillary Columns. *Anal. Chem.* **2017**, *89* (16), 8177–8191.
- (171) Reising, A. E.; Godinho, J. M.; Bernzen, J.; Jorgenson, J. W.; Tallarek, U. Axial heterogeneities in capillary ultrahigh pressure liquid chromatography columns: Chromatographic and bed morphological characterization. *J. Chromatogr A* **2018**, *1569*, 44–52.
- (172) Vaast, A.; Terryn, H.; Svec, F.; Eeltink, S. Nanostructured porous polymer monolithic columns for capillary liquid chromatography of peptides. *J. Chromatogr A* **2014**, *1374*, 171–179.
- (173) Dores-Sousa, J. L.; Terryn, H.; Eeltink, S. Morphology optimization and assessment of the performance limits of high-porosity nanostructured polymer monolithic capillary columns for proteomics analysis. *Anal. Chim. Acta* **2020**, *1124*, 176–183.
- (174) Gritti, F.; Cavazzini, A.; Marchetti, N.; Guiochon, G. Comparison between the efficiencies of columns packed with fully

- and partially porous C18-bonded silica materials. *Journal of Chromatography A* **2007**, *1157* (1–2), 289–303.
- (175) Daneyko, A.; Holtzel, A.; Khirevich, S.; Tallarek, U. Influence of the Particle Size Distribution on Hydraulic Permeability and Eddy Dispersion in Bulk Packings. *Anal. Chem.* **2011**, *83* (10), 3903–3910.
- (176) Bruns, S.; Stoeckel, D.; Smarsly, B. M.; Tallarek, U. Influence of particle properties on the wall region in packed capillaries. *J. Chromatogr A* **2012**, *1268*, 53–63.
- (177) Gritti, F.; Bell, D. S.; Guiochon, G. Particle size distribution and column efficiency. An ongoing debate revived with 1.9 μm Titan-C18 particles. *J. Chromatogr A* **2014**, *1355*, 179–92.
- (178) Ishihama, Y.; Rappaport, J.; Andersen, J. S.; Mann, M. Microcolumns with self-assembled particle frits for proteomics. *Journal of Chromatography A* **2002**, *979* (1–2), 233–239.
- (179) Knox, J. H. Band dispersion in chromatography - a universal expression for the contribution from the mobile zone. *Journal of Chromatography A* **2002**, *960* (1–2), 7–18.
- (180) Gzil, P.; Vervoort, N.; Baron, G. V.; Desmet, G. Advantages of perfectly ordered 2-D porous pillar arrays over packed bed columns for LC separations: a theoretical analysis. *Anal. Chem.* **2003**, *75* (22), 6244–50.
- (181) De Malsche, W.; Gardeniers, H.; Desmet, G. Experimental study of porous silicon shell pillars under retentive conditions. *Anal. Chem.* **2008**, *80* (14), 5391–5400.
- (182) Op De Beeck, J.; Callewaert, M.; Ottevaere, H.; Gardeniers, H.; Desmet, G.; De Malsche, W. On the advantages of radially elongated structures in microchip-based liquid chromatography. *Anal. Chem.* **2013**, *85* (10), 5207–12.
- (183) Desmet, G.; Callewaert, M.; Ottevaere, H.; De Malsche, W. Merging Open-Tubular and Packed Bed Liquid Chromatography. *Anal. Chem.* **2015**, *87* (14), 7382–8.
- (184) Vangelooen, J.; De Malsche, W.; Op De Beeck, J.; Eghbali, H.; Gardeniers, H.; Desmet, G. Design and evaluation of flow distributors for microfabricated pillar array columns. *Lab Chip* **2010**, *10* (3), 349–356.
- (185) Vangelooen, J.; Schlautman, S.; Detobel, F.; Gardeniers, H.; Desmet, G. Experimental optimization of flow distributors for pressure-driven separations and reactions in flat-rectangular micro-channels. *Anal. Chem.* **2011**, *83* (2), 467–77.
- (186) Miyabe, K.; Guiochon, G. Surface diffusion in reversed-phase liquid chromatography. *J. Chromatogr A* **2010**, *1217* (11), 1713–34.
- (187) Renkin, E. M. Filtration, diffusion, and molecular sieving through porous cellulose membranes. *J. Gen. Physiol.* **1954**, *38* (2), 225–243.
- (188) Brenner, H.; Gaydos, L. J. The constrained brownian movement of spherical particles in cylindrical pores of comparable radius: Models of the diffusive and convective transport of solute molecules in membranes and porous media. *J. Colloid Interface Sci.* **1977**, *58* (2), 312–356.
- (189) Gritti, F.; Guiochon, G. Possible resolution gain in enantioseparations afforded by core-shell particle technology. *J. Chromatogr A* **2014**, *1348*, 87–96.
- (190) Suzuki, M. *Adsorption Engineering*; Kodansha; Elsevier: Tokyo; Amsterdam; New York, 1990; p ix, 295 p.
- (191) Gritti, F. Quantification of Individual Mass Transfer Phenomena in Liquid Chromatography for Further Improvement of Column Efficiency. *LCGC North America* **2014**, *32* (12), 928–940.
- (192) Desmet, G.; Broeckhoven, K. Equivalence of the Different C-m- and C-s-Term Expressions Used in Liquid Chromatography and a Geometrical Model Uniting Them. *Anal. Chem.* **2008**, *80* (21), 8076–8088.
- (193) Fekete, S.; Rudaz, S.; Veuthey, J. L.; Guillarme, D. Impact of mobile phase temperature on recovery and stability of monoclonal antibodies using recent reversed-phase stationary phases. *J. Sep. Sci.* **2012**, *35* (22), 3113–23.
- (194) Dillon, T. M.; Bondarenko, P. V.; Rehder, D. S.; Pipes, G. D.; Kleemann, G. R.; Ricci, M. S. Optimization of a reversed-phase high-performance liquid chromatography/mass spectrometry method for characterizing recombinant antibody heterogeneity and stability. *J. Chromatogr A* **2006**, *1120* (1–2), 112–20.
- (195) Halász, I.; Ende, R.; Asshauer, J. Ultimate limits in high-pressure liquid chromatography. *Journal of Chromatography A* **1975**, *112*, 37–60.
- (196) Gritti, F.; Guiochon, G. Complete temperature profiles in ultra-high-pressure liquid chromatography columns. *Anal. Chem.* **2008**, *80* (13), 5009–20.
- (197) Wolcott, R. G.; Dolan, J. W.; Snyder, L. R.; Bakalyar, S. R.; Arnold, M. A.; Nichols, J. A. Control of column temperature in reversed-phase liquid chromatography. *Journal of Chromatography A* **2000**, *869* (1), 211–230.
- (198) Thompson, J. D.; Brown, J. S.; Carr, P. W. Dependence of thermal mismatch broadening on column diameter in high-speed liquid chromatography at elevated temperatures. *Anal. Chem.* **2001**, *73* (14), 3340–7.
- (199) Pruss, A.; Kempfer, C.; Gysler, J.; Jira, T. Extracolumn band broadening in capillary liquid chromatography. *Journal of Chromatography A* **2003**, *1016* (2), 129–141.
- (200) Gritti, F.; Guiochon, G. On the minimization of the band-broadening contributions of a modern, very high pressure liquid chromatograph. *J. Chromatogr A* **2011**, *1218* (29), 4632–48.
- (201) Buckenmaier, S.; Miller, C. A.; van de Goor, T.; Dittmann, M. M. Instrument contributions to resolution and sensitivity in ultra high performance liquid chromatography using small bore columns: comparison of diode array and triple quadrupole mass spectrometry detection. *J. Chromatogr A* **2015**, *1377*, 64–74.
- (202) Gritti, F.; Guiochon, G. On the extra-column band-broadening contributions of modern, very high pressure liquid chromatographs using 2.1 mm I.D. columns packed with sub-2 μm particles. *J. Chromatogr A* **2010**, *1217* (49), 7677–89.
- (203) Fountain, K. J.; Neue, U. D.; Grumbach, E. S.; Diehl, D. M. Effects of extra-column band spreading, liquid chromatography system operating pressure, and column temperature on the performance of sub-2-micron porous particles. *J. Chromatogr A* **2009**, *1216* (32), 5979–88.
- (204) Koutsky, J. A.; Adler, R. J. Minimisation of axial dispersion by use of secondary flow in helical tubes. *Canadian Journal of Chemical Engineering* **1964**, *42* (6), 239–246.
- (205) Engelhardt, H.; Neue, U. D. Reaction detector with three dimensional coiled open tubes in HPLC. *Chromatographia* **1982**, *15* (7), 403–408.
- (206) Katz, E. D.; Scott, R. P. W. Low-dispersion connecting tubes for liquid chromatography systems. *J. Chromatogr. A* **1983**, *268* (2), 169–175.
- (207) Engelhardt, H.; Lillig, B. Practical applications of open tubes in liquid chromatography. *Journal of High Resolution Chromatography* **1985**, *8* (9), 531–534.
- (208) Meiring, H. D.; van der Heeft, E.; ten Hove, G. J.; de Jong, A. P. J. M. Nanoscale LC-MS(n): technical design and applications to peptide and protein analysis. *J. Sep. Sci.* **2002**, *25* (9), 557–568.
- (209) Stankovich, J. J.; Gritti, F.; Stevenson, P. G.; Guiochon, G. The impact of column connection on band broadening in very high pressure liquid chromatography. *J. Sep. Sci.* **2013**, *36* (17), 2709–17.
- (210) Vissers, J. P.; Blackburn, R. K.; Moseley, M. A. A novel interface for variable flow nanoscale LC/MS/MS for improved proteome coverage. *J. Am. Soc. Mass Spectrom.* **2002**, *13* (7), 760–71.
- (211) Licklider, L. J.; Thoreen, C. C.; Peng, J.; Gygi, S. P. Automation of nanoscale microcapillary liquid chromatography-tandem mass spectrometry with a vented column. *Anal. Chem.* **2002**, *74* (13), 3076–83.
- (212) Shen, Y.; Moore, R. J.; Zhao, R.; Blonder, J.; Auberry, D. L.; Masselon, C.; Pasa-Tolic, L.; Hixson, K. K.; Auberry, K. J.; Smith, R. D. High-efficiency on-line solid-phase extraction coupling to 15–150-microm-i.d. column liquid chromatography for proteomic analysis. *Anal. Chem.* **2003**, *75* (14), 3596–3605.
- (213) Mitulovic, G.; Smoluch, M.; Chervet, J. P.; Steinmacher, I.; Kunig, A.; Mechtler, K. An improved method for tracking and

- reducing the void volume in nano HPLC-MS with micro trapping columns. *Anal Bioanal Chem.* **2003**, *376* (7), 946–51.
- (214) Noga, M.; Sucharski, F.; Suder, P.; Silberring, J. A practical guide to nano-LC troubleshooting. *J. Sep Sci.* **2007**, *30* (14), 2179–89.
- (215) Lauber, M. A.; Koza, S. M.; Fountain, K. J. Optimizing Peak Capacity in Nanoscale Trap-Elute Peptide Separations with Differential Column Heating; Application Note; Waters, 2014; 720005047EN.
- (216) Gritti, F.; Guiochon, G. Band broadening in fast gradient high-performance liquid chromatography: Application to the second generation of 4.6 mm ID silica monolithic columns. *Journal of Chromatography A* **2012**, *1238*, 77–90.
- (217) Kocher, T.; Pichler, P.; Swart, R.; Mechtler, K. Analysis of protein mixtures from whole-cell extracts by single-run nanoLC-MS/MS using ultralong gradients. *Nat. Protoc.* **2012**, *7* (5), 882–90.
- (218) Vanderlinden, K.; Desmet, G.; Broeckhoven, K. Measurement of the Band Broadening of UV Detectors used in Ultra-high Performance Liquid Chromatography using an On-tubing Fluorescence Detector. *Chromatographia* **2019**, *82* (1), 489–498.
- (219) Spaggiari, D.; Fekete, S.; Eugster, P. J.; Veuthey, J. L.; Geiser, L.; Rudaz, S.; Guillarme, D. Contribution of various types of liquid chromatography-mass spectrometry instruments to band broadening in fast analysis. *J. Chromatogr A* **2013**, *1310*, 45–55.
- (220) Gritti, F.; Felinger, A.; Guiochon, G. Influence of the errors made in the measurement of the extra-column volume on the accuracies of estimates of the column efficiency and the mass transfer kinetics parameters. *J. Chromatogr A* **2006**, *1136* (1), 57–72.
- (221) Broeckhoven, K.; De Vos, J.; Desmet, G. Particles, pressure, and system contribution: The holy trinity of ultrahigh-performance liquid chromatography. *LCGC Europe* **2017**, *30* (11), 618–625.
- (222) Bell, D. S. New Chromatography Columns and Accessories for 2020. *LCGC North America* **2020**, *38*, (4).
- (223) Bell, D. S. New liquid chromatography columns and accessories for 2019. *LCGC North America* **2019**, *37* (4), 222–243.
- (224) Bell, D. S. New Liquid Chromatography Columns and Accessories for 2021. *LCGC North America* **2021**, *39* (5), 214–227.
- (225) Dolan, J. Detective Work, Part III: Strong Retention and Chemical Problems with the Column. *LCGC North America* **2016**, *34* (1), 20–25.
- (226) Muller-Reif, J. B.; Hansen, F. M.; Schweizer, L.; Treit, P. V.; Geyer, P. E.; Mann, M. A New Parallel High-Pressure Packing System Enables Rapid Multiplexed Production of Capillary Columns. *Mol. Cell Proteomics* **2021**, *20*, 100082.
- (227) Kovalchuk, S. I.; Jensen, O. N.; Rogowska-Wrzesinska, A. FlashPack: Fast and Simple Preparation of Ultrahigh-performance Capillary Columns for LC-MS. *Mol. Cell Proteomics* **2019**, *18* (2), 383–390.
- (228) González-Ruiz, V.; Olives, A. I.; Martín, M. A. Core-shell particles lead the way to renewing high-performance liquid chromatography. *TrAC Trends in Analytical Chemistry* **2015**, *64*, 17–28.
- (229) Hayes, R.; Ahmed, A.; Edge, T.; Zhang, H. Core–shell particles: Preparation, fundamentals and applications in high performance liquid chromatography. *Journal of Chromatography A* **2014**, *1357*, 36–52.
- (230) Horvath, C.; Lipsky, S. R. Rapid analysis of ribonucleosides and bases at the picomole level using pellicular cation exchange resin in narrow bore columns. *Anal. Chem.* **1969**, *41* (10), 1227–34.
- (231) Kirkland, J. J. Controlled Surface Porosity Supports for High Speed Gas and Liquid Chromatography. *Anal. Chem.* **1969**, *41* (1), 218–220.
- (232) Kirkland, J. J. Superficially Porous Silica Microspheres for the Fast High-Performance Liquid Chromatography of Macromolecules. *Anal. Chem.* **1992**, *64* (11), 1239–1245.
- (233) Cunliffe, J. M.; Maloney, T. D. Fused-core particle technology as an alternative to sub-2-micron particles to achieve high separation efficiency with low backpressure. *J. Sep Sci.* **2007**, *30* (18), 3104–9.
- (234) Ruta, J.; Zurlino, D.; Grivel, C.; Heinisch, S.; Veuthey, J.-L.; Guillarme, D. Evaluation of columns packed with shell particles with compounds of pharmaceutical interest. *Journal of Chromatography A* **2012**, *1228*, 221–231.
- (235) Gritti, F.; Farkas, T.; Heng, J.; Guiochon, G. On the relationship between band broadening and the particle-size distribution of the packing material in liquid chromatography: theory and practice. *J. Chromatogr A* **2011**, *1218* (45), 8209–21.
- (236) Gritti, F.; Guiochon, G. Performance of columns packed with the new shell Kinetex-C18 particles in gradient elution chromatography. *J. Chromatogr A* **2010**, *1217* (10), 1604–15.
- (237) Gritti, F.; Guiochon, G. The mass transfer kinetics in columns packed with Halo-ES shell particles. *J. Chromatogr A* **2011**, *1218* (7), 907–21.
- (238) Schuster, S. A.; Wagner, B. M.; Boyes, B. E.; Kirkland, J. J. Optimized superficially porous particles for protein separations. *J. Chromatogr A* **2013**, *1315*, 118–26.
- (239) Bobaly, B.; Lauber, M.; Beck, A.; Guillarme, D.; Fekete, S. Utility of a high coverage phenyl-bonding and wide-pore superficially porous particle for the analysis of monoclonal antibodies and related products. *J. Chromatogr A* **2018**, *1549*, 63–76.
- (240) Bobaly, B.; Veuthey, J. L.; Guillarme, D.; Fekete, S. New developments and possibilities of wide-pore superficially porous particle technology applied for the liquid chromatographic analysis of therapeutic proteins. *J. Pharm. Biomed. Anal.* **2018**, *158*, 225–235.
- (241) Fallas, M. M.; Buckenmaier, S. M.; McCalley, D. V. A comparison of overload behaviour for some sub 2 µm totally porous and sub 3 µm shell particle columns with ionised solutes. *J. Chromatogr A* **2012**, *1235*, 49–59.
- (242) Urban, J.; Jandera, P.; Kucerova, Z.; van Straten, M. A.; Claessens, H. A. A study of the effects of column porosity on gradient separations of proteins. *J. Chromatogr A* **2007**, *1167* (1), 63–75.
- (243) Kawashima, Y.; Ohara, O. Development of a NanoLC-MS/MS System Using a Nonporous Reverse Phase Column for Ultrasensitive Proteome Analysis. *Anal. Chem.* **2018**, *90* (21), 12334–12338.
- (244) Issaeva, T.; Kourganov, A.; Unger, K. Super-high-speed liquid chromatography of proteins and peptides on non-porous Micra NPS-RP packings. *Journal of Chromatography A* **1999**, *846* (1–2), 13–23.
- (245) Majors, R. E. Fast and Ultrafast HPLC on sub-2 µm Porous Particles — Where Do We Go From Here? *LCGC Europe* **2006**, *19* (6), 352–362.
- (246) Swartz, M. E.; Murphy, B. J. Ultra performance liquid chromatography: Tomorrow's HPLC technology today. *LabPlus Int.* **2004**, *18* (3), 6–9.
- (247) Sanders, K. L.; Edwards, J. L. Nano-liquid chromatography-mass spectrometry and recent applications in omics investigations. *Anal Methods* **2020**, *12* (36), 4404–4417.
- (248) Sestak, J.; Moravcova, D.; Kahle, V. Instrument platforms for nano liquid chromatography. *J. Chromatogr A* **2015**, *1421*, 2–17.
- (249) Wilson, S. R.; Vehus, T.; Berg, H. S.; Lundanes, E. Nano-LC in proteomics: recent advances and approaches. *Bioanalysis* **2015**, *7* (14), 1799–815.
- (250) Kirkland, J. J.; Schuster, S. A.; Johnson, W. L.; Boyes, B. E. Fused-core particle technology in high-performance liquid chromatography: An overview. *J. Pharm. Anal.* **2013**, *3* (5), 303–312.
- (251) Dolan, J. How Fast Can a Gradient Be Run? *LCGC North America* **2011**, *29* (8), 652–657.
- (252) DeStefano, J. J.; Schuster, S. A.; Lawhorn, J. M.; Kirkland, J. J. Performance characteristics of new superficially porous particles. *Journal of Chromatography A* **2012**, *1258*, 76–83.
- (253) MacNair, J. E.; Patel, K. D.; Jorgenson, J. W. Ultrahigh-pressure reversed-phase capillary liquid chromatography: isocratic and gradient elution using columns packed with 1.0-micron particles. *Anal. Chem.* **1999**, *71* (3), 700–8.
- (254) Jerkovich, A. D.; Mellors, J. S.; Thompson, J. W.; Jorgenson, J. W. Linear velocity surge caused by mobile-phase compression as a source of band broadening in isocratic ultrahigh-pressure liquid chromatography. *Anal. Chem.* **2005**, *77* (19), 6292–9.
- (255) Wang, X.; Barber, W. E.; Carr, P. W. A practical approach to maximizing peak capacity by using long columns packed with

- pellicular stationary phases for proteomic research. *J. Chromatogr A* **2006**, *1107* (1–2), 139–51.
- (256) Sneekes, E.-J.; Dekker, K.; de Haan, B.; Swartz, M. E. Optimizing Particle Size and Column Length: What Is the Best Way to Utilize Nano UHPLC in Proteomics? In *HUPO 2011 - 10th World Congress*, Geneva, September 4–7, 2011; P1739.
- (257) Han, J.; Ye, L.; Xu, L.; Zhou, Z.; Gao, F.; Xiao, Z.; Wang, Q.; Zhang, B. Towards high peak capacity separations in normal pressure nanoflow liquid chromatography using meter long packed capillary columns. *Anal. Chim. Acta* **2014**, *852*, 267–73.
- (258) Wang, X.; Stoll, D. R.; Carr, P. W.; Schoenmakers, P. J. A graphical method for understanding the kinetics of peak capacity production in gradient elution liquid chromatography. *J. Chromatogr A* **2006**, *1125* (2), 177–81.
- (259) Poppe, H. Some reflections on speed and efficiency of modern chromatographic methods. *Journal of Chromatography A* **1997**, *778* (1), 3–21.
- (260) Desmet, G.; Clicq, D.; Nguyen, D. T.; Guillarme, D.; Rudaz, S.; Veuthey, J. L.; Vervoort, N.; Torok, G.; Cabooter, D.; Gzil, P. Practical constraints in the kinetic plot representation of chromatographic performance data: theory and application to experimental data. *Anal. Chem.* **2006**, *78* (7), 2150–62.
- (261) Desmet, G.; Clicq, D.; Gzil, P. Geometry-independent plate height representation methods for the direct comparison of the kinetic performance of LC supports with a different size or morphology. *Anal. Chem.* **2005**, *77* (13), 4058–70.
- (262) Broeckhoven, K.; Cabooter, D.; Lynen, F.; Sandra, P.; Desmet, G. The kinetic plot method applied to gradient chromatography: theoretical framework and experimental validation. *J. Chromatogr A* **2010**, *1217* (17), 2787–95.
- (263) Neue, U. Kinetic Plots Made Easy. *LCGC North America* **2009**, *27* (11), 974–983.
- (264) Broeckhoven, K.; Stoll, D. R. But Why Doesn't It Get Better? Kinetic Plots for Liquid Chromatography, Part 1: Basic Concepts. *LCGC EUROPE* **2022**, *35* (2), 52–56.
- (265) Broeckhoven, K.; Stoll, D. R. But Why Doesn't It Get Better? Kinetic Plots for Liquid Chromatography, Part 2: Making and Interpreting the Plots. *LCGC EUROPE* **2022**, *35* (3), 93–97.
- (266) Broeddloven, K.; Gunnareon, C.; Stoll, D. R. But Why Doesn't It Get Better? Kinetic Plots for Liquid Chromatography, Part 3: Pulling It All Together. *LCGC EUROPE* **2022**, *35* (4), 130–134.
- (267) Godinho, J. M.; Naese, J. A.; Toler, A. E.; Boyes, B. E.; Henry, R. A.; DeStefano, J. J.; Grinias, J. P. Importance of Particle Pore Size in Determining Retention and Selectivity in Reversed Phase Liquid Chromatography. *J. Chromatogr A* **2020**, *1634*, 461678.
- (268) Wang, G.; Tomasella, F. P. Ion-pairing HPLC methods to determine EDTA and DTPA in small molecule and biological pharmaceutical formulations. *J. Pharm. Anal.* **2016**, *6* (3), 150–156.
- (269) Getaz, D.; Dogan, N.; Forrer, N.; Morbidelli, M. Influence of the pore size of reversed phase materials on peptide purification processes. *J. Chromatogr A* **2011**, *1218* (20), 2912–22.
- (270) Vellaichamy, A.; Tran, J. C.; Catherman, A. D.; Lee, J. E.; Kellie, J. F.; Sweet, S. M. M.; Zamdborg, L.; Thomas, P. M.; Ahlf, D. R.; Durbin, K. R.; Valaskovic, G. A.; Kelleher, N. L. Size-Sorting Combined with Improved Nanocapillary Liquid Chromatography–Mass Spectrometry for Identification of Intact Proteins up to 80 kDa. *Anal. Chem.* **2010**, *82* (4), 1234–1244.
- (271) Washburn, E. W. The dynamics of capillary flow. *Phys. Rev.* **1921**, *17* (3), 273–283.
- (272) Walter, T. H.; Iraneta, P.; Capparella, M. Mechanism of retention loss when C8 and C18 HPLC columns are used with highly aqueous mobile phases. *J. Chromatogr A* **2005**, *1075* (1–2), 177–83.
- (273) Gritt, F.; Gilar, M.; Walter, T. H.; Wyndham, K. Retention loss of reversed-phase chromatographic columns using 100% aqueous mobile phases from fundamental insights to best practice. *J. Chromatogr A* **2020**, *1612*, 460662.
- (274) Bidlingmeyer, B. A.; Broske, A. D. The role of pore size and stationary phase composition in preventing aqueous-induced retention time loss in reversed-phase HPLC. *J. Chromatogr Sci.* **2004**, *42* (2), 100–6.
- (275) Claessens, H. A.; van Straten, M. A. Review on the chemical and thermal stability of stationary phases for reversed-phase liquid chromatography. *Journal of Chromatography A* **2004**, *1060* (1), 23–41.
- (276) Borges, E. M.; Volmer, D. A. Silica, Hybrid Silica, Hydride Silica and Non-Silica Stationary Phases for Liquid Chromatography. Part II: Chemical and Thermal Stability. *J. Chromatogr Sci.* **2015**, *53* (7), 1107–22.
- (277) McCalley, D. V. Rationalization of retention and overloading behavior of basic compounds in reversed-phase HPLC using low ionic strength buffers suitable for mass spectrometric detection. *Anal. Chem.* **2003**, *75* (14), 3404–10.
- (278) Gritt, F.; Guiochon, G. Peak shapes of acids and bases under overloaded conditions in reversed-phase liquid chromatography, with weakly buffered mobile phases of various pH: a thermodynamic interpretation. *J. Chromatogr A* **2009**, *1216* (1), 63–78.
- (279) Borges, E. M. Silica, Hybrid Silica, Hydride Silica and Non-Silica Stationary Phases for Liquid Chromatography. *Journal of Chromatographic Science* **2015**, *53* (4), 580–597.
- (280) Mendez, A.; Bosch, E.; Roses, M.; Neue, U. D. Comparison of the acidity of residual silanol groups in several liquid chromatography columns. *J. Chromatogr A* **2003**, *986* (1), 33–44.
- (281) Iraneta, P. C.; Wyndham, K. D.; McCabe, D. R.; Walter, T. H. A Review of Waters Hybrid Particle Technology, Part 3, Charge Surface Hybrid (CSH) Technology and Its Use in Liquid Chromatography; White Paper; Waters, 2011; 720003929EN.
- (282) Kadlecová, Z.; Kozlík, P.; Tesařová, E.; Gilar, M.; Kalíková, K. Characterization and comparison of mixed-mode and reversed-phase columns; interaction abilities and applicability for peptide separation. *Journal of Chromatography A* **2021**, *1648*, 462182.
- (283) Kadlecová, Z.; Kalíková, K.; Folprechtová, D.; Tesařová, E.; Gilar, M. Method for evaluation of ionic interactions in liquid chromatography. *Journal of Chromatography A* **2020**, *1625*, 461301.
- (284) Majors, R. The Top 10 HPLC and UHPLC Column Myths: Part 1. *LCGC Europe* **2013**, *26* (10), 584–592.
- (285) Gritt, F.; Walter, T. Retention Loss of Reversed-Phase Columns Using Highly Aqueous Mobile Phases: Fundamentals, Mechanism, and Practical Solutions. *LCGC North America* **2021**, *39* (1), 33–40.
- (286) Layne, J. Characterization and comparison of the chromatographic performance of conventional, polar-embedded, and polar-endcapped reversed-phase liquid chromatography stationary phases. *Journal of Chromatography A* **2002**, *957* (2), 149–164.
- (287) Majors, R. E.; Przybycien, M. Columns for reversed-phase LC separations in highly aqueous mobile phases. *LCGC North America* **2002**, *20* (7), 584–593.
- (288) Shen, Y.; Tolic, N.; Piehowski, P. D.; Shukla, A. K.; Kim, S.; Zhao, R.; Qu, Y.; Robinson, E.; Smith, R. D.; Pasa-Tolic, L. High-resolution ultrahigh-pressure long column reversed-phase liquid chromatography for top-down proteomics. *J. Chromatogr A* **2017**, *1498*, 99–110.
- (289) Fekete, S.; Ritchie, H.; Lawhorn, J.; Veuthey, J.-L.; Guillarme, D. Improving selectivity and performing online on-column fractioning in liquid chromatography for the separation of therapeutic biopharmaceutical products. *Journal of Chromatography A* **2020**, *1618*, 460901.
- (290) Khalikova, M. A.; Skarbalius, L.; Naplekov, D. K.; Jadeja, S.; Svec, F.; Lenco, J. Evaluation of strategies for overcoming trifluoroacetic acid ionization suppression resulted in single-column intact level, middle-up, and bottom-up reversed-phase LC-MS analyses of antibody biopharmaceuticals. *Talanta* **2021**, *233*, 122512.
- (291) Bobaly, B.; D'Atri, V.; Lauber, M.; Beck, A.; Guillarme, D.; Fekete, S. Characterizing various monoclonal antibodies with milder reversed phase chromatography conditions. *J. Chromatogr B Analyt Technol. Biomed. Life Sci.* **2018**, *1096*, 1–10.
- (292) Fekete, S.; Murisier, A.; Beck, A.; Lawhorn, J.; Ritchie, H.; Boyes, B.; Guillarme, D. New wide-pore superficially porous

- stationary phases with low hydrophobicity applied for the analysis of monoclonal antibodies. *J. Chromatogr A* **2021**, *1642*, 462050.
- (293) Donnelly, D. P.; Rawlins, C. M.; DeHart, C. J.; Fornelli, L.; Schachner, L. F.; Lin, Z.; Lippens, J. L.; Aluri, K. C.; Sarin, R.; Chen, B.; Lantz, C.; Jung, W.; Johnson, K. R.; Koller, A.; Wolff, J. J.; Campuzano, I. D. G.; Auclair, J. R.; Ivanov, A. R.; Whitelegge, J. P.; Pasa-Tolic, L.; Chamot-Rooke, J.; Danis, P. O.; Smith, L. M.; Tsybin, Y. O.; Loo, J. A.; Ge, Y.; Kelleher, N. L.; Agar, J. N. Best practices and benchmarks for intact protein analysis for top-down mass spectrometry. *Nat. Methods* **2019**, *16* (7), 587–594.
- (294) Tweenet, K. A.; Tweenet, T. N. Reversed-phase chromatography of proteins on resin-based wide-pore packings. *Journal of Chromatography A* **1986**, *359*, 111–119.
- (295) Svec, F.; Frechet, J. M. J. Continuous rods of macroporous polymer as high-performance liquid chromatography separation media. *Anal. Chem.* **1992**, *64* (7), 820–822.
- (296) Wang, Q. C.; Svec, F.; Frechet, J. M. J. Macroporous polymeric stationary-phase rod as continuous separation medium for reversed-phase chromatography. *Anal. Chem.* **1993**, *65* (17), 2243–2248.
- (297) Minakuchi, H.; Nakanishi, K.; Soga, N.; Ishizuka, N.; Tanaka, N. Effect of skeleton size on the performance of octadecylsilylated continuous porous silica columns in reversed-phase liquid chromatography. *J. Chromatogr A* **1997**, *762* (1–2), 135–46.
- (298) Eeltink, S.; Wouters, S.; Dores-Sousa, J. L.; Svec, F. Advances in organic polymer-based monolithic column technology for high-resolution liquid chromatography-mass spectrometry profiling of antibodies, intact proteins, oligonucleotides, and peptides. *Journal of Chromatography A* **2017**, *1498*, 8–21.
- (299) Eeltink, S.; Meston, D.; Svec, F. Recent developments and applications of polymer monolithic stationary phases. *Analytical Science Advances* **2021**, *2* (3–4), 250–260.
- (300) Vaast, A.; Novakova, L.; Desmet, G.; de Haan, B.; Swart, R.; Eeltink, S. High-speed gradient separations of peptides and proteins using polymer-monolithic poly(styrene-co-divinylbenzene) capillary columns at ultra-high pressure. *J. Chromatogr A* **2013**, *1304*, 177–82.
- (301) Iwasaki, M.; Sugiyama, N.; Tanaka, N.; Ishihama, Y. Human proteome analysis by using reversed phase monolithic silica capillary columns with enhanced sensitivity. *J. Chromatogr A* **2012**, *1228*, 292–7.
- (302) Khoo, H. T.; Leow, C. H. Advancements in the preparation and application of monolithic silica columns for efficient separation in liquid chromatography. *Talanta* **2021**, *224*, 121777.
- (303) Svec, F.; Lv, Y. Advances and recent trends in the field of monolithic columns for chromatography. *Anal. Chem.* **2015**, *87* (1), 250–73.
- (304) Ikegami, T.; Tanaka, N. Recent Progress in Monolithic Silica Columns for High-Speed and High-Selectivity Separations. *Annu. Rev. Anal. Chem. (Palo Alto Calif.)* **2016**, *9* (1), 317–42.
- (305) Gama, M. R.; Rocha, F. R. P.; Bottoli, C. B. G. Monoliths: Synthetic routes, functionalization and innovative analytical applications. *TrAC Trends in Analytical Chemistry* **2019**, *115*, 39–51.
- (306) Hara, T.; Izumi, Y.; Hata, K.; Baron, G. V.; Bamba, T.; Desmet, G. Performance of small-domain monolithic silica columns in nano-liquid chromatography and comparison with commercial packed bed columns with 2 microm particles. *J. Chromatogr. A* **2020**, *1616*, 460804.
- (307) Xiang, P.; Yang, Y.; Chen, H.; Chen, A.; Liu, S. Liquid chromatography using $\leq 5 \mu\text{m}$ open tubular columns. *TrAC Trends in Analytical Chemistry* **2021**, *142*, 116321.
- (308) Lam, S. C.; Sanz Rodriguez, E.; Haddad, P. R.; Paull, B. Recent advances in open tubular capillary liquid chromatography. *Analyst* **2019**, *144* (11), 3464–3482.
- (309) Jorgenson, J. W.; Guthrie, E. J. Liquid chromatography in open-tubular columns: Theory of column optimization with limited pressure and analysis time, and fabrication of chemically bonded reversed-phase columns on etched borosilicate glass capillaries. *Journal of Chromatography A* **1983**, *255* (Jan), 335–348.
- (310) Causon, T. J.; Shellie, R. A.; Hilder, E. F.; Desmet, G.; Eeltink, S. Kinetic optimization of open-tubular liquid-chromatography capillaries coated with thick porous layers for increased loadability. *Journal of Chromatography A* **2011**, *1218* (46), 8388–8393.
- (311) Golay, M. J. Height equivalent to a theoretical plate of an open tubular column lined with a porous layer. *Anal. Chem.* **1968**, *40* (2), 382–384.
- (312) Hara, T.; Futagami, S.; Eeltink, S.; De Malsche, W.; Baron, G. V.; Desmet, G. Very High Efficiency Porous Silica Layer Open-Tubular Capillary Columns Produced via in-Column Sol-Gel Processing. *Anal. Chem.* **2016**, *88* (20), 10158–10166.
- (313) Xiang, P.; Zhu, Y.; Yang, Y.; Zhao, Z.; Williams, S. M.; Moore, R. J.; Kelly, R. T.; Smith, R. D.; Liu, S. Picoflow Liquid Chromatography-Mass Spectrometry for Ultrasensitive Bottom-Up Proteomics Using 2-mum-i.d. Open Tubular Columns. *Anal. Chem.* **2020**, *92* (7), 4711–4715.
- (314) Roberg-Larsen, H.; Lundanes, E.; Nyman, T. A.; Berven, F. S.; Wilson, S. R. Liquid chromatography, a key tool for the advancement of single-cell omics analysis. *Anal. Chim. Acta* **2021**, *1178*, 338551.
- (315) Kennedy, R. T.; Oates, M. D.; Cooper, B. R.; Nickerson, B.; Jorgenson, J. W. Microcolumn separations and the analysis of single cells. *Science* **1989**, *246* (4926), 57–63.
- (316) De Malsche, W.; Op De Beeck, J.; De Bruyne, S.; Gardeniers, H.; Desmet, G. Realization of 1×10^6 theoretical plates in liquid chromatography using very long pillar array columns. *Anal. Chem.* **2012**, *84* (3), 1214–9.
- (317) De Beeck, J. O.; Pauwels, J.; Van Landuyt, N.; Jacobs, P.; De Malsche, W.; Desmet, G.; Argentini, A.; Staes, A.; Martens, L.; Impens, F.; Gevaert, K. A well-ordered nanoflow LC-MS/MS approach for proteome profiling using 200 cm long micro pillar array columns. *bioRxiv* **2019**, 472134.
- (318) Stadlmann, J.; Hudacek, O.; Krssakova, G.; Ctortecka, C.; Van Raemdonck, G.; Op De Beeck, J.; Desmet, G.; Penninger, J. M.; Jacobs, P.; Mechtler, K. Improved Sensitivity in Low-Input Proteomics Using Micropillar Array-Based Chromatography. *Anal. Chem.* **2019**, *91* (22), 14203–14207.
- (319) Muller, J. B.; Geyer, P. E.; Colaco, A. R.; Treit, P. V.; Strauss, M. T.; Oroshi, M.; Doll, S.; Virreira Winter, S.; Bader, J. M.; Kohler, N.; Theis, F.; Santos, A.; Mann, M. The proteome landscape of the kingdoms of life. *Nature* **2020**, *582* (7813), 592–596.
- (320) Desmet, G.; de Beeck, J. O.; Van Raemdonck, G.; Van Mol, K.; Claerebout, B.; Van Landuyt, N.; Jacobs, P. Separation efficiency kinetics of capillary flow micro-pillar array columns for liquid chromatography. *J. Chromatogr A* **2020**, *1626*, 461279.
- (321) Rozing, G. Micropillar array columns for advancing nanoflow HPLC. *Microchem. J.* **2021**, *170*, 106629.
- (322) Abian, J.; Oosterkamp, A. J.; Gelpí, E. Comparison of conventional, narrow-bore and capillary liquid chromatography/mass spectrometry for electrospray ionization mass spectrometry: practical considerations. *Journal of Mass Spectrometry* **1999**, *34* (4), 244–254.
- (323) Vissers, J. P. C.; Claessens, H. A.; Cramers, C. A. Microcolumn liquid chromatography: instrumentation, detection and applications. *Journal of Chromatography A* **1997**, *779* (1), 1–28.
- (324) Cutillas, P. Principles of Nanoflow Liquid Chromatography and Applications to Proteomics. *Current Nanosci.* **2005**, *1* (1), 65–71.
- (325) Rozing, G. Trends in HPLC column formats - Microbore, nanobore and smaller. *LCGC Europe* **2003**, *6* (6a), 1–7.
- (326) Urban, P. L. Clarifying Misconceptions about Mass and Concentration Sensitivity. *J. Chem. Educ.* **2016**, *93* (6), 984–987.
- (327) Michalski, A.; Cox, J.; Mann, M. More than 100,000 detectable peptide species elute in single shotgun proteomics runs but the majority is inaccessible to data-dependent LC-MS/MS. *J. Proteome Res.* **2011**, *10* (4), 1785–93.
- (328) Bell, D. Perspectives on the adoption and utility of 1.0-mm internal diameter liquid chromatography columns. *LCGC Europe* **2019**, *32* (3), 140–143.
- (329) Zhu, Y.; Zhao, R.; Piehowski, P. D.; Moore, R. J.; Lim, S.; Orphan, V. J.; Pasa-Tolic, L.; Qian, W. J.; Smith, R. D.; Kelly, R. T. Subnanogram proteomics: impact of LC column selection, MS

- instrumentation and data analysis strategy on proteome coverage for trace samples. *Int. J. Mass Spectrom.* **2018**, *427*, 4–10.
- (330) Bian, Y.; Bayer, F. P.; Chang, Y. C.; Meng, C.; Hoefer, S.; Deng, N.; Zheng, R.; Boychenko, O.; Kuster, B. Robust Microflow LC-MS/MS for Proteome Analysis: 38000 Runs and Counting. *Anal. Chem.* **2021**, *93* (8), 3686–3690.
- (331) Bian, Y.; Zheng, R.; Bayer, F. P.; Wong, C.; Chang, Y. C.; Meng, C.; Zolg, D. P.; Reinecke, M.; Zecha, J.; Wiechmann, S.; Heinzlmeir, S.; Scherr, J.; Hemmer, B.; Baynham, M.; Gingras, A. C.; Boychenko, O.; Kuster, B. Robust, reproducible and quantitative analysis of thousands of proteomes by micro-flow LC-MS/MS. *Nat. Commun.* **2020**, *11* (1), 157.
- (332) Gonzalez Fernandez-Nino, S. M.; Smith-Moritz, A. M.; Chan, L. J.; Adams, P. D.; Heazlewood, J. L.; Petzold, C. J. Standard flow liquid chromatography for shotgun proteomics in bioenergy research. *Front Bioeng Biotechnol* **2015**, *3*, 44.
- (333) Pergande, M. R.; Zarate, E.; Haney-Ball, C.; Davidson, C. D.; Scesa, G.; Givogri, M. I.; Bongarzone, E. R.; Cologna, S. M. Standard-flow LC and thermal focusing ESI elucidates altered liver proteins in late stage Niemann–Pick, type C1 disease. *Bioanalysis* **2019**, *11* (11), 1067–1083.
- (334) Orsburn, B. C.; Miller, S. D.; Jenkins, C. J. Standard Flow Multiplexed Proteomics (SFloMPro)—An Accessible Alternative to NanoFlow Based Shotgun Proteomics. *Proteomes* **2022**, *10* (1), 3.
- (335) Percy, A. J.; Chambers, A. G.; Yang, J.; Domanski, D.; Borchers, C. H. Comparison of standard- and nano-flow liquid chromatography platforms for MRM-based quantitation of putative plasma biomarker proteins. *Anal Bioanal Chem.* **2012**, *404* (4), 1089–101.
- (336) Hsieh, E. J.; Bereman, M. S.; Durand, S.; Valaskovic, G. A.; MacCoss, M. J. Effects of column and gradient lengths on peak capacity and peptide identification in nanoflow LC-MS/MS of complex proteomic samples. *J. Am. Soc. Mass Spectrom.* **2013**, *24* (1), 148–53.
- (337) Kocher, T.; Swart, R.; Mechtler, K. Ultra-high-pressure RPLC hyphenated to an LTQ-Orbitrap Velos reveals a linear relation between peak capacity and number of identified peptides. *Anal. Chem.* **2011**, *83* (7), 2699–704.
- (338) Gritti, F.; Dion, M.; Felinger, A.; Savaria, M. Characterization of radial and axial heterogeneities of chromatographic columns by flow reversal. *J. Chromatogr A* **2018**, *1567*, 164–176.
- (339) Miyamoto, K.; Hara, T.; Kobayashi, H.; Morisaka, H.; Tokuda, D.; Horie, K.; Koduki, K.; Makino, S.; Nunez, O.; Yang, C.; Kawabe, T.; Ikegami, T.; Takubo, H.; Ishihama, Y.; Tanaka, N. High-efficiency liquid chromatographic separation utilizing long monolithic silica capillary columns. *Anal. Chem.* **2008**, *80* (22), 8741–50.
- (340) Wang, X.; Stoll, D. R.; Schellinger, A. P.; Carr, P. W. Peak capacity optimization of peptide separations in reversed-phase gradient elution chromatography: fixed column format. *Anal. Chem.* **2006**, *78* (10), 3406–16.
- (341) Gilar, M.; Daly, A. E.; Kele, M.; Neue, U. D.; Gebler, J. C. Implications of column peak capacity on the separation of complex peptide mixtures in single- and two-dimensional high-performance liquid chromatography. *J. Chromatogr A* **2004**, *1061* (2), 183–92.
- (342) Xu, P.; Duong, D. M.; Peng, J. Systematical optimization of reverse-phase chromatography for shotgun proteomics. *J. Proteome Res.* **2009**, *8* (8), 3944–50.
- (343) Kocher, T.; Pichler, P.; De Pra, M.; Rieux, L.; Swart, R.; Mechtler, K. Development and performance evaluation of an ultralow flow nanoliquid chromatography-tandem mass spectrometry set-up. *Proteomics* **2014**, *14* (17–18), 1999–2007.
- (344) Williams, J. S.; Donahue, S. H.; Gao, H.; Brummel, C. L. Universal LC-MS method for minimized carryover in a discovery bioanalytical setting. *Bioanalysis* **2012**, *4* (9), 1025–37.
- (345) Schellinger, A. P.; Stoll, D. R.; Carr, P. W. High speed gradient elution reversed-phase liquid chromatography. *J. Chromatogr A* **2005**, *1064* (2), 143–56.
- (346) Schellinger, A. P.; Stoll, D. R.; Carr, P. W. High-speed gradient elution reversed-phase liquid chromatography of bases in buffered eluents. Part I. Retention repeatability and column re-equilibration. *J. Chromatogr A* **2008**, *1192* (1), 41–53.
- (347) John, W. D. Gradient Elution, Part IV: Dwell-Volume Problems. *LCGC North America* **2013**, *31* (6), 456–463.
- (348) Moruz, L.; Pichler, P.; Stranzl, T.; Mechtler, K.; Kall, L. Optimized nonlinear gradients for reversed-phase liquid chromatography in shotgun proteomics. *Anal. Chem.* **2013**, *85* (16), 7777–85.
- (349) Trudgian, D. C.; Fischer, R.; Guo, X.; Kessler, B. M.; Mirzaei, H. GOAT-a simple LC-MS/MS gradient optimization tool. *Proteomics* **2014**, *14* (12), 1467–71.
- (350) Moruz, L.; Kall, L. GradientOptimizer: an open-source graphical environment for calculating optimized gradients in reversed-phase liquid chromatography. *Proteomics* **2014**, *14* (12), 1464–6.
- (351) Bian, Y.; The, M.; Giansanti, P.; Mergner, J.; Zheng, R.; Wilhelm, M.; Boychenko, A.; Kuster, B. Identification of 7000–9000 Proteins from Cell Lines and Tissues by Single-Shot Microflow LC-MS/MS. *Anal. Chem.* **2021**, *93* (25), 8687–8692.
- (352) Majors, R. E. The continuing acetonitrile shortage: To combat it or live with it. *LCGC North America* **2009**, *27* (6), 458–471.
- (353) Dolan, J. W. Mobile-phase degassing: What, why, and how. *LCGC Europe* **2014**, *27* (7), 347–352.
- (354) Dolan, J. W. How does it work? Part II: Mixing and degassing. *LCGC North America* **2016**, *34*, 400–407.
- (355) Budamgunta, H.; Maes, E.; Willems, H.; Menschaert, G.; Schildermans, K.; Kumar, A. A.; Boonen, K.; Baggerman, G. Multiple solvent elution, a method to counter the effects of coelution and ion suppression in LC-MS analysis in bottom up proteomics. *J. Chromatogr B Analyt Technol. Biomed Life Sci.* **2019**, *1124*, 256–264.
- (356) Keppel, T. R.; Jacques, M. E.; Weis, D. D. The use of acetone as a substitute for acetonitrile in analysis of peptides by liquid chromatography/electrospray ionization mass spectrometry. *Rapid Commun. Mass Spectrom.* **2010**, *24* (1), 6–10.
- (357) Giorgianni, F.; Cappiello, A.; Beranova-Giorgianni, S.; Palma, P.; Trufelli, H.; Desiderio, D. M. LC-MS/MS analysis of peptides with methanol as organic modifier: improved limits of detection. *Anal. Chem.* **2004**, *76* (23), 7028–38.
- (358) Gangnus, T.; Burckhardt, B. B. Improving sensitivity for the targeted LC-MS/MS analysis of the peptide bradykinin using a design of experiments approach. *Talanta* **2020**, *218*, 121134.
- (359) Cech, N. B.; Enke, C. G. Practical implications of some recent studies in electrospray ionization fundamentals. *Mass Spectrom Rev.* **2001**, *20* (6), 362–87.
- (360) Katz, J. J. Anhydrous trifluoroacetic acid as a solvent for proteins. *Nature* **1954**, *174* (4428), 509.
- (361) Mahoney, W. C.; Hermodson, M. A. Separation of large denatured peptides by reverse phase high performance liquid chromatography. Trifluoroacetic acid as a peptide solvent. *J. Biol. Chem.* **1980**, *255* (23), 11199–203.
- (362) Winkler, G.; Wolschann, P.; Briza, P.; Heinz, F. X.; Kunz, C. Spectral properties of trifluoroacetic acid—acetonitrile gradient systems for separation of picomole quantities of peptides by reversed-phase high-performance liquid chromatography. *Journal of Chromatography A* **1985**, *347* (1), 83–88.
- (363) Bennett, H. P.; Hudson, A. M.; McMartin, C.; Purdon, G. E. Use of octadecasilyl-silica for the extraction and purification of peptides in biological samples. Application to the identification of circulating metabolites of corticotropin-(1–24)-tetracosapeptide and somatostatin in vivo. *Biochem. J.* **1977**, *168* (1), 9–13.
- (364) Gustavsson, S. A.; Samskog, J.; Markides, K. E.; Langstrom, B. Studies of signal suppression in liquid chromatography-electrospray ionization mass spectrometry using volatile ion-pairing reagents. *J. Chromatogr A* **2001**, *937* (1–2), 41–7.
- (365) Zhou, S.; Hamburger, M. Effects of solvent composition on molecular ion response in electrospray mass spectrometry: Investigation of the ionization processes. *Rapid Commun. Mass Spectrom.* **1995**, *9* (15), 1516–1521.

- (366) Apffel, A.; Fischer, S.; Goldberg, G.; Goodley, P. C.; Kuhlmann, F. E. Enhanced sensitivity for peptide mapping with electrospray liquid chromatography-mass spectrometry in the presence of signal suppression due to trifluoroacetic acid-containing mobile phases. *J. Chromatogr A* **1995**, *712* (1), 177–90.
- (367) Kuhlmann, F. E.; Apffel, A.; Fischer, S. M.; Goldberg, G.; Goodley, P. C. Signal enhancement for gradient reverse-phase high-performance liquid chromatography-electrospray ionization mass spectrometry analysis with trifluoroacetic and other strong acid modifiers by postcolumn addition of propionic acid and isopropanol. *J. Am. Soc. Mass Spectrom.* **1995**, *6* (12), 1221–5.
- (368) Zhou, Z.; Zhang, J.; Xing, J.; Bai, Y.; Liao, Y.; Liu, H. Membrane-based continuous remover of trifluoroacetic acid in mobile phase for LC-ESI-MS analysis of small molecules and proteins. *J. Am. Soc. Mass Spectrom.* **2012**, *23* (7), 1289–92.
- (369) Chan, C. C.; Bolgar, M. S.; Dalpathado, D.; Lloyd, D. K. Mitigation of signal suppression caused by the use of trifluoroacetic acid in liquid chromatography mobile phases during liquid chromatography/mass spectrometry analysis via post-column addition of ammonium hydroxide. *Rapid Commun. Mass Spectrom.* **2012**, *26* (12), 1507–14.
- (370) Wang, S.; Xing, T.; Liu, A. P.; He, Z.; Yan, Y.; Daly, T. J.; Li, N. Simple Approach for Improved LC-MS Analysis of Protein Biopharmaceuticals via Modification of Desolvation Gas. *Anal. Chem.* **2019**, *91* (4), 3156–3162.
- (371) Mao, Y.; Kleinberg, A.; Zhao, Y.; Raidas, S.; Li, N. Simple Addition of Glycine in Trifluoroacetic Acid-Containing Mobile Phases Enhances the Sensitivity of Electrospray Ionization Mass Spectrometry for Biopharmaceutical Characterization. *Anal. Chem.* **2020**, *92* (13), 8691–8696.
- (372) Bobaly, B.; Toth, E.; Drahos, L.; Zsila, F.; Visy, J.; Fekete, J.; Vekey, K. Influence of acid-induced conformational variability on protein separation in reversed phase high performance liquid chromatography. *J. Chromatogr A* **2014**, *1325*, 155–62.
- (373) Bobaly, B.; Beck, A.; Fekete, J.; Guillarme, D.; Fekete, S. Systematic evaluation of mobile phase additives for the LC-MS characterization of therapeutic proteins. *Talanta* **2015**, *136*, 60–7.
- (374) Nguyen, J. M.; Smith, J.; Rzewuski, S.; Legido-Quigley, C.; Lauber, M. A. High sensitivity LC-MS profiling of antibody-drug conjugates with difluoroacetic acid ion pairing. *MAbs* **2019**, *11* (8), 1358–1366.
- (375) Marakova, K.; Rai, A. J.; Schug, K. A. Effect of difluoroacetic acid and biological matrices on the development of a liquid chromatography-triple quadrupole mass spectrometry method for determination of intact growth factor proteins. *J. Sep Sci.* **2020**, *43* (9–10), 1663–1677.
- (376) Schindler, P. A.; Van Dorsselaer, A.; Falick, A. M. Analysis of hydrophobic proteins and peptides by electrospray ionization mass spectrometry. *Anal. Biochem.* **1993**, *213* (2), 256–63.
- (377) Doucette, A. A.; Vieira, D. B.; Orton, D. J.; Wall, M. J. Resolubilization of precipitated intact membrane proteins with cold formic acid for analysis by mass spectrometry. *J. Proteome Res.* **2014**, *13* (12), 6001–12.
- (378) Cheng, Y. C.; Ku, W. C.; Tseng, T. T.; Wu, C. P.; Li, M.; Lee, S. C. Anchorage independence altered vasculogenic phenotype of melanoma cells through downregulation in aminopeptidase N/syndecan-1/integrin beta4 axis. *Aging (Albany NY)* **2020**, *12* (17), 16803–16819.
- (379) Voichek, M.; Maass, S.; Kroniger, T.; Becher, D.; Sorek, R. Peptide-based quorum sensing systems in Paenibacillus polymyxia. *Life Sci. Alliance* **2020**, *3* (10), No. e202000847.
- (380) Hahne, H.; Pachl, F.; Ruprecht, B.; Maier, S. K.; Klaeger, S.; Helm, D.; Medard, G.; Wilm, M.; Lemeer, S.; Kuster, B. DMSO enhances electrospray response, boosting sensitivity of proteomic experiments. *Nat. Methods* **2013**, *10* (10), 989–91.
- (381) Meyer, J. G.; Komives, E. A. Charge state coalescence during electrospray ionization improves peptide identification by tandem mass spectrometry. *J. Am. Soc. Mass Spectrom.* **2012**, *23* (8), 1390–9.
- (382) Yu, P.; Hahne, H.; Wilhelm, M.; Kuster, B. Ethylene glycol improves electrospray ionization efficiency in bottom-up proteomics. *Anal. Bioanal. Chem.* **2017**, *409* (4), 1049–1057.
- (383) He, Y.; Rashan, E. H.; Linke, V.; Shishkova, E.; Hebert, A. S.; Jochem, A.; Westphall, M. S.; Pagliarini, D. J.; Overmyer, K. A.; Coon, J. J. Multi-Omic Single-Shot Technology for Integrated Proteome and Lipidome Analysis. *Anal. Chem.* **2021**, *93* (9), 4217–4222.
- (384) Mitulovic, G.; Stingl, C.; Steinmacher, I.; Hudecz, O.; Hutchins, J. R.; Peters, J. M.; Mechler, K. Preventing carryover of peptides and proteins in nano LC-MS separations. *Anal. Chem.* **2009**, *81* (14), 5955–60.
- (385) Maes, K.; Smolders, I.; Michotte, Y.; Van Eeckhaut, A. Strategies to reduce aspecific adsorption of peptides and proteins in liquid chromatography-mass spectrometry based bioanalyses: an overview. *J. Chromatogr A* **2014**, *1358*, 1–13.
- (386) Birdsall, R. E.; Kellett, J.; Yu, Y. Q.; Chen, W. Application of mobile phase additives to reduce metal-ion mediated adsorption of non-phosphorylated peptides in RPLC/MS-based assays. *J. Chromatogr. B* **2019**, *1126–1127*, 121773.
- (387) Winter, D.; Seidler, J.; Ziv, Y.; Shiloh, Y.; Lehmann, W. D. Citrate boosts the performance of phosphopeptide analysis by UPLC-ESI-MS/MS. *J. Proteome Res.* **2009**, *8* (1), 418–24.
- (388) Siegel, D.; Permentier, H.; Bischoff, R. Controlling detrimental effects of metal cations in the quantification of energy metabolites via ultrahigh pressure-liquid chromatography-electrospray-tandem mass spectrometry by employing acetylacetone as a volatile eluent modifier. *J. Chromatogr A* **2013**, *1294*, 87–97.
- (389) Schöbinger, M.; Klein, O.-J.; Mitulović, G. Low-Temperature Mobile Phase for Peptide Trapping at Elevated Separation Temperature Prior to Nano RP-HPLC-MS/MS. *Separations* **2016**, *3* (1), 6.
- (390) Young, C.; Podtelejnikov, A. V.; Nielsen, M. L. Improved Reversed Phase Chromatography of Hydrophilic Peptides from Spatial and Temporal Changes in Column Temperature. *J. Proteome Res.* **2017**, *16* (6), 2307–2317.
- (391) Colin, H.; Diezmasa, J. C.; Guiochon, G.; Czjkowska, T.; Miedziak, I. Role of the Temperature in Reversed-Phase High-Performance Liquid-Chromatography Using Pyrocarbon-Containing Adsorbents. *J. Chromatogr. A* **1978**, *167* (Dec), 41–65.
- (392) Antia, F. D.; Horvath, C. High-Performance Liquid-Chromatography at Elevated-Temperatures - Examination of Conditions for the Rapid Separation of Large Molecules. *J. Chromatogr. A* **1988**, *435* (1), 1–15.
- (393) Moskovets, E. V.; Ivanov, A. R. Comparative studies of peak intensities and chromatographic separation of proteolytic digests, PTMs, and intact proteins obtained by nanoLC-ESI MS analysis at room and elevated temperatures. *Anal. Bioanal. Chem.* **2016**, *408* (15), 3953–68.
- (394) Speers, A. E.; Blackler, A. R.; Wu, C. C. Shotgun analysis of integral membrane proteins facilitated by elevated temperature. *Anal. Chem.* **2007**, *79* (12), 4613–20.
- (395) Farias, S. E.; Kline, K. G.; Klepacki, J.; Wu, C. C. Quantitative improvements in peptide recovery at elevated chromatographic temperatures from microcapillary liquid chromatography-mass spectrometry analyses of brain using selected reaction monitoring. *Anal. Chem.* **2010**, *82* (9), 3435–40.
- (396) Griffiths, S. W.; Cooney, C. L. Development of a peptide mapping procedure to identify and quantify methionine oxidation in recombinant human alpha1-antitrypsin. *J. Chromatogr A* **2002**, *942* (1–2), 133–43.
- (397) Yang, X.; Ma, L.; Carr, P. W. High temperature fast chromatography of proteins using a silica-based stationary phase with greatly enhanced low pH stability. *Journal of Chromatography A* **2005**, *1079* (1), 213–220.
- (398) Heidorn, M. Optimization of Chromatographic Results by Using Mobile Phase Preheating; Technical Note 150, Thermo Fisher Scientific, 2016.
- (399) Vanhoenacker, G.; Sandra, P. High temperature and temperature programmed HPLC: possibilities and limitations. *Anal. Bioanal. Chem.* **2008**, *390* (1), 245–8.

- (400) Hebert, A. S.; Prasad, S.; Belford, M. W.; Bailey, D. J.; McAlister, G. C.; AbbatIELLO, S. E.; Huguet, R.; Wouters, E. R.; Dunyach, J. J.; Brademan, D. R.; Westphall, M. S.; Coon, J. J. Comprehensive Single-Shot Proteomics with FAIMS on a Hybrid Orbitrap Mass Spectrometer. *Anal. Chem.* **2018**, *90* (15), 9529–9537.
- (401) Wang, H.; Yang, Y.; Li, Y.; Bai, B.; Wang, X.; Tan, H.; Liu, T.; Beach, T. G.; Peng, J.; Wu, Z. Systematic optimization of long gradient chromatography mass spectrometry for deep analysis of brain proteome. *J. Proteome Res.* **2015**, *14* (2), 829–38.
- (402) McCalley, D. V. Study of overloading of basic drugs and peptides in reversed-phase high-performance liquid chromatography using pH adjustment of weak acid mobile phases suitable for mass spectrometry. *J. Chromatogr A* **2005**, *1075* (1–2), 57–64.
- (403) Maia, T. M.; Staes, A.; Plasman, K.; Pauwels, J.; Boucher, K.; Argentini, A.; Martens, L.; Montoye, T.; Gevaert, K.; Impens, F. Simple Peptide Quantification Approach for MS-Based Proteomics Quality Control. *ACS Omega* **2020**, *5* (12), 6754–6762.
- (404) Chervet, J. P.; Ursem, M.; Salzmann, J. P. Instrumental Requirements for Nanoscale Liquid Chromatography. *Anal. Chem.* **1996**, *68* (9), 1507–1512.
- (405) Heaton, J. C.; McCalley, D. V. Some factors that can lead to poor peak shape in hydrophilic interaction chromatography, and possibilities for their remediation. *J. Chromatogr A* **2016**, *1427*, 37–44.
- (406) Dolan, J. How Does It Work? Part 1: Pumps. *LCGC Europe* **2016**, *29* (5), 258–261.
- (407) Dolan, J. How Does It Work? Part II: Mixing and Degassing. *LCGC North America* **2016**, *34* (6), 400–407.
- (408) Dolan, J. How Does It Work? Part III: Autosamplers. *LCGC North America* **2016**, *34* (7), 472–478.
- (409) Dolan, J. How Does It Work? Part IV: Ultraviolet Detectors. *LCGC North America* **2016**, *34* (8), 534–539.
- (410) Broeckhoven, K.; Konstantin, S.; Michael, W. D. Modern HPLC Pumps: Perspectives, Principles, and Practices. *LCGC North America* **2019**, *37* (6), 374–384.
- (411) Stoll, D. Mixing and Mixers in Liquid Chromatography—Why, When, and How Much? Part I, The Pump. *LCGC North America* **2018**, *36* (10), 746–751.
- (412) Steiner, F.; Dong, M.; Carsten, P. HPLC Autosamplers: Perspectives, Principles, and Practices. *LCGC North America* **2019**, *37* (8), 514–529.
- (413) Perez-Riverol, Y.; Bai, J.; Bandla, C.; Garcia-Seisdedos, D.; Hewapathirana, S.; Kamatchinathan, S.; Kundu, D. J.; Prakash, A.; Frericks-Zipper, A.; Eisenacher, M.; Walzer, M.; Wang, S.; Brazma, A.; Vizcaino, J. A. The PRIDE database resources in 2022: a hub for mass spectrometry-based proteomics evidences. *Nucleic Acids Res.* **2022**, *50* (D1), D543–D552.

□ Recommended by ACS

Deep Proteome Profiling with Reduced Carryover Using Superficially Porous Microfabricated nanoLC Columns

Karel Stejskal, Karl Mechtler, *et al.*
NOVEMBER 10, 2022
ANALYTICAL CHEMISTRY

READ ▾

Size-Based Proteome Fractionation through Polyacrylamide Gel Electrophoresis Combined with LC–FAIMS–MS for In-Depth Top-Down Proteomics

Ayako Takemori, Andreas Tholey, *et al.*
SEPTEMBER 07, 2022
ANALYTICAL CHEMISTRY

READ ▾

Chromatography at –30 °C for Reduced Back-Exchange, Reduced Carryover, and Improved Dynamic Range for Hydrogen–Deuterium Exchange Mass Spectrometry

Kyle W. Anderson and Jeffrey W. Hudgens
JUNE 22, 2022
JOURNAL OF THE AMERICAN SOCIETY FOR MASS SPECTROMETRY

READ ▾

High-Throughput Screening Using a Synchronized Pulsed Self-aspiration Vacuum Electrospray Ionization Miniature Mass Spectrometer

Yanping Zhu, Quan Yu, *et al.*
MAY 09, 2022
ANALYTICAL CHEMISTRY

READ ▾

[Get More Suggestions >](#)